1-1-2012

Induced Gene Expression In Bladder Cancer: Kindlin-2 And Metallothionein-1x

Sherine Talaat

INDUCED GENE EXPRESSION IN BLADDER CANCER: KINDLIN-2 AND METALLOTHIONEIN-1X

by

SHERINE TALAAT
Bachelor of Medicine, Bachelor of Surgery, University of Alexandria, Egypt, 1995

A Dissertation

Submitted to the Graduate Faculty

of the

University of North Dakota

in partial fulfillment of the requirements

for the degree of

Doctor of Philosophy

Grand Forks, North Dakota
August
2012

This dissertation, submitted by Sherine Talaat, in partial fulfillment of the requirements for the Degree of Doctor of Philosophy from the University of North Dakota, has been read by the Faculty Advisory Committee under whom the work has been done and is hereby approved.

Dr. Mary Ann Sens

_____
Chairperson

Dr. Scott Garrett

_____

Dr. Seema Somji

_____

Dr. Roxanne Vaughan

_____

Dr. Holly Brown-Borg

_____

This dissertation meets the standards for appearance, conforms to the style and format requirements of the Graduate School of the University of North Dakota, and is hereby approved.

Dr. Wayne Swisher

_____
Dean of the Graduate School

July 5, 2012

_____
Date

PERMISSION

Title	INDUCED GENE EXPRESSION IN BLADDER CANCER: KINDLIN-2 AND METALLOTHIONEIN-1X
Department	Biochemistry and Molecular Biology
Degree	Doctor of Philosophy

In presenting this dissertation in partial fulfillment of the requirements for a graduate degree from the University of North Dakota, I agree that the library of this University shall make it freely available for inspection. I further agree that permission for extensive copying for scholarly purposes may be granted by the professor who supervised my dissertation work or, in her absence, by the chairperson of the department or the dean of the Graduate School. It is understood that any copying or publication or other use of this dissertation or part thereof for financial gain shall not be allowed without my written permission. It is also understood that due recognition shall be given to me and to the University of North Dakota in any scholarly use which may be made of any material in my dissertation.

Sherine Talaat

Signature_____

July 5, 2012

Date_____

TABLE OF CONTENTS

LIST OF FIGURES

Figure Page

LIST OF TABLES

Table Page

ABBREVIATIONS

°C	Degree Celsius
As^{+3}	Arsenite
ATSDR	Agency for the Toxic Substances and Disease Registry
BCA	Bicinchoninic acid
BCP	1-bromo-3 chloropropane
bp	Base pairs
BSA	Bovine serum albumin
CBP	cAMP-responsive element binding protein-binding protein
Cd^{+2}	Cadmium
$CdCl_2$	Cadmium chloride
cDNA	Copy of DNA made from mRNA
ChIP	Chromatin immunoprecipitation
Cr	Chromium
Cu	Copper
DAB	Diaminobenzidine
DMA^{+5}	Dimethyl arsenate
DMEM	Dulbecco's modified Eagle's medium

DNA	Deoxy-ribonucleic acid
ELK1	Ets domain-containing protein Elk-1
FERM	Four point one protein, Ezrin, Radixin, and Moesin
GSH	Glutathione
h	Hour
H2A.z	H2A histone family, member Z
H3.3	H3 histone, family 3A
H3K27	Histone H3 trimethyl lysine 27
H3K4	Histone H3 trimethyl lysine 4
H3K9	Histone H3 trimethyl lysine 9
HDACi	Histone deacetylase inhibitor
IARC	International Agency on Research in Cancer
IP	Intra-peritoneal
LBP-1	Upstream binding protein 1
min	Minute
ml	Millilter
mM	Millimolar
µg	Microgram
µl	Microliter
µm	Micrometer
µM	Micromolar

MMA^{+5}	Monomethyl arsenate
MRE	Metal responsive elements
mRNA	Messenger RNA
MT	Metallothionein
MTF-1	Metal-responsive-element-binding transcription factor 1
$NaAsO_2$	Sodium arsenite
NF-I	CCAAT-binding transcription factor
p300	E1A binding protein p300
PAGE	Polyacramide gel electrophoresis
PCR	Polymerase Chain Reaction
PMSF	Phenylmethylsulfonylfluoride
RNA	Ribonucleic acid
ROS	Reactive Oxygen Species
RT-PCR	Reverse transcription Polymerase Chain Reaction
s	Second
SC	Subcutaneous
SDS	Sodium dodecyl sulphate
SP1	The Sp1 transcription factor
TBS	Tris buffered saline
TCF-1	T cell-specific transcription factor 1
TESS	Transcription Element Search System

TSS	Transcription start site
USF1	Upstream transcription factor 1
YY1	Yin and Yang 1 protein
Zn^{+2}	Zinc
$ZnSO_4$	Zinc sulphate

ACKNOWLEDGMENTS

I wish to express my sincere appreciation to the members of my advisory committee: Drs. Mary Ann Sens, Scott Garrett, Seema Somji, Roxanne Vaughan and Holly Brown-Borg for their guidance and support during my time in the doctoral program at the University of North Dakota.

ABSTRACT

Arsenic and cadmium (Cd^{+2}) are environmental agents that have been classified as human carcinogens by the International Agency on Research in Cancer (IARC). Numerous epidemiological studies have linked arsenite (As^{+3}) and Cd^{+2} to the development of bladder cancer. Bladder cancer is the second most common genitourinary malignancy in the United States, and one of the first cancers to be associated with an environmental component. Currently, there are no stand-alone biomarkers for this type of cancer.

Kindlin-2 and Metallothionein (MT) isoform-1X (MT-1X) are two genes that are the focus of this dissertation. Both genes were selected for further experimental analysis based on their common association with bladder cancer. Metallothionein isoforms 1 & 2 (MT I/II) are over-expressed in high-grade muscle-invasive bladder cancers, and in one study, MT-1X showed increased levels of expression compared to the other isoforms. The main goal of the MT-1X study was to investigate the mechanism by which this isoform is over expressed in bladder cancer, and it was predicted that both transcriptional and epigenetic processes were involved in the regulation of the MT-1X promoter. The model system used in this study was the normal human urothelial (UROtsa) cell line and its As^{+3} or Cd^{+2} transformed counterparts. The experimental approach was to assess MT-1X mRNA expression, transcription factor binding, as well as,

histone modifications in the MT-1X promoter of metal-transformed cells and compare it to that of the non-transformed parent. In addition, the effect of the histone deacetylase inhibitor (HDACi) MS-275 on factor binding and histone modifications was also examined. Results of this study revealed that exposure to MS-275 induced the levels of MT-1X mRNA, and that this induction was further enhanced when the cells were exposed to a combined treatment of zinc (Zn^{+2}), a known inducer of MT transcription, and MS-275. ChIP analysis of the MT-1X promoter showed that there was increased transcription factor binding and histone modifications in the As^{+3} and Cd^{+2} transformed cells when compared to the non-transformed parent. Treatment with MS-275 further increased the binding of the transcription factors to the MT-1X promoter. Additionally, the histone modifications that correlated to a transcriptional active state were also increased with MS-275 treatment. The results also highlighted a possible role for the CCAAT-binding transcription factor (NF-I) in the initiation of transcription in the MT-1X promoter.

Kindlin-2 was selected for further investigation in an effort to confirm a microarray analysis that suggested that it might play a role in tumor metastasis. The microarray study revealed that Kindlin-2 was the most consistently repressed gene in the As^{+3} and Cd^{+2} transformed UROtsa cell lines that were capable of forming peritoneal tumors. To confirm these results, and to assess whether Kindlin-2 expression correlates with the ability to form tumors in the peritoneum, a common metastatic site in bladder cancer, the current study utilized a combination of RT-PCR, Western, and immunohistochemical

analyses to characterize Kindlin-2 expression in As^{+3} and Cd^{+2} transformed human cell lines, their tumor transplants in immunocompromised mice, and in archival specimens of normal human bladder and bladder cancer. Results of these experiments did not correlate with the results of the microarray study, but never the less, it was significant since it pointed to a potential role for Kindlin-2 as a prognostic biomarker in a subset of high-grade invasive urothelial cancers that are destined to progression and metastasis.

CHAPTER I

INTRODUCTION

Overview

The search for the ideal biomarker that can be the hallmark of, or the "signature" for a certain type of tumor, is a sought-after commodity for many investigators in the cancer research field. Biomarkers that are disease-specific represent an appealing option due to their ease of assessment and the invaluable insight they offer to monitoring the disease progression, metastasis, and the response to treatment.

Despite the fact that bladder cancer is one of the best-studied malignancies, and the fourth and fifth most common malignancy in men and women respectively, in the United States, there are no stand-alone biomarkers that can replace the gold standard for diagnosis consisting of a combination of cystoscopy and urinary cytology.

Bladder cancer was one of the first cancers to be associated with environmental factors as etiological agents, when Ludwig Rehn, in 1895, reported its increased incidence among factory workers in the aniline dye industry (Rehn 1895). Arsenic and Cd^{+2} are two of the most notorious environmental agents that were classified as human carcinogens (IARC 1987 and 2004). Both carcinogens are widespread in our environment, from drinking water and foodstuffs to being inhaled as particles in the air. Until 2004, there was no direct evidence, other than numerous epidemiological studies, that linked As^{+3} and Cd^{+2} to the development of bladder cancer. In an effort to develop

an *in vitro* model system of agent-induced bladder cancer, Sens & colleagues were the first to report the successful malignant transformation of UROtsa cells after long-term exposure to As^{+3} and Cd^{+2} (Sens *et al*., 2004). All of the transformed cell lines were able to form tumors in nude mice when injected SC, but only a subset of these cells were able to form tumors when injected in the peritoneal cavities of nude mice (Cao *et al*., 2010). A microarray study was done to characterize the individual patterns of gene expression for these cell lines, and the results of this analysis showed that Kindlin-2 was the most consistently repressed gene in the cell lines forming peritoneal tumors. Kindlin-2 was thus selected for further analysis to explore the possibility of its utilization as a biomarker for bladder cancer. Kindlin-2 belongs to the family of Kindlins, which are focal adhesion proteins with recently discovered roles in integrin activation. The expression of Kindlin-2 has not been previously characterized in bladder cancer.

Among the genes that showed variable expression in different types of tumors is the MT family of genes. Metallothioneins are small, cysteine-rich metal binding proteins. The MT family has four major isoforms (MT 1-4) that are widely distributed among eukaryotes, and show differential expression in various types of cancers. Metallothionein isoform III (MT-3) expression was reported to be down-regulated in ependymomas, oesophageal adenocarcinomas and lung cancer (Peyre *et al*., 2010, Peng *et al*., 2011, and Zhong *et al*., 2007). On the other hand, the overexpression of MT-3 in breast cancer tissues signaled a poor prognosis and further progression of the disease (Sens *et al*., 2001). Another study noted that there was a significant up-regulation of

MT-3 in bladder cancer, and proposed its use as a biomarker for this disease (Sens *et al*., 2000).

In addition to its over expression in different types of cancers, several studies have associated the increased levels of Metallothionein isoforms I & II (MT I/II) protein and mRNA in bladder cancer with increased aggressiveness and a worse response to treatment with chemotherapeutic agents (Siu *et al*., 1998, and Wulfing *et al*., 2007). Evidence presented in one study suggested that MT I/II is elevated in human bladder tumors, and that MT I/II might be developed as a prognostic biomarker in the progression of advanced bladder cancer (Zhou *et al*., 2006). In another study, it was concluded that the MT I/II up regulation in bladder cancer was due to the over expression of the MT-1X isoform (Somji *et al*., 2001).

Somji and colleagues concluded that the promoter of MT-3 gene in MCF-10 cells was influenced by epigenetic control mechanisms (Somji *et al.*, 2010). In another study, the promoter of MT-3 was examined for its enrichment in several histone modifications. Results of this study revealed that the MT-3 promoter was under epigenetic control, and that it was in a "poised state" carrying both marks of activation and repression in a "transcription-ready" state (Somji *et al*., 2011). Therefore, it seemed like a relevant possibility that the MT-1X promoter could also be under epigenetic control, and that this type of regulation caused its long-term up-regulation in bladder cancer tissues. Thus the hypothesis that MT-1X was epigenetically regulated in bladder cancer was the second different angle through which bladder cancer was examined in this study.

In conclusion, Kindlin-2 and MT-1X are two genes that are the focus of this dissertation. Both genes were selected for further experimental analysis based on their common association with bladder cancer. At the present time, there are no studies that link Kindlin-2 expression to bladder cancer, and the experiments on Kindlin-2 conducted herein are an effort to confirm a microarray analysis that suggested that it might play a role in the development and progression of bladder cancer. As for MT-1X, it will be discussed later in this chapter that there is strong evidence linking it to bladder cancer, and to the ability of such tumors to resist the effect of treatment with chemotherapeutic agents. This document will attempt to shed light on the possible roles that these two genes play in the pathogenesis of bladder cancer.

Arsenic

For more than twenty years, Arsenic has been classified as a "Group I human carcinogen" (IARC 1987 and 2012). Arsenic is also the first out of 50 most hazardous substances on a priority list prepared by the Agency for the Toxic Substances and Disease Registry (ATSDR 1999).

Arsenic has been used as a component in the production of various pharmaceutical and industrial compounds, and until the 1970s, it was a component of different medicinal preparations. The inorganic arsenical compounds were used in the treatment of chronic bronchial asthma, psoriasis, and leukemia, and the organic arsenicals were used in the treatment of protozoal and spirochetal diseases. Other industries that utilize arsenic include agricultural chemicals, wood preservatives, glass making, and semiconductors production.

Arsenic has been classified as the twentieth most common element of the earth's crust. Sources of arsenic include volcanic eruptions, industrial activities, and landscapes historically contaminated by arsenic-containing pesticides. Drinking water is the major source for arsenic contamination. The concentration of arsenic in water depends on several factors including the water's oxidative state, the type of water and the water source's proximity to arsenic-contaminated areas. Consumption of contaminated foods is another source for arsenic's accumulation in the human body, although it is less significant than the consumption of contaminated drinking water. The most common arsenic-containing foods are seafood followed by meats, cereals, fruits, vegetables and dairy products, and the estimated daily intake of arsenic is between 20-300 μg per day. Less common routes of contamination are the air-borne, and the trans-dermal routes (IARC 2004). Arsenic accumulates in keratin-rich tissues such as the hair, fingernails and toenails, and thus these tissues are used for the measurement of previous arsenic exposures. On the other hand, and because of the metal's rapid clearance from the body, blood and urine arsenic levels are considered as measurements of recent exposures.

Based on its chemical and physical properties, arsenic has been classified as a metalloid, which is an intermediate class between a metal and a non-metal element. Depending on its oxidation/reduction state, arsenic can exist in five different states, the most common of which are the trivalent As^{+3} when reduced, or the pentavalent arsenate (As^{+5}) when oxidized. From the biological and toxicological aspect, arsenical compounds can be classified into three major groups: organic and inorganic arsenical

compounds, and the arsine gas. The organic arsenicals include arsanilic acid and methyl arsonic acid, and the inorganic compounds include arsenic trichloride and sodium arsenite ($NaAsO_2$) as some of the common trivalent arsenicals, while arsenic pentoxide and arsenic acid are the most common pentavalent compounds. The inorganic compounds are generally considered the most toxic of the three groups.

The metabolism of inorganic arsenic compounds inside the body involves two steps: a reduction step and an oxidative methylation step. Approximately 50-70% of the As^{+5} are rapidly reduced to As^{+3} while still in the blood stream, and before they enter the cells (Tseng *et al.*, 2007). This reaction can occur non-enzymatically via glutathione (GSH) acting as an electron donor, or through the action of arsenate reductase enzyme (Vahter, 1999, and Kitchin, 2001). The liver is the major site for the metabolism of arsenic compound. Whereas As^{+3} enters the cells through the aquaglyceroporin channels, which are members of the aquaporin superfamily, the As^{+5} gains entrance to the cell with the help of phosphate transporters. The cells have a higher affinity for the intake of As^{+3} due to its presence in an undissociated form, when compared to As^{+5} that are present in an ionized state (Vahter, 2002). Once inside the cells, As^{+3} is oxidized into monomethyl arsenate (MMA^{+5}) and dimethyl arsenate (DMA^{+5}) compounds (Carter *et al.*, 2003). This methylation step occurs in the cytosol through the action of a methyl transferase enzyme, and with S-adenosyl methionine acting as the methyl donor. Recent studies have confirmed the presence of trivalent intermediates of As^{+3} metabolism that are formed through the reduction of MMA^{+5} and DMA^{+5} compounds. These As^{+3} intermediates have a higher toxicity than the non-methylated trivalent

arsenites. This enhanced toxicity is due to the fact that upon methylation, the negatively charged hydroxyl group is replaced by an uncharged methyl group that can bind negatively charged molecules such as the DNA with a higher affinity. Therefore, the trivalent compounds are generally considered more toxic than the pentavalent ones, owing mostly to their higher reactivity, and to a less extent to their more rapid rates of absorption (Bertolero *et al.*, 1987).

Cadmium

Cadmium has been classified as a "Group I human carcinogen" (IARC 1987 and 2012). Cadmium is also the seventh out of 50 most hazardous substances on a priority list prepared by the ATSDR (ATSDR 1999). It has been noted that Cd^{+2} release into the environment is a direct consequence of human activities. Three main sources of exposure to Cd^{+2} have been reported and these are: occupational exposure, smoking, and consumption of foods that have been contaminated with Cd^{+2}. Among the occupations with a high risk of exposure to Cd^{+2} are nickel-cadmium battery manufacturing, Cd^{+2} production and refining, and zinc (Zn^{+2}) smelting. The most common route for occupational Cd^{+2} exposure is through air-borne dust and fumes (Kellen *et al*., 2007). Cigarette smoking is a major contributor to Cd^{+2} accumulation in the human body, and it indirectly links Cd^{+2} to bladder cancer, since it is one of the predisposing factors for the development of this type of malignancy. It has been estimated that the Cd^{+2} content per cigarette is between 0-6.67 mg (Smith *et al*. 1997). The third major route of accumulation is through the consumption of foods contaminated with Cd^{+2}. Increase in the Cd^{+2} soil content through environmental

contamination increases its uptake by plants, and the leafy green vegetables in particular accumulate the highest amounts. Other food sources that are known to accumulate Cd^{+2} include fruits, meat, and fish. Drinking water generally has low levels of Cd^{+2}, and is not considered a major source for its exposure (Rojas *et al.,* 1999).

Owing to the fact that Cd^{+2} is a non-essential metal, it has been hypothesized that it utilizes the transport mechanisms of other essential metals to gain entry into the cell's interior. To date, the transporters for iron, calcium, Zn^{+2}, manganese, and magnesium have been directly involved in the transport of Cd^{+2} to the cell's interior. Zinc transporters ZIP8 and ZIP14, together with calcium channels are recent candidates of interest in Cd^{+2} transport (Himeno *et al*., 2009). Cadmium has a long half-life that is estimated to be between 15-20 years, and the major predicament from Cd^{+2} exposure stems from the fact that it is poorly metabolized into less toxic byproducts by the human body. Cadmium is also weakly excreted, and tends to accumulate in different body organs particularly the liver and kidneys. Metallothioneins, which are small proteins, are directly involved in Cd^{+2} accumulation, and are induced at the transcriptional level by Cd^{+2}, upon which they bind to it and favor its sequestration in the different body organs (Waalkes 2003). Cadmium's toxic effects stem mainly from its interference with Zn^{+2} metabolism. Both Cd^{+2} and Zn^{+2} are closely related in the periodic table, and they compete with each other for binding to MT. One consequence for this competition is that it drastically decreases the intracellular Zn^{+2} reserves (Goering *et al*., 1994).

Bladder Cancer

Bladder cancer is the second most common genitourinary malignancy in the United States, with a peak incidence in the age group between 50-70 years of age. Men are three times more afflicted with this malignancy when compared to women. Bladder cancer is one of the most costly cancers among all other types of cancer, from the time of its diagnosis until the time of death, and is associated with a high risk for recurrence and progression (Cheng *et al*., 2011). There are no stand-alone biomarkers that can replace the gold standard for diagnosis, which consists of a combination of cystoscopy and urinary cytology. In addition to being an invasive procedure, cystoscopy can have complications including post-procedure pain, and it requires specialized clinical equipment and set-up (Schwamborn *et al.*, 2010).

Three major risk factors have been identified for this disease, namely: molecular or genetic factors, environmental factors, and chronic irritation. Out of the different environmental factors, cigarette smoking is the single most important risk factor associated with this disease. Other environmental causative agents include aniline dyes, aromatic amines, arsenic, acrolein, coal, nitrites, and nitrates (Kaufman *et al.,* 2009). The current general consensus is that urothelial carcinomas can be classified into two distinct subgroups: the first is a low-grade papillary non-invasive tumor with a frequent recurrence, and the second is a high-grade invasive one that can often progress to lethality (Zlotta *et al*., 2010).

Arsenic and Bladder Cancer

Several studies conducted on the population in Taiwan have established a close relationship between the exposure to arsenic compounds from contaminated water sources and the development of cancers of the urinary bladder and the kidney. All of these studies showed an increase in the mortality rates among both men and women in a dose-dependent relationship that is directly proportional to the amount of consumption of arsenic-contaminated water from under-ground wells (Chen *et al*., 1985, Wu *et al*., 1989, and Tsai *et al.,* 1999). In addition to cancers of the bladder and kidneys, chronic arsenic exposure predisposes the body to the risk of development of several other types of cancer including lung, skin, liver, and prostate cancers (IARC 1987).

Arsenite was successfully used to induce malignant transformation of UROtsa cells in one study. This study found that the heterotransplants formed by the SC injection of As^{+3} transformed UROtsa cells had the characteristic histological features of squamous cell carcinoma of the urinary bladder. This squamous differentiation can be a used as a useful biomarker for As^{+3} exposure (Sens *et al*., 2004). The molecular mechanisms behind the As^{+3} induced carcinogenesis are not fully understood but might be in part, due its ability to generate reactive oxygen species (ROS) that can cause DNA damage and predispose to malignant changes (Jacobson-Kram *et al.,* 1985, and Schwerdtle *et al.,* 2003). Another theory suggests that As^{+3} causes alterations in the sinaling pathways including the activation of the mitogen activated protein kinase, c-Jun

N-terminal kinases, and Notch pathways. This disruption of the signaling pathways can lead to chronic increase in the cellular proliferation and malignant transformation (Ludwig et *al.,* 1998, Huang *et al*., 2001 and Ahlborn *et al*., 2008).

Cadmium and Bladder Cancer

Exposure to Cd^{+2} has been associated with several kinds of cancers including: lung, kidney, prostate, and female breast and genitourinary cancers. Several mechanisms are thought be responsible for the carcinogenic effects of Cd^{+2}. One of these mechanisms is its ability to interfere with the DNA damage repair responses including: nucleotide excision repair, base excision repair, and the mismatch repair. The deregulation of these types of repair mechanisms has been known to be associated with different types of cancers (Hartwig, 2010). A second mechanism that is thought to be involved in Cd^{+2} induced carcinogenesis is its ability to generate ROS (Eneman *et al*., 2000). These species are detoxified through the action of GSH or one of its related enzymes. Prolonged Cd^{+2} exposure can overwhelm these antioxidant defense mechanisms and leave the cell unprotected against the toxic effects of Cd^{+2}.

Several studies have implicated Cd^{+2} as a causative agent for bladder cancer. In Belgium, a case-control study was conducted to explore the possibility of a link between Cd^{+2} exposure and the development of bladder cancer (Kellen *et al*., 2007). Belgium is one of the major Cd^{+2} producing countries worldwide, and although Cd^{+2} emissions from Zn^{+2} smelting have been reduced drastically in the last three decades, several regions in this country are still known for heavy Cd^{+2} contamination. The study examined the blood Cd^{+2} levels and found an increased risk to the development of bladder cancer in

subjects with increased blood Cd^{+2} levels. It is noteworthy that while blood Cd^{+2} levels reflect the current exposure levels, urine levels measure the whole body Cd^{+2} burden. In another study in Canada, a correlation was found between the occupational exposure to Cd^{+2} and bladder cancer (Siemiatycki *et al*., 1994). The findings from these studies are further supported by the fact that Cd^{+2} was successfully used to induce malignant transformation of UROtsa cells (Sens *et al*., 2004). This study found that the heterotransplants formed by the subcutaneous injection of Cd^{+2} transformed human urothelial cells, had the characteristic histological features of transitional cell carcinoma of the urinary bladder.

Metallothionein

Metallothioneins are small, cysteine-rich proteins that have a high affinity for binding metal ions. The initial discovery of MT came about in 1957, when Margoshes and Vallee noted the presence of a small protein in an equine renal cortex sample that bound most of the Cd^{+2} and a sizable amount of Zn^{+2} in that sample (Thirumoorthy *et al*., 2007). By 1961, Kagi and Vallee (Kagi *et al.*, 1961) had completed the initial characterization of that protein and named it MT (Namdarghanbari *et al*., 2011). Five decades and extensive research later, it is now an established fact that the mammalian MT cluster originated from a succession of duplication events that resulted in the formation of four major MT genes (MT-1, MT-2, MT-3 & MT-4). During the process of primate evolution to the modern human, MT-1 has undergone additional duplication events leading to the formation of eight functional genes (MT-1A, MT-1B, MT-1E, MT-

1F, MT-1G, MT-1H, MT-1M, and MT-1X) and five pseudogenes (MT-1C, MT-1D, MT-1I, MT-1J, and MT-1L) (Moleirinho *et al*., 2011).

Metallothioneins are widely distributed across the different species, from bacteria and fungi to plant and animal cells. While MT-1 & MT-2 are ubiquitous proteins that are present in almost all mammalian cells (Haq *et al.,* 2003), MT-3 is expressed mainly in the brain particularly in the glutamatergic neuronal tissues, and has a very limited expression in the intestines and pancreas (Ebadi *et al.,* 1995). On the other hand, MT-4 expression is limited to the stratified squamous epithelia of the skin and tongue (Quiafe *et al.,* 1994). The high degree of structural homology between the MTs of different species points to an important function for that protein that resulted in its conservation. Although no single crucial role has been assigned to the MTs, they are known to play several roles in preserving the homeostasis in response to tissue and cellular stressors. Among these roles are heavy metal detoxification, the protection of the body against the different oxidative insults, and the regulation of several essential metals including copper (Cu) and Zn^{+2} (Haq *et al.,* 2003).

Structurally, MTs contain between 61-68 amino acid residues and are composed of two metal-binding domains (alpha and beta). The alpha domain occupies the C-terminal end of the protein and contains 11 cysteines. The beta domain occupies the N-terminal end and contains 9 cysteines. It is through the thiol (-SH) moieties of these cysteine residues that the MTs interact with, and bind the different metal ions (Haq *et al.,* 2003, and Laukens *et al*., 2009).

Metallothionein isoforms 1 & 2 are highly responsive to induction by several metal ions including, Zn^{+2}, Cd^{+2}, mercury, Cu and bismuth. The metal-induction of MTs is highly dependent on the presence of the metal-responsive-element-binding transcription factor 1 (MTF-1). This transcription factor is both Zn^{+2} dependent and Zn^{+2} responsive, and upon Zn^{+2} stimulation it translocates from the cytoplasm to the nucleus where it recognizes and binds to several non-identical metal responsive elements (MREs). The binding of MTF-1 to the DNA controls MT transcription through the recruitment of, and interactions with, elements of the RNA polymerase II transcriptional machinery. MTF-1 is essential for both the basal and heavy metal-induction of MTs (Haq *et al.,* 2003, Smirnova et al., 2000, Westin *et al*., 1988, and Heuchel *et al*., 1994).

The Expression of MT I/II in Bladder Cancer

Immunohistochemical studies performed on transitional cell carcinomas of the bladder revealed that MT I/II was highly over expressed in cancers resistant to the chemotherapeutic agent cis-diamminedichloroplatinum II (cisplatin) and alkylating agents often used in cancer treatment (Bahnson *et al*., 1991). This correlation between the level of MT I/II over-expression and the degree of cisplatin resistance was proposed to be a useful marker for predicting cisplatin resistance in transitional cell carcinomas of the bladder (Kotoh *et al.,* and Bahnson *et al.,* 1994).

The previous findings, along with the complexity of the human MT gene cluster when compared to other species, led to a study by Somji and colleagues (Somji *et al*., 2001). One goal of this study was to determine the expression levels of MT I/II in the normal bladder and bladder cancer and correlate the expression to the stage and grade

of bladder cancer. The results determined the absence of MT I/II expression in normal bladder tissues, and a correlation between the intensity of MT I/II staining and the tumor grade. This study also found positive staining for MT I/II in all high-grade tumor samples. Due to the fact that the antibody used in immunohistochemical staining cannot distinguish between the MT-I & MT-II isoforms (hence the designation MT I/II), mRNA analysis was employed to discern the different MT I/II isoforms expressed. Findings showed that there was a significant increase in the MT-1X mRNA expression in all three grades of bladder cancer (carcinoma in situ, and low and high grade transitional cell carcinomas).

Another study reported the absence of MT I/II immunohistochemical staining in benign lesions and in low-grade bladder cancer, and a high degree of expression in high-grade muscle-invasive bladder cancer. Another finding in this study was the presence of positive stromal staining for MT I/II in heterotransplant tumors formed following the subcutaneous injection of As^{+3} and Cd^{+2} transformed tumor cells in athymic nude mice (Zhou *et al*., 2006).

The Effects of Metal Exposure on Altering the Epigenetic State of the Cell

"Epigenetics" is a term that was invented by C.H.Waddington in the 1940s. It originated from a combination of the words "genetics" and "epigenesis", with the latter signifying the theory of the gradual changes that occur in the embryo until it reaches adulthood as contrasted to being fully preformed in the zygote stage. It was Waddington's intention to establish a new discipline of studying the genetic control of development through a combined study of embryology and genetics (Waddington,

1942). A recent review proposed the following modern definition of epigenetics as: "the inheritance of variation (-genetics) above and beyond (epi-) changes in the DNA sequence" (Bonasio *et al*., 2010). This definition encompasses both the *cis*- and *trans*-epigenetic signals. An example of trans- epigenetic states is transcription factors that maintain an epigenetic state through feedback loops, and that may propagate their own transcription. On the other hand, *cis*- regulatory signals are physically associated with the DNA structure, examples are: the post-translational histone modifications and the covalent DNA modifications, as in the case of DNA methylation.

In order to accommodate the large amount of genetic information that is contained in the DNA within the small confined space offered by the nucleus, the cells use a "packaging" mechanism. This DNA packaging within the nucleus involves the formation of a protein-DNA complex known as "chromatin" that has a basic repeating "nucleosomal" unit (Glatt *et al*., 2011). The major part of the nucleosome is termed the "chromatosome" and this consists of a stretch of approximately 147 base pairs of DNA that are wound around an octamer histone core and are associated with a linker histone protein (Bednar et al., 2011). The octamer histone core consists of a pair of each of the four core histones: H2A, H2B, H3 and H4. The histone bodies have a globular structure with highly dynamic N-terminal tails that protrude from the nucleosomal unit, and a distinguishing feature of these histones is the presence of a large number of modified residues, particularly on their N-terminal tails. At least eight types of post-translational modifications have been identified, and these include: acetylation, methylation,

phosphorylation, ubiquitylaion, sumoylation, and ADP-ribosylation (Kouzarides *et al.*, 2007).

The acetylation of lysine residues on histone tails has been extensively studied. This acetylation is kept in tight balance through the opposing actions of HATs that add acetyl groups to these lysine residues and result in transcriptional activation, and the HDACs that remove these groups leading to transcriptional repression (Lombardi *et al*., 2011). Some transcriptional activators possess intrinsic HAT activity such as the CBP/p300 coactivator complex (Ogryzko *et al.*, 1996). To date, 18 human HDACs have been identified and were subdivided into 4 classes (I-IV) (Gregoretti *et al*., 2004). MS-275 is a pharmacologic agent that selectively inhibits the HDAC1 of the class I HDACs (Hu *et al*., 2003), and has been used in the experimental studies on the MT-1X promoter for this dissertation.

Chronic exposure to metals, due to environmental contamination or occupational exposure, has been linked to the development of many types of cancer and other diseases. Some of the metals that have been implicated as causative agents in organ carcinogenesis include arsenic, Cd^{+2}, nickel, and chromium (Cr) (Gibb *et al*., 2000, and Smith *et al.,* 1992). The exact molecular mechanisms behind the development of metal induced carcinogenesis are not fully understood but several theories have been formulated. Some of the theories include: the disruption of the signaling pathways by metals, the ability of these metals to generate damaging ROS, and their interference with the cellular metabolism (Martinez-Zamudio *et al.*, 2011).

The notoriety of these metals is a result of their indestructible nature, and their tendency to accumulate in the body over long periods of time. Most of these metals, with the exception of Cr**,** are none to weakly mutagenic as documented by several bacterial and mammalian mutagenesis assays. This fact led to the theory that alterations in the epigenetic marks caused by exposure to these metals may play a significant role in metal-induced carcinogenesis (Kerckaert *et al*., 1996). These epigenetic alterations include inhibition of the DNA repair mechanisms and the silencing of tumor suppressor genes (Ali *et al*., 2011, and Kondo *et al*., 2006).

Arsenite and Cd^{+2} as Agents of Epigenetic Change

The post-translational modifications of histone tails, along with DNA methylation are epigenetic marks that are essential in the regulation and propagation of heritable gene expression (Martinez-Zamudio *et al*., 2011). Changes in the DNA methylation states have been known to alter the levels of gene transcription; with hypermethylation leading to a "silencing" effect, and hypomethylation leading to an "activating" one. Several studies have tied both the short and long term As^{+3} exposure to the production of global DNA hyper- and hypomethylation states (Zhong *et al*., 2001, Zhao *et al*., 1997, and Reichard *et al*., 2007). Other studies have concluded that the DNA hypomethylation states are strongly associated with the development of hepatocarcinogenesis in individuals with chronic exposure to inorganic arsenicals (Chen *et al.*, 2004, and Waalkes *et al.,* 2003). Arsenite exposure also leads to gene-specific alterations in the DNA methylation status. One study has shown that cells from bladder cancer tissues obtained from individuals chronically exposed to arsenic were associated with

hypermethylation of the promoters of the tumor suppressor genes: Ras Association Domain Family Protein 1A (RASSF1A) and Serine Protease 3. This hypermethylation led to silencing of these genes, and this silencing showed a correlation with an increase in the size and invasiveness of the bladder tumor (Marsit *et al.*, 2006). Evidence from recent studies suggests that As^{+3} exposure is associated with changes in gene expression due to alterations in histone modifications. One study documented an increase in the level of phosphoacetylation of histone H3 at lysine 9/serine 10 (which is a mark of transcriptional activation) in the promoter of c-fos and c-jun protooncogenes in fibroblast cells exposed to $NaAsO_2$ (Li *et al.*, 2003). Several other histone modifications have been linked to chronic As^{+3} exposure (Zhou *et al*., 2009, and He *et al*., 2003).

Likewise, Cd^{+2} has been associated with altered levels of DNA methylation states, where the DNA hypermethylation of some gene promoters such as the RASSF1A and MT-1 has been observed in cell lines chronically exposed to Cd^{+2}. What is further significant is that the expression of these genes can be restored by treating the cells with DNA methyl transferase inhibitors, which further strengthens the association between the DNA methylation status and gene expression (Benbrahim-Tallaa *et al.,* 2007 and Takiguchi *et al.,* 2003). A recent study examined the promoter of MT-3 in parental, Cd^{+3} and As^{+3} transformed UROtsa cells (Somji *et al*., 2011). The findings from this study establish the fact that the promoter of this gene is epigenetically regulated; in the parental cells it is silenced, and in the transformed cells it is in a "poised" state, where it has both marks of transcriptional activation and transcriptional repression.

Kindlin-2

Kindlin-2 is one of three family members belonging to the Kindlin family of focal adhesion proteins. Although the Kindlins have been only studied for a few years, they have been discovered to play a significant role in integrin activation. The Kindlins (1-3) share significant structural homology, are evolutionarily conserved, and they have the function of an "adaptor protein" that is recruited to the intracellular integrin-containing adhesion sites termed focal adhesions. The Kindlins possess what is known as the FERM (four point one protein, ezrin, radixin, and moesin) domain that has been deemed essential in integrin activation. The FERM domain is bipartite and is interrupted by a Pleckstrin homology domain. Due to the fact that the Kindlin proteins have no catalytic domains in their structure, it is thought that their primary function is protein-protein interactions. Four proteins have been identified as interaction partners of the Kindlins and these are: integrin-linked kinase (ILK), migfilin, and the beta-1 and beta-3 integrins (Larjava *et al*., 2008).

Kindlin-2 is known by several other names in the literature: MIG2, KIND2, mig-2, UNC112, PLEKHC1, UNC112B, FLJ34213, FLJ44462, DKFZp686G11125, and FERMT2. Kindlin-2 deficient mice have been generated and the knockout animals died at or before embryonic age of 7.5 days due to epiblast and endodermal detachment that consequently resulted in peri-implantation lethality. On the other hand, heterozygote mice were viable and did not show any associated abnormalities. Northern analysis showed the Kindlin-2 mRNA to be present in the heart, lung, skeletal muscle, kidney, bladder, and stomach. A review of the literature on Kindlin-2 further confirmed that

this protein has not been localized within the normal human bladder or expressed in urothelial cancer (Ussar *et al*., 2006).

Despite the absence of its expression in urothelial cancers, Kindlin-2 has been characterized in several different types of cancers where its expression was variable. In the aggressive breast cancer cell line TMX2-28, Kindlin-2 mRNA was highly over-expressed and Kindlin-2 siRNA succeeded in reducing the tumor's aggressiveness and invasive capabilities (Gozgit *et al*., 2006). In leimyosarcoma cells of uterine origin, Kindlin-2 levels were considerably lower when compared to the benign leiomyoma uterine tumor cells (Kato *et al*., 2004). It has been theorized that Kindlin-2 may play a significant role in the regulation of the invasiveness of cancers of mesenchymal origin (Shi and Wu, 2008).

The Role of Kindlin-2 in Integrin Activation

In recent years more insight has been gained about the role that Kindlin-2 plays in integrin activation. Integrins are glycosylated heterodimeric type I cell receptors that play an important role in mediating cell-cell and cell-extracellular matrix (ECM) adhesion. Structurally, they are composed of an alpha and a beta subunit. Each of these subunits is further subdivided into a large extracellular domain, a transmembrane domain, and a cytoplasmic tail. In mammals, there are about 18 alpha and 8 beta subunits that inter-associate to give rise to a total of 24 integrin receptors thus discovered so far. These receptors exhibit ligand and tissue specificity, and thus cells that possess a specific type of integrin receptors, can associate with and migrate towards certain regions where their integrin-specific ligand is located (Hynes, 2002).

Data comparison from different types of studies such as nuclear magnetic resonance, fluorescence resonance energy transfer, crystallography and electron microscopy, provided the sequential changes that occur in the structure of integrin in response to its activation. In the resting inactive state, the integrins are in a "low-affinity" binding conformation, where they are in a bent state, and upon activation, the receptors assume an "extended" conformation (Lai-Cheong *et al*., 2010).

In addition to their role as adhesion receptors, integrins can convey information about the chemical and physical status of the extracellular surroundings to the cell's interior, in a phenomenon known as "Outside-in signaling". This communication enables the cell to regulate its growth, survival and migration. The integrins cytoplasmic tails possess no known enzymatic activities, and therefore, this type of communication is dependent on the presence of certain "adaptor" proteins that form a link between integrins and kinases such as the Src protooncogene and focal adhesion kinases. Talins and Kindlins are examples of such adaptor proteins that are involved in integrin activation.

Signaling in the opposite direction is named "inside-out signaling", where intracellular signals are relayed to the outside, and it is through this type of signaling that the cell controls its adhesiveness and migration (Kim *et al*., 2011). Kindlin-2 localizes to the sites of cell-ECM adhesions through the direct binding of its C-terminal end to the beta integrin receptor. Through its N-terminal end, Kindlin-2 interacts with the protein migfilin that associates with other proteins such as filamin, which acts as a "cross-linking" protein through its ability to connect together two actin filament, and to

promote the formation of loose gel-like actin “sheets”. These “sheets” of actin can form projections from the cell surface that are termed “lamellipodia” that help the cell move on solid surfaces (Alberts *et al*., 2008). It has been observed that depletion of Kindlin-2 or migfilin results in the impairment of cell spreading (Tu *et al*., 2003). This observation established a role for Kindlin-2 and migfilin in the control of the actin cytoskeleton and cell-ECM adhesions (Wu, 2005).

Chapter II

STATEMENT OF PURPOSE

Part I: MT-1X

The goal of this study is to investigate the mechanism by which MT-1X is over expressed in bladder cancer. This mechanism is predicted to involve transcriptional and epigenetic processes at the MT-1X promoter. The model system that will be utilized is the UROtsa cell line, transformed by either As^{+3} or Cd^{+2}, and the approach is to assess transcription factor binding as well as histone modifications in the MT-1X promoter of metal-transformed cells in comparison to that of the non-transformed parent. This approach will seek to identify those transcription factors whose binding to the MT-1X promoter correlates to expression differences between the normal and metal-transformed cells. Likewise, histone modifications that correlate to the MT-1X expression differences in these cells will also be implicated in the mechanism by which MT-1X is induced in bladder cancer. Additional insights are expected to be gained by assessing transcription factor binding and histone modifications while perturbing the MT-1X promoter with two unique MT transcriptional inducing agents. One agent class is metals and is particularly important since these metals are the transforming agents. Cadmium and, to a lesser extent, As^{+3} are known MT inducers, working through the MRE which is the binding site for MTF-1, a factor that confers metal induction. Perturbation of the MT-1X promoter will also be done with MS-275. This agent is useful since the MT

genes in general have been shown to be especially sensitive to the effects of histone deacetylase inhibitors (Gius *et al*., 2004). Thus the first experimental strategy is to identify the potential transcription factor binding sites in the proximal promoter of MT-1X, and to design MT-1X-unique primers that would specifically amplify these promoter sequences and the immediate regions flanking them. The initial focus will be on identifying the MREs that are known to exist in all MT genes. This will be achieved through an *in silico* analysis of the of the MT-1X proximal promoter region, and through the utilization of the primer designing software Oligo 7 to design MT-1X - specific primers.

The second experimental strategy is to compare the MT-1X mRNA expression between UROtsa cells exposed to As^{+3} or Cd^{+2} for a short duration (48 h), UROtsa cells subcultured in the continued presence of As^{+3} or Cd^{+2} for 5 passages (P5), and UROtsa cells transformed by As^{+3} or Cd^{+2}. In addition to treatment with As^{+3} or Cd^{+2}, the effect of two MT inducers, MS-275 and Zn^{+2}, will be tested to assess their potential to increase MT-1X expression. This comparison will be achieved through the use of RT-PCR analysis on the RNA extracts obtained from the cells subjected to these treatments.

The third experimental strategy is to assess the difference in the accessibility of MTF-1 to the MT-1X MREs between the parental and As^{+3} and Cd^{+2} transformed UROtsa cells. The effect of treatment of the cells with either MS-275, Zn^{+2}, or with the combined exposure on MTF-1 binding will be evaluated. This assessment will be achieved through the ChIP assay for MTF-1 binding followed by RT-PCR of the immunoprecipitated chromatin.

The fourth experimental strategy is to utilize the ChIP technique to assess transcription factor binding and histone modifications across the non-transformed parent, compared to the Cd^{+2} and As^{+3} transformed cells. Superimposed on these experiments will be the effects of MS-275 exposure on factor binding and histone modifications. The transcription factors to be tested will be chosen based on the results of the *in silico* analysis of the transcription factor binding sites in the MT-1X proximal promoter. The histone modifications that will be tested will be for activating marks (acetyl H4, trimethyl H3K4, H2A.z, and histones H3 & H3.3), and repressive marks (trimethyl H3K27, and trimethyl H3K9). The ChIP assays will be followed by RT-PCR of the immunoprecipitated chromatin.

Part II: Kindlin-2

The goal of this study is to confirm a microarray analysis that suggested that Kindlin-2 might play a role in the development and progression of bladder cancer. In an effort to develop an *in vitro* model system of agent-induced bladder cancer, Sens & colleagues were the first to report the successful malignant transformation of UROtsa cells after long-term exposure to As^{+3} and Cd^{+2} (Sens *et al*., 2004). In total, 6 As^{+3} and 7 Cd^{+2} transformed cell lines have been isolated from the parental cells. All of the transformed cell lines were able to form tumors in nude mice when injected SC, but only a subset of these cells were able to form tumors when injected in the peritoneal cavities of nude mice (Cao *et al*., 2010). The microarray study was done to characterize the individual patterns of gene expression for these cell lines, and the results of this analysis showed that Kindlin-2 was the most consistently repressed gene in the cell lines forming

peritoneal tumors. To confirm these results and to assess whether Kindlin-2 expression correlates to the ability to form tumors in the peritoneum, a common metastatic site in bladder cancer, a combination of RT-PCR, Western, and immunohistochemical analyses will be utilized to characterize Kindlin-2 expression in As^{+3} and Cd^{+2} transformed human cell lines, their tumor transplants in immunocompromised mice, and in archival specimens of normal human bladder and bladder cancer.

CHAPTER III

MATERIALS AND METHODS

Materials

Animals

The Hsd:Athymic Nude-*Foxn1*^{nu} mice were purchased from Harlan Laboratories (Madison, WI), and were housed in accordance with the guidelines established by the University of North Dakota's Institutional Animal Care and Use committee and the National Institutes of Health.

Reagents

TRI reagent and the 1-bromo-3-chloropropane (BCP) phase separation reagent were purchased from Molecular Research Center, Inc. (Cincinnati, OH). Bovine serum albumin (BSA) standards, and Pierce bicinchoninic acid (BCA) protein assay reagents A and B were purchased from Thermo Scientific (Rockford, IL). Dulbecco's modified Eagle's medium (DMEM), Isopropanol, Methanol, $CdCl_2$, and zinc sulphate ($ZnSO_4$) were purchased from Sigma Aldrich (St.Louis, MO). Chromatin immunoprecipitation (ChIP) validated antibodies against histone H3 trimethyl Lysine 9 (H3K9), histone H3 trimethyl Lysine 4 (H3K4), histone H3 trimethyl Lysine 27 (H3K27), and H2A histone family, member Z (H2A.z), and the CHIP-IT Express Enzymatic kit were purchased from Active Motif (Carlsbad, CA). QIAquick PCR purification kit and the primers for Kindlin-2 were purchased from Qiagen (Valencia, CA). Tris-HCl (0.5 M), Tris-HCl (1.5 M), 10X

Tris/Glycine/SDS buffer, Ammonium persulfate, Acrylamide/Bis (30%), Beta-mercaptoethanol, TEMED, Tween 20 (10%), 2-mercaptoethanol, Laemmli sample buffer, iScript cDNA synthesis kit, and the SYBR Green Kit were purchased from Bio-Rad (Hercules, CA). Hybond-P polyvinylidine difluoride membrane was purchased from Amersham Biosciences (Piscataway, NJ). The custom-designed primers for ChIP analysis were purchased from Invitrogen (Frederick, MD). Bovine fetal calf serum and Trypsin-EDTA (1X 0.05% Trypsin, 0.53 mM EDTA **.** 4 Na) were purchased from Gibco (Grand Island, NY). Agarose for the separation of GeneAmp PCR products, and Agarose low melting genetic analysis grade were purchased from Fisher scientific (Fair Lawn, NJ). Target Retrieval Solution, and DakoCytomation liquid DAB substrate chromogen system were purchased from Dako (Carpenteria, CA). The ChIP validated antibodies against the ETS domain-containing protein Elk-1 (ELK1), the upstream binding protein 1 (LBP-1), the CCAAT-binding transcription factor (NF-I), the E1A binding protein p300 (p300), MTF-1, the Sp1 transcription factor (SP1), the T cell-specific transcription factor 1 (TCF-1), the upstream transcription factor 1 (USF1), and the Yin and Yang 1 protein (YY1) were purchased from Santa Cruz Biotechnology Inc. (Santa Cruz, CA). The ChIP validated antibody against histone H4 acetyl was purchased from Millipore (Billerica, MA). The ChIP validated antibody against the H3 histone, family 3A (H3.3), and the antibody against beta-Actin were purchased from Abcam (Cambridge, MA). Kindlin-2 primary antibody was purchased from Proteintech (Chicago, IL). The $NaAsO_2$

was purchased from Fluka, (Hannover, Germany). The MS-275 was purchased from ALEXIS Biochemicals (Lausen, Switzerland). Phototope-HRP western blot detection system was purchased from Cell Signaling (Boston, MA). GeneChip human Genome U133 plus 2.0 arrays was purchased from Affymetrix (Santa Clara, CA). GraphPad PRISM 5.0 software was purchased from GraphPad (San Diego, CA).

Equipment

Centrifuges

The Eppendorf 5810R centrifuge (Hamburg, Germany) was used for harvesting the cells used in the cell culture experiments. The Eppendorf 5415R centrifuge (Hamburg, Germany) was used for RNA isolation purposes, and for the purification of the eluted ChIP DNA following the QIAquick PCR purification kit manufacturer's guidelines.

Spectroscopy

The NanoDrop 1000 spectrophotometer used for RNA quantitation was purchased from Thermo Scientific (Willmington, DE). The BioTek ELx800 absorbance microplate reader was used for protein quantitation using the BCA protein assay, and was purchased from BioTek (Winooski, VT).

Electrophoresis

Sodium dodecyl sulphate (SDS) polyacramide gel electrophoresis (PAGE) was performed using the Mini-Protean II electrophoresis device purchased from Bio-Rad (Hercules, CA). Agarose gel electrophoresis for the separation of the PCR products of ChIP DNA, and for confirming the ribosomal band integrity of the purified RNA were

done using the OWL horizontal minigel system purchased from Thermo Scientific (Rockford, IL).

Polymerase Chain Reaction (PCR)

Real-time reverse transcription PCR (RT-PCR) was performed using the Bio-Rad iCycler iQ Real Time PCR Detection System 584 BR 01989s purchased from Bio-Rad (Hercules, CA). The cDNA synthesis was performed using the Gene AMP PCR system 9700 purchased from Applied Biosystems (Carlsbad, CA).

Immunohistochemistry

A Dako Autostainer Universal Staining System used for Immunohistochemical staining of fixed tissue sections, and a DakoCytomation peroxidase-conjugated EnVision Dual Link System used for Kindlin-2 primary antibody localization, were both purchased from Dako (Carpenteria, CA).

Cell Culture

The UROtsa parent and transformed cell lines were handled in a sterile Sterilgard III Advance hood purchased from the Baker company (Sanford, ME), and maintained in an Incusafe MCO-17AIC water-jacketed CO_2 incubator purchased from Sanyo (Japan). The cells were visualized using the PhotoZoom inverted microscope purchased from Bausch & Lomb (Rochester, NY).

Methods

Cell Culture

Stock cultures of the UROtsa cell line were maintained in 75-cm^2 tissue culture flasks in DMEM containing 5% v/v fetal calf serum, and the cultures were incubated at

37°C in a 5% CO_2: 95% air atmosphere. Confluent flasks were subcultured at a 1:4 ratio using trypsin-EDTA, and the cells were fed fresh growth medium every 3 days.

Short-term Exposure of UROtsa Cells to As^{+3} and Cd^{+2} (48 h)

UROtsa cells (10^6) were seeded at a 1:4 ratio and were treated with 1 μM $CdCl_2$ or 1 μM $NaAsO_2$ on the following day. The cells were allowed to grow in the presence of the metals for 48 hrs, following which they were treated with 10 μM MS-275 for another 24 hours. The following day the cells were exposed to 100 μM $ZnSO_4$ for 4 hours. The cells were then harvested for RNA isolation and ChIP analysis.

Multiple Subculturing of UROtsa Cells in the Continued Presence of As^{+3} and Cd^{+2} (P5)

UROtsa cells (10^6) were seeded at a 1:4 ratio and were treated with 1 μM $CdCl_2$ or 1 μM $NaAsO_2$ on the following day. The cells were allowed to reach confluency, following which they were sub-cultured for 5 passages in media containing 1 μM $CdCl_2$ or 1 μM $NaAsO_2$. After the 5^{th} passage, the cells were exposed to 10 μM MS-275 for 24 hours. The following day the cells were exposed to 100 μM $ZnSO_4$ for 4 hours. The cells were then harvested for RNA isolation and ChIP analysis.

Arsenite and Cd^{+2} Induced Transformation of UROtsa Cells

For As^{+3} and Cd^{+2} transformation, the cells were subcultured and maintained continuously in media containing 1 μM $CdCl_2$ or 1 μM $NaAsO_2$. The strategy was to hold the cultures at confluency with continued feeding until cell death ensued, then allowing the surviving cells in the culture to proliferate to confluency. Serial passaging of the cells was done in the continued presence of As^{+3} and Cd^{+2} until the cells were able to produce colonies in soft agar. In total, 6 As^{+3} and 7 Cd^{+2} transformed cell lines have

been isolated from the parental cells. The As^{+3} and Cd^{+2} transformed cell lines were serially passaged 10 times in As^{+3} and Cd^{+2} free growth media before use in any experimental protocols.

Subcutaneous and Intra-Peritoneal (IP) Tumors' Production

To test for malignant transformation, the respective cultures that showed colony formation in soft agar, along with the UROtsa parent cell line, were each inoculated in the SC tissues at a dose of 1×10^6 cells in 200 µl of phosphate-buffered saline (PBS) in the dorsal thoracic midline of 5 nude (*Foxn1*^{nu}) mice. Tumor formation and growth were assessed weekly. All mice were sacrificed by 10 weeks after injection or when the clinical conditions dictated euthanasia.

To determine the ability of the transformed isolates to colonize internal organs of the peritoneum, As^{+3} and Cd^{+2} transformed isolates were each injected in the peritoneal cavity of 6 nude (*Foxn1*^{nu}) mice. The IP injection was performed according to the online protocol of the American Association of Laboratory Animal Science learning library. A one inch 23 gauge needle was inserted in the abdominal cavity in the lower right quadrant and each mouse received 1×10^6 cells in 200 µl of PBS. All the mice were euthanized at 53 days after injection when the tumors in some groups became large and observable by visual examination of the abdomen. Necropsy was performed on each mouse according to the online dissection guide published by the National Institutes of Health.

Immunohistochemical Staining for Kindlin-2 in Tumor Hetertransplants and Archival Specimens of Human Bladder Cancer

Archival bladder specimens were routinely fixed in 10% neutral buffered formalin for 16–18 h. All tissues were transferred to 70% ethanol and dehydrated in 100% ethanol. Dehydrated tissues were cleared in xylene, infiltrated, and embedded in paraffin. Serial sections were cut at 3–5 μm for use in immunohistochemical protocols. Prior to immunostaining, the sections were immersed in preheated Target Retrieval Solution and heated in a steamer for 20 minutes (min). The sections were allowed to cool to room temperature and immersed into Tris-buffered saline (TBS) with Tween 20 (TBS/T) for 5 min. The immunostaining was performed on a Dako Autostainer Universal Staining System. Kindlin-2 was localized using the DakoCytomation peroxidase-conjugated EnVision Dual Link System. Liquid diaminobenzidine (DAB) was used for visualization (DakoCytomation liquid DAB substrate chromogen system). Slides were rinsed in distilled water, dehydrated in graded ethanol, cleared in xylene, and cover-slipped. Tumor tissues of nude mice heterotransplants from the As^{+3} and Cd^{+2} transformed UROtsa cell lines were used to determine the localization and expression of Kindlin-2. Tissue sections for the immunohistochemical analysis of Kindlin-2 expression in human bladder were obtained from archival paraffin blocks that originated from previously completed patient diagnostic procedures. These archival specimens contained no patient identifiers and their use was approved by the University of North Dakota Internal Review Board.

RNA Isolation for Kindlin-2 mRNA Expression

Total RNA from cultures of each UROtsa parental and transformed cell lines was isolated using the TRI reagent following the manufacturer's protocol. Growth media were removed from the culture flasks and 2 mL of TRI reagent was added per 25 cm^2 tissue culture flasks and the homogenate was incubated at room temperature for five min. The cell lysate was passed several times through a plastic pipette to ensure the complete shearing of DNA, and then the lysate was transferred to sterile 1.5 mL microcentrifuge tubes. 0.1 mL of BCP was added per 1 mL of TRI reagent and the samples were vigorously mixed by vortexing for 30 seconds (s), and then incubated at room temperature for 15 min. This was followed by centrifugation at 12,000 g for 15 min at 4 °C. The aqueous phase was transferred to a clean tube and 0.5 mL Isopropanol was added per 1 mL TRI reagent and mixed gently. This was followed by centrifugation at 12,000 g for 8 min at 4 °C. The precipitated RNA pellet was washed with 0.75 mL of 75% ethanol and centrifuged at 7,500 g for 15 min at 4 °C. The pellet was then left to air-dry for 5-10 min and then resuspended in 25 µl of RNAse-free water. The samples were quantified and stored at -80 °C. The samples were analyzed using the NanoDrop spectrophotometer, and the absorbance was measured at 260 (A_{260}) nm. The ratio of A_{260}/A_{280}, which should be close to 2.0, was used to check the purity of RNA samples. The RNA was checked for the integrity of its ribosomal bands using 1% agarose gel electrophoesis.

RNA Isolation for MT-1X mRNA Expression

The UROtsa parent and the As^{+3} and Cd^{+2} transformed cells (10^6) were seeded at a 1:10 ratio. After 24 h, the cells were treated with 10 µM of MS-275. The cells were allowed to grow to confluency (24 h). Following this, the cells received either no further treatment or were treated with 100 µM $ZnSO_4$ for 4 h. The cells were then harvested and the total RNA from cultures of the As^{+3} and Cd^{+2} transformed cells, as well as total RNA from cells harvested from 48h and P5 experiments, were isolated using the TRI reagent and following the manufacture's protocol, as discussed previously.

Real-Time RT-PCR Analysis

MT-1X

The measurement of MT-1X mRNA was assessed utilizing MT-1X isoform-specific primers with the sense primer being: TCTCCITGCCTCGAAATGGAC and antisense: GGGCACACITGGCACAGC. Total RNA isolated from confluent cultures from each of the UROtsa parental and transformed cell lines was used. A total of 1 µg of RNA was subjected to cDNA synthesis using the iScript cDNA synthesis kit in a total volume of 20 µl. For the MT-1X mRNA analysis, Real-time RT-PCR analysis was done using 2 µl of cDNA, and 0.2 µl of MT-1X primer using the SYBR Green Kit in a total volume of 20 µl in an iQ iCycler Real-Time detection system. The amplification of MT-1X was monitored by SYBR Green fluorescence, with the cycling parameters of annealing at 68 °C for 30 s, extension at 72 °C for 30 s, and denaturation at 95 °C for 15 s. The level of MT-1X mRNA was determined relative to MT-1X serial dilutions as the standard curve.

Kindlin-2

Real-time RT-PCR analysis was used to measure the expression levels of Kindlin-2 mRNA. The measurement of Kindlin-2 mRNA was assessed using a commercially available Kindlin-2 primer. Total RNA isolated from confluent cultures from each of the UROtsa parental and transformed cell lines was used. A total of 1 µg of RNA was subjected to cDNA synthesis using the iScript cDNA synthesis kit in a total volume of 20 µl. For Kindlin-2 mRNA analysis, Real-time RT-PCR analysis was done using 2 µl of cDNA, and 0.2 µl of the commercial primer using the SYBR Green Kit in a total volume of 20 µl in an iQ iCycler Real-Time detection system. The amplification of Kindlin-2 was monitored by SYBR Green fluorescence, with the cycling parameters of annealing at 55 °C for 30 s, extension at 72 °C for 30 s, and denaturation at 95 °C for 15 s. The level of Kindlin-2 mRNA was determined relative to the UROtsa cells grown in serum-containing medium using serial dilutions of this sample as the standard curve. The resulting relative levels were then normalized to the fold change in beta-Actin expression assessed by the same assay using the primers being sense: CGACAACGGCTCCGGCATGT and antisense: TGCCGTGCTCGATGGGGTACT, and with the cycling parameters of annealing/extension at 62 °C for 45 s and denaturation at 95 °C for 15 s.

Microarray Analysis

For each of the transformed cell lines, aliquots of the 3 parallel samples of RNA were mixed in equal amounts (1:1:1) before submission for array analysis and they represented 1 sample for array hybridization. Global gene expression analysis was

performed by Genome Explorations (Memphis, TN) using the GeneChip human Genome U133 plus 2.0 arrays. For analysis, each probe set was filtered for MAS5 Detection on each array using *P* values <0.05. Induced and repressed genes were identified that were expressed differentially between the cell lines based on their ability to form peritoneal tumors by using a *t* test with *P* values <0.05 and an absolute fold change of at least 2. The microarray study has been deposited in the National Institutes of Health's GEO database.

Protein Extraction and Quantitation

Confluent cell cultures were harvested in 2% SDS and 50 mM Tris-HCL, pH 6.8. The lysate was then passed through a 23-gauge needle for several times to ensure the complete shearing of the DNA. The BCA protein assay was used to determine the protein concentration of the samples. Briefly, BSA standards were prepared with final concentrations of 0, 1, 2, 4, 6, 8, 12, 16, 18, and 20 µg /10 µl. The working reagent was made with 1 part copper sulfate (BCA reagent B) and 50 parts of BCA solution (BCA reagent A). The standards were added in duplicates (10 µl of standard solution mixed with 10 µl of water). The samples were added in triplicates (5 µl of the sample protein mixed with 10 µl of water). To each well, 200 µl of working reagent was added and the samples were incubated at 37 °C for 30 min. The samples were analyzed using the BioTek ELx800 absorbance microplate reader using an absorbance of 562 nm. The concentrations of the protein samples were calculated by the regression of standard optical densities using the GraphPad PRISM 5.0 software.

Western Blot Analysis

The expression of Kindlin-2 protein was determined by Western blotting using 20 µg of total cellular protein on a 12.5% SDS-PAGE gel and transferred to a Hybond-P polyvinylidine difluoride membrane. The membranes were blocked in TBS/T and 5% (w/v) nonfat dry milk for 1 h at room temperature. After blocking, the membranes were probed with a 1:1500 dilution of the Kindlin-2 primary antibody in blocking buffer for 1 h at room temperature. After washing 3 times in TBS/T, the membranes were incubated with the anti-rabbit secondary antibody (1:2000) in antibody dilution buffer for 1 h. The blots were visualized using the Phototope-HRP Western blot detection. To determine equal loading of samples, membranes were stripped of bound proteins by incubating in 100 mM 2-mercaptoethanol, 2% SDS, 62.5 mM Tris–HCl, pH 6.7 at 50 °C for 30 min. The membranes were washed twice with TBS/T at room temperature and blocked following the previously mentioned protocol. The membranes were reprobed using 0.2 µg/ml of the anti beta-Actin antibody followed by incubation with a 1:10,000 dilution of the anti-mouse secondary antibody.

ChIP Assays

ChIP assays were carried out using the ChIP-IT™ Express kit. The protocols and reagents were supplied by the manufacturer. The UROtsa parent and the transformed cell lines were seeded at 10^6 cells/75 cm^2 flask and 24 h later treated with 10 µM MS-275. Following incubation for 48 h, the cells were fixed with 1% formaldehyde for 10 min. Cross-linking was stopped by the addition of glycine stop solution (0.125 M). The cells were scraped in 2 ml of PBS containing 0.5 mM phenylmethylsulfonylfluoride (PMSF). The cells were pelleted and re-

suspended in ice-cold lysis buffer and homogenized in an ice-cold dounce homogenizer. The released nuclei were pelleted and re-suspended in a digestion buffer supplemented with PMSF and protease inhibitor cocktail. The chromatin was sheared using the enzymatic shearing cocktail at 37°C for 5 min for the UROtsa parental cells, and 7.5 min for the transformed cell lines, to an average length of 200-1500 base pairs (bp). Approximately 7 µg of sheared chromatin was used to coat the protein G-coated magnetic beads along with a total of 3 µg of the antibody. The following 15 antibodies were used in the immunoprecipitations: ELK1, LBP-1, NF-I, p300, MTF-1, SP1, TCF-1, USF1, YY1, trimethyl H3K9, trimethyl H3K4, trimethyl H3K27, H2A.z, acetyl H4, and H3.3. The coating was performed overnight at 4°C following which the beads were washed and the immune complexes eluted using the elution buffer. The cross linking was reversed using the reverse cross-linking buffer.

ChIP DNA Purification

Following the recommendation of the CHIP-IT Express chromatin immunoprecipitation kit, the eluted DNA was purified using the QIAquick PCR purification kit. The protocols and reagents were supplied by the manufacturer. To bind the DNA, 150 µl of PB buffer was added to the 30 µl of the eluted DNA and mixed thoroughly, and the mix was added to the supplied spin column and centrifuged for 30-60 s. To wash, the flow through was discarded and 750 ml of buffer PE was added to the column and centrifuged for 30-60 s. The flow through was discarded and the column was re-centrifuged for an additional 30-60 s. To elute the DNA, the spin column was placed in a new 1.5 ml microcentrifuge tube, and 30 µl of elution buffer EB was added to the center of the column's membrane and allowed to stand for 1 min. The column was centrifuged for 30-60 s and the eluted DNA was stored at -20 °C.

Real-Time RT-PCR Analysis of the MT-1X Proximal Promoter Region

RT-PCR analysis was used to assess transcription factors binding and histone modifications, using the custom-designed primers covering the MREs in the proximal promoter region of MT-1X. The primers were designated MRE-a, MRE-d, & MRE-e. For the MRE-a-specific primer pair, the sequence for the sense primer being: TCTGCGCCCGGCCCTCTTC and for the antisense being: CGGCGGCTCTCTTTATAGTCC, with annealing temperatures of 66 & 60 °C. For the MRE-d-specific primer pair, the sequence for the sense primer being: CCACGTACTGCCAGGTTCTCA and for the antisense primer being: GTGCAGCAACCCGTGAGCC, with annealing temperatures of 68 & 65 °C.

For the MRE-e-specific primer pair, the sequence for the sense primer being: ATGCAGGAAATCCGAGTGTCA and for the antisense primer being:

TTTGCATTTCCCAGAGTCCCT, with annealing temperatures of 60 °C. MREs-a, d, and e each had a PCR product size of 42, 86, and 115 base pairs (bp), respectively. The ChIP DNA was assessed for histone modifications and transcription factors binding. RT-PCR analysis was done using 2 µl of genomic DNA, and 0.4 µl of the custom primers using the SYBR Green Kit in a total volume of 20 µl in an iQ iCycler Real-Time detection system. For quantitative PCR analysis, the quantity of the PCR template found in each specific precipitate was normalized to the amount of the corresponding DNA sequence found in the fragmented chromatin solution present before antibody-based precipitation (normalized to the value of DNA input). This was done using the following calculations: The value for the sample PCR starting quantity was divided by the value of the input PCR starting quantity. The result was multiplied by 0.1/3 x100 and expressed as % of input,

where the (0.1) represents the concentration of the input used relative to the concentration of the genomic DNA (3) used in the ChIP assay.

Statistical Analysis

Statistical analysis consisted of analysis of variance (ANOVA) with Tukey post-hoc testing performed with GraphPad PRISM 5.0 software. Real time data is plotted as the mean +/- SEM of triplicate determinations. All statistical significance is denoted at $P < 0.05$.

Prediction of MT-1X Transcription Start Site (TSS)

Determining TSS for MT-1X was done using the University of California at Santa Cruz (UCSC) Genome Bioinformatics web-site, which is an online resource containing annotated genome sequence data from various organisms, (http://genome.ucsc.edu/). In the UCSC Genome Browser home page, the button leading to the Gene Sorter page was selected. Once in that page, the genome of interest (Human) was selected along with the latest gene assembly [Feb.2009 (GRCh37/hg19)]. The gene symbol for MT-1X was entered in the Search box. A page that has a list of genes followed and the MT-1X gene was selected from that list. The next screen displayed the genome region of the MT-1X gene. The direction of the arrows indicates the orientation of the gene and it is essential that the sequence of the promoter region be downloaded in the correct orientation. MT-1X was found to be a forward-oriented gene. The numbers in the position/ search field mark the beginning and end of transcription and were used to isolate the transcription start site, as detailed in the website's help page.

Prediction of Transcription Factors Binding Sites

The transcription factors potential binding sites were mapped out using The Transcription Element Search System (TESS), which is a website that predicts transcription factors binding sites in a DNA sequence (http://www.cbil.upenn.edu/cgi-bin/tess/tess). Briefly, after identification of the TSS, MT-1X gene sequence was downloaded to cover 100 bp downstream to 1000 bp upstream of the TSS. This sequence was pasted in the specified box. Search parameters can be adjusted using the "Full Search" mode, which was used to limit the search to the human species. To increase the likelihood of the accuracy of the prediction, only the highest scoring transcription factors predicted binding sites were picked for further analysis. Among the binding sites predicted, five MREs were predicted and were assigned the letters a-e according to their proximity from the TSS, with "a" being the closest and "e" the farthest from the TSS. These MREs are DNA sequences were MTF-1 is predicted to bind, and were found to be essential for the induction of the MT gene transcription (Haq et al., 2003).

CHAPTER IV

RESULTS

Part I: MT-1X

Predicted Transcription Factors Binding Sites in the MT-1X Proximal Promoter Region

Results of the *in Silico* analysis of the MT-1X proximal promoter region revealed that that the binding site for the transcription factor IID (TFIID) is at 29 bp upstream of the TSS. Five MREs were detected that have the consensus sequence of TGCRCNC (R = A or G, N = any nucleotide) shared by all MREs (Gunther *et al*., 2012). These MREs were labeled a-e based on their proximity to the TSS; MRE-a being the closest and MRE-e being the farthest from the TSS (Figures 1 A and B). Five custom primer pairs were designed to cover the area surrounding each of the MREs. A bacterial artificial chromosome containing the MT gene cluster was used to test the specificity of the designed primers, and to optimize the PCR cycling conditions. Of the five designed primer sets tested, only three (primers a, d, & e) were deemed specific to MT-1X, and their cycling conditions were favorably optimized to allow for an efficiency of amplification close to 100% (Figure 2). These three sets of primers were selected to characterize the histone modifications and transcription factor binding in the region they amplify. The primer set covering the MRE-a region amplifies the area of the promoter from -30 to -50 bp upstream of the TSS, and has a PCR product size of 42 bp.

The primer set covering the MRE-d region amplifies the area of the promoter from -135 to -199 bp upstream of the TSS, and has a PCR product size of 86 bp. The primer set covering the MRE-e region amplifies the area of the promoter from -348 to -448 bp upstream of the TSS, and has a PCR product size of 115 bp.

Several transcription factors binding sites were predicted along the proximal promoter region; of special interest were the transcription factors predicted to bind the promoter regions surrounding three MREs that were selected for further analysis (Tables 1 A-C)

A

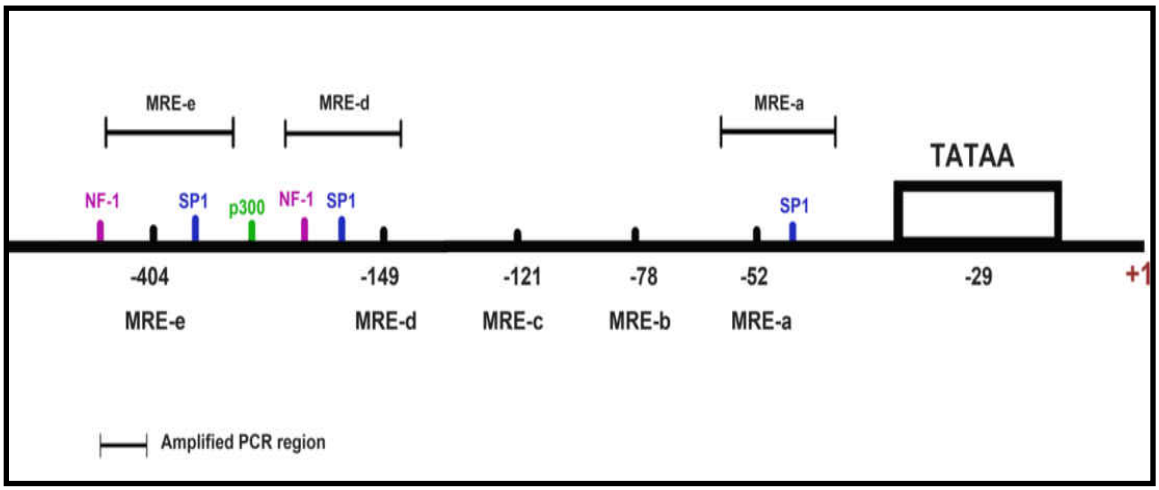

B

MRE-a: TGCGCCC **MRE-b**: GGGTGCA **MRE-c**: TGCACCC **MRE-d**: TGCGCCC **MRE-e**: TGCACAC

Figure 1. Predicted binding site for TFIID, MREs, and some selected transcription factor binding sites (A). The five MREs predicted by TESS to occupy the proximal MT-1X promoter region and their DNA sequences (B).

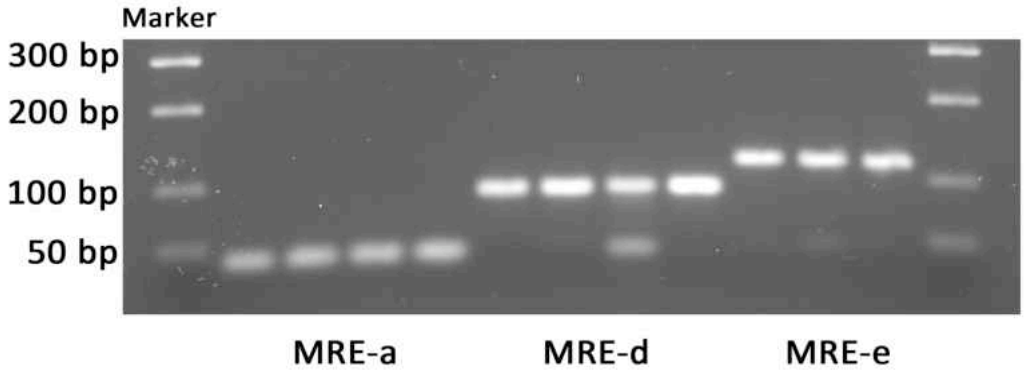

Figure 2. Agarose gel electrophoresis of PCR products for MREs a, d, and e. A bacterial artificial chromosome (BAC) clone containing the MT gene cluster was used as the DNA template in the PCR reaction to test the specificity of the designed primers, and to optimize the PCR cycling conditions.

Table 1: Transcription factor binding sites in the MRE-a (A), MRE-d (B), and MRE-e (C) regions as predicted by the TESS software.

A

MRE-a (-30 to -50 from TSS)
1- SP1
2- GR
3- GCF
4- ETF
5- ESR1
6- MTF-1

B

MRE-d (-135 to -199 from TSS)
1- USF1
2- LBP-1
3- SP1
4- NF-I
5- AP-2
6- GCF
7- TCF-1
8- YY1
9- MTF-1

C

MRE-e (-348 to -448 from TSS)
1- HIST2H4A
2- CEBPA
3- ELK1
4- ETV4
5- NFATC1
6- NFATC3
7- TGIF
8- AP-1
9- c-Ets-1
10- YY1
11- MTF-1
12- E2F1
13- MYB
14- ESR1
15- SP1
16- LBP-1
17- PAX2/PAX5/PAX8

MT-1X mRNA Expression

Cadmium and, to a lesser extent, As^{+3} are known MT inducers, working through the MREs which are the binding sites for MTF-1. The experiments for the MT-1X mRNA expression were designed so as to create a comparison between the effects of different lengths of exposure to As^{+3} and Cd^{+2} on the MT-1X expression. The comparative analysis was between UROtsa cells exposed to As^{+3} or Cd^{+2} for a short duration (48 h), UROtsa cells subcultured in the continued presence of As^{+3} or Cd^{+2} for 5 passages (P5), and UROtsa cells transformed by As^{+3} or Cd^{+2}. In addition to treatment with As^{+3} or Cd^{+2}, the effect of two MT inducers, MS-275 and Zn^{+2}, were also tested to assess their potential to increase MT-1X expression. Exposure of the cells to high levels of Zn^{+2} (100 µM) for 4 h is a protocol classically used to assess MT induction and the binding of MTF-1 to the MRE.

MT-1X mRNA Expression in UROtsa Cells Exposed to Short-term Treatments with As^{+3} & Cd^{+2} (48 h)

The results of this experiment demonstrated that the 48 h exposure of the UROtsa cells to As^{+3} & Cd^{+2} resulted in a significant increase in expression in the Cd^{+2} exposed cells when compared to the non-exposed parent cells and the As^{+3} exposed cells (Figure 3). Treatment with MS-275 resulted in an increased expression in all three groups, however the Cd^{+2} exposed cells had the highest expression level compared to the untreated cells and the As^{+3} exposed cells. Furthermore, treatment of the cells with

Zn^{+2} only, or Zn^{+2} plus As^{+3} and Cd^{+2} exposure resulted in a significant increase in MT-1X expression in all three groups. Treatment of the cells with Zn^{+2} and MS-275 resulted in a significant increase all the three groups when compared to the non-treated cells.

MT-1X mRNA Expression in UROtsa Cells Sub-cultured in the Continuous Presence of As^{+3} & Cd^{+2} for Five Passages (P5)

The results of this experiment demonstrated that the continuous exposure of the UROtsa cells to As^{+3} or Cd^{+2} up to 5 passages resulted in a significant increase in expression in the Cd^{+2} exposed cells when compared to the non-exposed and the As^{+3} exposed cells (Figure 4), a finding that is similar what was seen with a 48 h As^{+3} or Cd^{+2} exposure. Treatment with MS-275 resulted in an increased expression in the non-metal exposed UROtsa cells as well as the As^{+3} or Cd^{+2} exposed cells. The increase in the Cd^{+2} exposed cells was much higher compared to the non-metal exposed cells and the As^{+3} exposed cells. Treatment with Zn^{+2} resulted in a significant increase in MT-1X expression in the cells that were not exposed to either As^{+3} or Cd^{+2} as well as in the cells exposed to As^{+3}. The Cd^{+2} exposed cells did not show a significant increase in MT-1X expression when compared to the Cd^{+2} exposed cells that were not treated with Zn^{+2}. Treatment with both Zn^{+2} and MS-275 resulted in a significant increase in MT-1X expression in the cells that were not exposed to either As^{+3} or Cd^{+2} and in the cells exposed to these heavy metals.

MT-1X mRNA Expression in Parental, As^{+3} & Cd^{+2} Transformed UROtsa Cells

The results of this experiment demonstrated that the As^{+3} & Cd^{+2} transformation of the UROtsa cells resulted in an increase in the mRNA expression levels in the As^{+3} transformed cells when compared to the parental and the Cd^{+2} transformed cells (Figure

5). Treatment with MS-275 resulted in a significant increase in the expression of MT-1X in the parental and the Cd^{+2} transformed cell lines when compared to the cells receiving no treatment, while the As^{+3} transformed cells did not show a significant increase in the expression levels of MT-1X. Treatment of the cells with Zn^{+2} resulted in a significant increase in the MT-1X mRNA expression levels in the parental and the As^{+3} transformed cells when compared to the non-treated cells. The combined Zn^{+2} and MS-275 treatments resulted in a significant increase in all the three cell lines when compared to the non-treated cells.

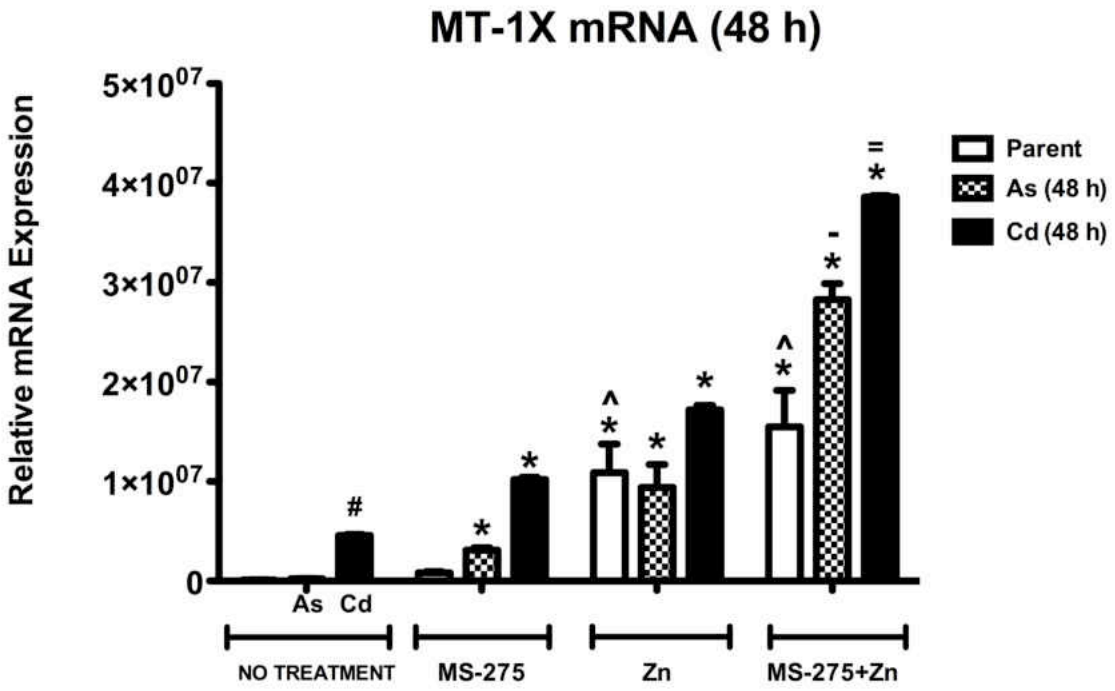

Figure 3. The effect of treatment with MS-275 +/- Zn^{+2} in the 48 h As^{+3} and Cd^{+2} exposed UROtsa cell lines. Statistically significant ($p < 0.05$) when compared to their corresponding cells receiving no treatment (*), to the non-metal exposed UROtsa and the As^{+3} exposed cells in the no treatment group (#), to parent MS-275 (^), to Cd^{+2} in the Zn^{+2} treated group and Cd^{+2} MS-275 (=), and when compared to As^{+3} cells in the Zn^{+} And in the MS-275+ Zn^{+} treated groups (-).

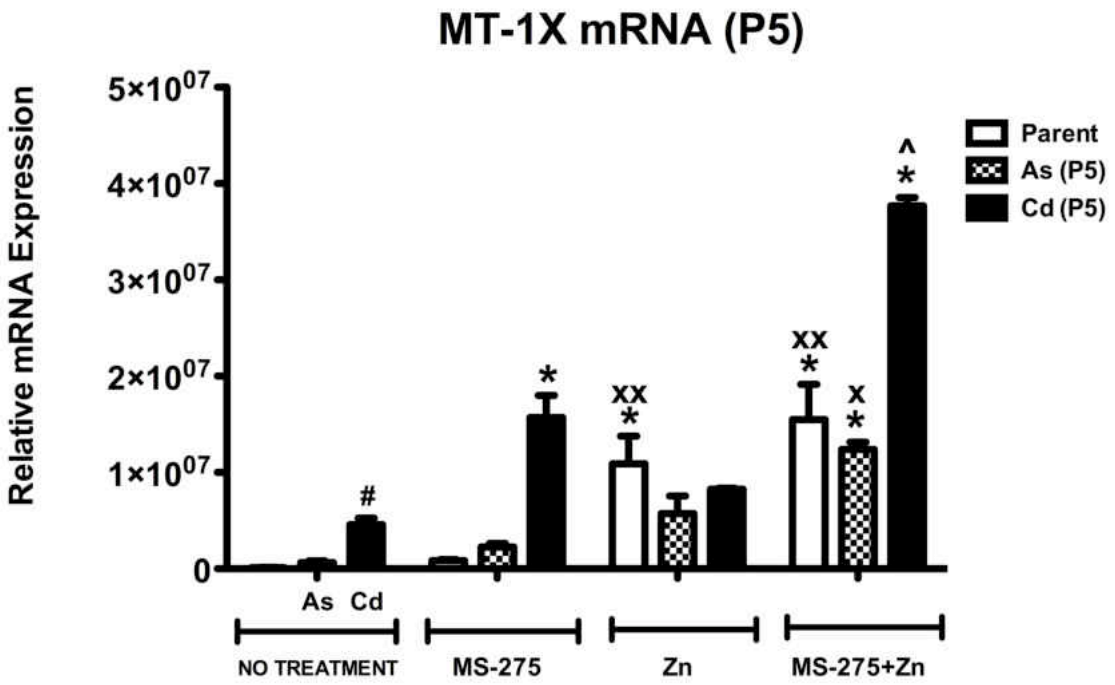

Figure 4. The effect of treatment with MS-275 +/- Zn^{+2} in the P5 UROtsa cells sub-cultured in the continued presence of As^{+3} and Cd^{+2}. Statistically significant ($p < 0.05$) when compared to their corresponding cells receiving no treatment (*), to the As^{+3} in the Zn^{+} treated group (x), to the parent MS-275 (xx), to the to Cd^{+2} in the Zn^{+2} treated group and Cd^{+2} MS-275 (^), and when compared to the non-metal exposed UROtsa and the As^{+3} exposed cells in the no treatment group (#).

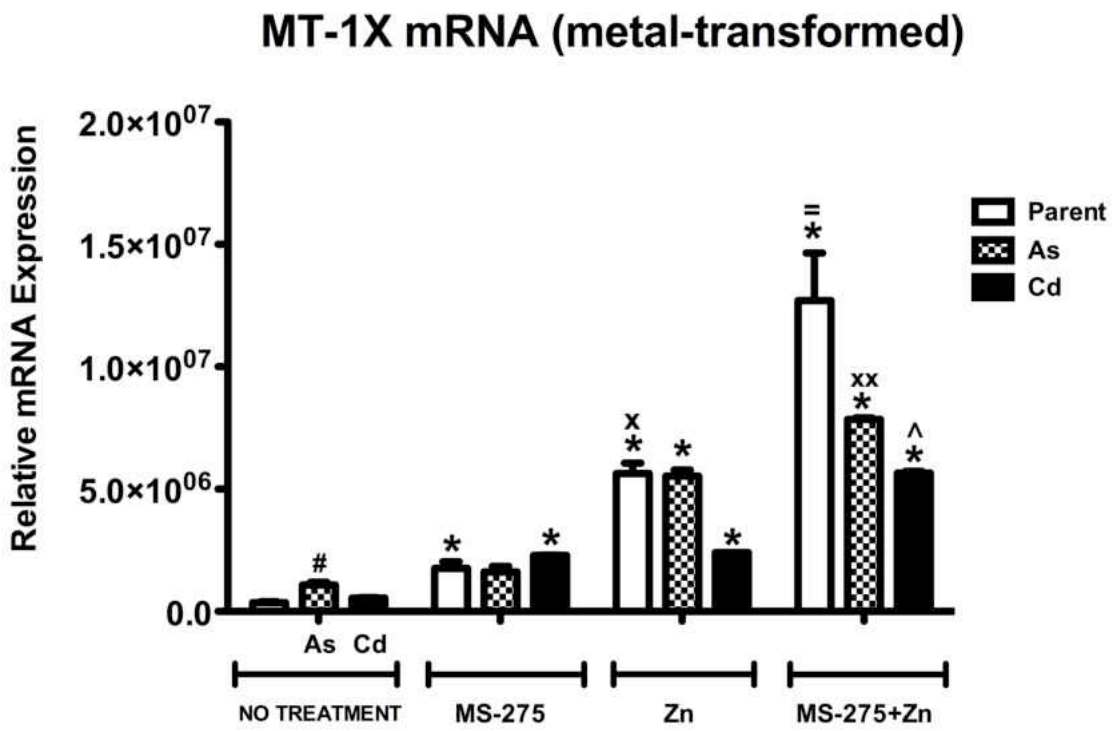

Figure 5. The effect of treatment with MS-275 +/- Zn^{+2} in the parent, As^{+3} and Cd^{+2} transformed UROtsa cells. Statistically significant ($p < 0.05$) when compared to their corresponding cells receiving no treatment (*), to parent MS-275 (x), to the to parent in the Zn^{+2} treated group and parent MS-275 (=), to the Cd^{+2} in the Zn^{+2} treated group and Cd^{+2} MS-275 (^), to the As^{+3} MS-275, and when compared to the UROtsa parent and the Cd^{+2} transformed cells in the no treatment group (#).

ChIP analysis to determine the binding of MTF-1 to the MREs

The purpose of this experiment was to assess the difference in the accessibility of MTF-1 to the MT-1X MREs between the parental and the As^{+3} and Cd^{+2} transformed UROtsa cells. The effect of treatment of the cells with either MS-275, Zn^{+2}, or both of them on MTF-1 binding was also evaluated. This assessment was achieved through ChIP assay for MTF-1 binding followed by RT-PCR of the immunoprecipitated chromatin, and was conducted in MREs a, d, & e.

The MTF-1 ChIP in the MRE-a Region

Results of this experiment showed that there was a significant degree of MTF-1 binding in the As^{+3} transformed cell lines when compared to the parent and the Cd^{+2} transformed ones, which showed no binding of MTF-1 (Figure 6). The MTF-1 binding in the no treatment group correlated with the MT-1X mRNA expression (Appendix B). Treatment with MS-275 resulted in a significant increase in MTF-1 binding in the Cd^{+2} transformed cell lines when compared to the parent UROtsa cells. There was no significant change in the level of MTF-1 binding in the As^{+3} transformed cells upon treatment with MS-275. The MTF-1 binding in the Cd^{+2} transformed cells was the only one in this treatment group that correlated to the MT-1X mRNA expression

There was no binding in any of the three cell lines when they were exposed to Zn^{+2}, and that did not correlate to the MT-1X mRNA expression which showed significant increase in the expression level following Zn^{+2} treatment. On the other hand,

treatment of the cells with MS-275 that was followed by the 4 h Zn^{+2} treatment resulted in a significant increase in the MTF-1 binding in the three cell lines with the As^{+3} transformed cell lines showing the greatest amount of binding, when compared to the same cells in the no treatment group. This finding correlated with the mRNA expression and suggests that in the MRE- a region, MTF-1 responds positively to the effect of epigenetic modulation by MS-275 through increased binding that is further accentuated by the 4 h Zn^{+2} treatment.

The MTF-1 ChIP in the MRE-d Region

Results of this experiment showed that there was a significant degree of binding in the parent cells when compared to the As^{+3} and Cd^{+2} transformed cell lines (Figure 7), and this did not correlate with the MT-1X mRNA expression (Appendix B). Treatment with MS-275 resulted in a slight increase in binding in the As^{+3} transformed cells when compared to the non-treated cells. There was no binding of MTF-1 in the UROtsa parent and the Cd^{+2} transformed cell lines when they were treated with MS-275. The MTF-1 binding correlated with the mRNA expression only in the As^{+3} transformed cells. Treatment of the cells with Zn^{+2} resulted in no detectable binding of MTF-1 in the three cell lines, which was similar to the results seen for the MRE-a region and did not correlate with the mRNA expression. Treatment of the cells with MS-275 followed by a 4 h Zn^{+2} treatment resulted in a significant increase in the MTF-1 binding in the As^{+3} and Cd^{+2} transformed cell lines, with the As^{+3} transformed cell line showing the greater amount of binding, when compared to the As^{+3} and Cd^{+2} transformed cell lines receiving

no treatment. The MTF-1 binding correlated with the mRNA expression in the As^{+3} and Cd^{+2} transformed cell lines.

The MTF-1 ChIP in the MRE-e Region

Results of this experiment showed that there was a significant degree of binding in the As^{+3} transformed cell lines when compared to the UROtsa parent and the Cd^{+2} transformed line (Figure 8), and that correlated with the MT-1X mRNA expression (Appendix B). Treatment with MS-275 resulted in a significant increase in MTF-1 binding in the Cd^{+2} transformed cell line, when compared to the parent and the As^{+3} transformed line. The UROtsa parent cells showed no increase in binding upon MS-275 treatment when compared to the non-treated cells whereas the As^{+3} transformed cells showed a decrease in binding when treated with MS-275 compared to the non- treated cells. The binding of MTF-1 in the Cd^{+2} transformed cell lines was the only one to show a correlation to the MT-1X mRNA expression. Treatment with Zn^{+2} did not show any binding in all the three cell lines which is similar to what was observed in the MREs a & d regions when similarly treated with Zn^{+2}, and does not correlate with the mRNA expression. Treatment of the cells with MS-275 that was followed by the 4 h Zn^{+2} treatment resulted in a significant increase in the MTF-1 binding in the As^{+3} and Cd^{+2} transformed cell lines when compared to the same cell lines receiving no treatment. Similar to the MRE-d region, the MTF-1 binding correlated with the mRNA expression in the As^{+3} and Cd^{+2} transformed cell lines.

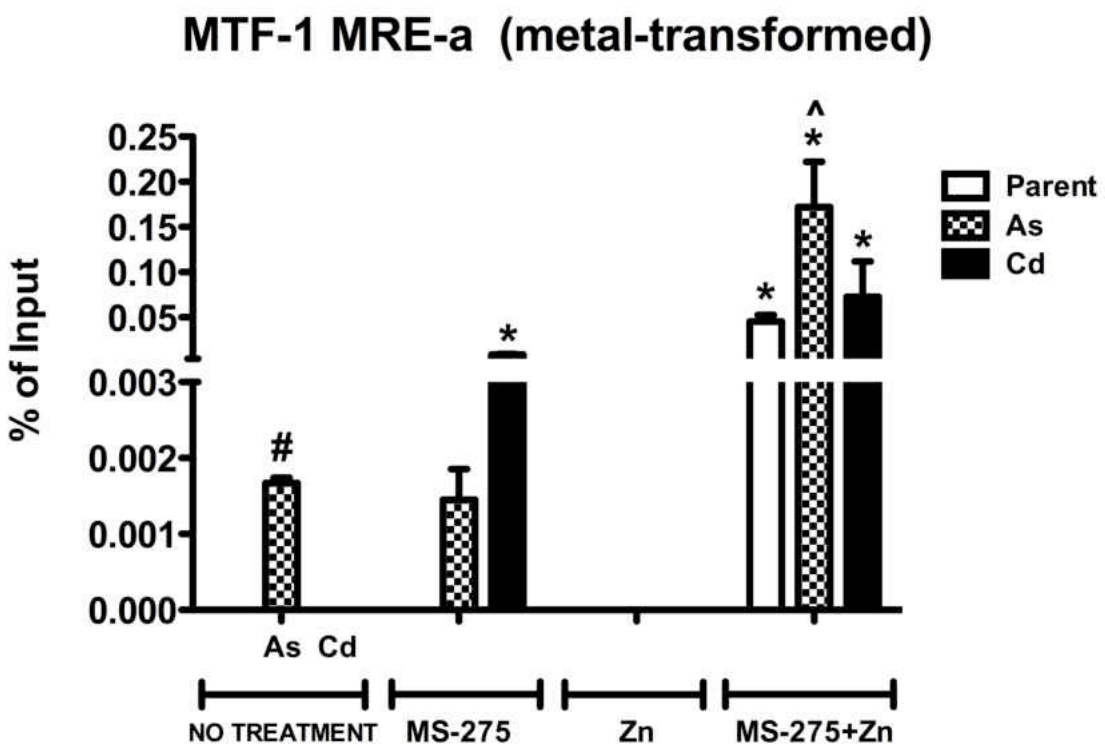

Figure 6. The effect of treatment with MS-275 +/- Zn^{+2} on MTF-1 binding in the parent, As^{+3} and Cd^{+2} transformed UROtsa cells in the MRE-a region. Statistically significant ($p < 0.05$) when compared to their corresponding cells receiving no treatment (*), to the As^{+3} MS-275 (^), and when compared to the UROtsa parent and the Cd^{+2} transformed cells in the no treatment group (#).

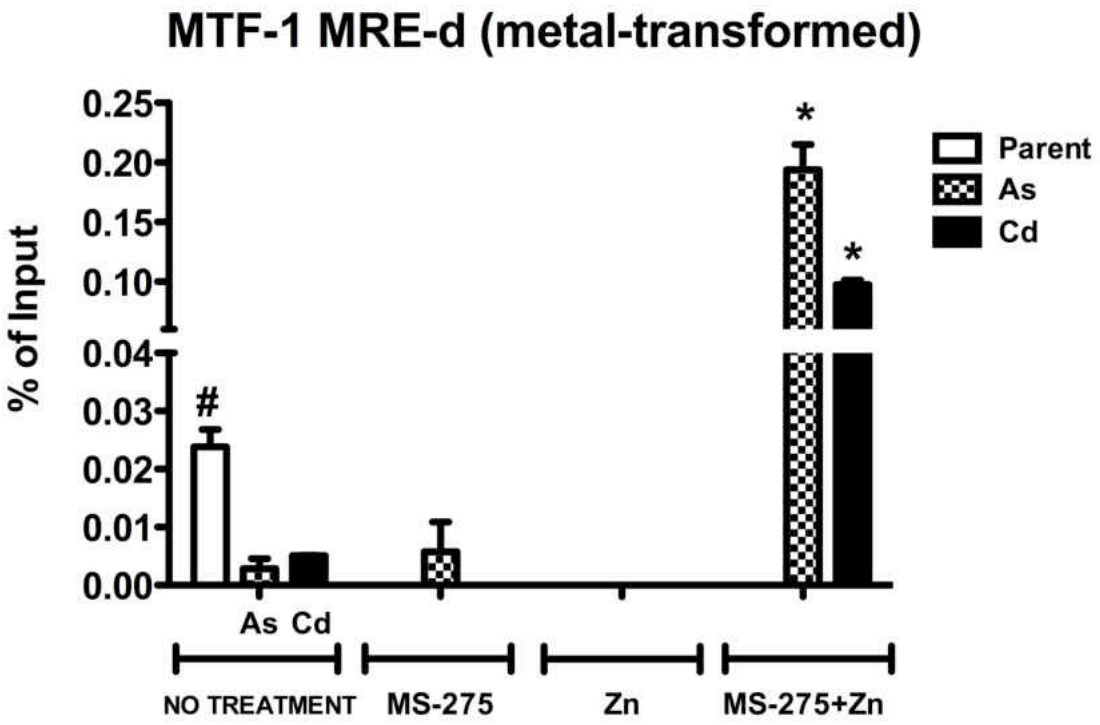

Figure 7. The effect of treatment with MS-275 +/- Zn^{+2} on MTF-1 binding in the parent, As^{+3} and Cd^{+2} transformed UROtsa cells in the MRE-d region. Statistically significant ($p < 0.05$) when compared to their corresponding cells receiving no treatment and to all other samples (*), and when compared to the As^{+3} and Cd^{+2} transformed cells in the no treatment group (#).

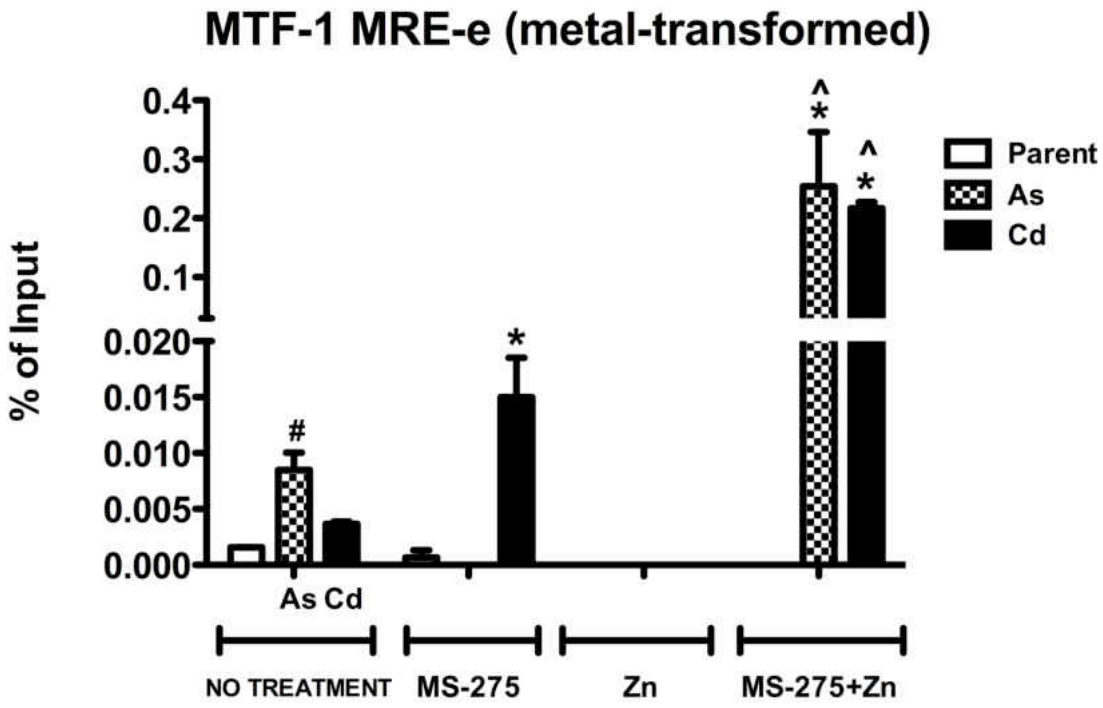

Figure 8. The effect of treatment with MS-275 +/- Zn^{+2} on MTF-1 binding in the parent, As^{+3} and Cd^{+2} transformed UROtsa cells in the MRE-e region. Statistically significant ($p < 0.05$) when compared to their corresponding cells receiving no treatment (*), to all other samples (^), and when compared to the UROtsa parent and Cd^{+2} transformed cells in the no treatment group (#).

Transcription Factor Binding in the MT-1X Proximal Promoter Region

The objective for these experiments was to utilize the ChIP technique to assess transcription factor binding in the non-transformed parent, compared to the Cd^{+2} and As^{+3} transformed cells. Superimposed on these experiments were the effects of MS-275 exposure on factor binding. This approach sought to identify the transcription factors whose binding to the MT-1X promoter correlated to expression differences between the normal and metal-transformed cells, and that might be implicated in the mechanism by which MT-1X is induced in bladder cancer.

The transcription factors tested were chosen based on the results of the *in silico* analysis, which predicted potential binding sites for these factors in the MT-1X proximal promoter and these were: ELK1, LBP-1, NF-I, p300, MTF-1, SP1, TCF-1, USF1, and YY1. The ChIP assays were followed by RT-PCR of the immunoprecipitated chromatin. The results for the MTF-1 binding were discussed in the previous section. ChIP assay for YY1 did not show any binding in all the MRE regions tested, in both the control and the MS-275 treatment groups.

Binding of p300 to the MT-1X promoter

The p300 transcription factor binding to the MT-1X promoter was selected for assessment based on the fact that, together with its coactivator cAMP-responsive element binding protein-binding protein (CBP), it is involved in the activation of numerous genes. Results of the ChIP assay for p300 in the MRE-a region revealed that

the As^{+3} transformed cell line showed the greatest amount of p300 binding when compared to the parent and the Cd^{+2} transformed cell lines (Figure 9). These results correlate to the expression levels of MT-1X mRNA in the transformed cell lines when compared to the UROtsa parent cell line (Figure 5). Treatment of the cells with MS-275 resulted in a significant increase in p300 binding in the Cd^{+2} transformed cell lines, which correlates to the MT-1X mRNA expression in the same treatment group. The UROtsa parent cells did not show an increase in p300 binding upon treatment with MS-275, whereas the As^{+3} transformed cell line showed a decrease in p300 binding. This binding does not correlate to the levels of MT-1X expression seen in the parent and the As^{+3} transformed cells treated with MS-275.

The binding of p300 to the MRE-d region showed that the As^{+3} transformed cell line showed the greatest amount of p300 binding when compared to the parent and the Cd^{+2} transformed cell lines (Figure 10). These results correlate to the expression levels of MT-1X mRNA in the transformed cell lines (Figure 5). Treatment of the cells with MS-275 resulted in a significant increase in the p300 binding in the Cd^{+2} transformed cell lines, which correlates to the MT-1X mRNA expression in the same treatment group. The UROtsa parent cells showed a decrease in the levels of p300 binding upon treatment with MS-275 when compared to the non-treated parent, whereas the As^{+3} transformed cell lines showed no change in the amount of p300 binding. This does not correlate with the expression levels of MT-1X, which increased after treatment with MS-275.

In the MRE-e region, the results for the p300 ChIP assay revealed that the As^{+3} transformed cell line showed the greatest amount of p300 binding when compared to the parent and the Cd^{+2} transformed cell lines (Figure 11). These results correlate to the expression levels of MT-1X mRNA as shown in Figure 5. Treatment of the cell lines with MS-275 resulted in an increase in p300 binding when compared to the non-treated cell lines. Both the As^{+3} and the Cd^{+2} transformed cell line showed a significant increase in p300 binding when compared to the non-treated cells. The increase in the p300 binding in the UROtsa parent cells was very small and was not statistically significant when compared to the non-treated UROtsa cells. The response to treatment with MS-275 generally reflected the changes observed in the MT-1X mRNA expression. Based on this response, the As^{+3} transformed cells showed an enhanced binding in the MRE-e region, while the Cd^{+2} transformed cells showed an increase in the binding levels of p300 in the MREs a & d regions.

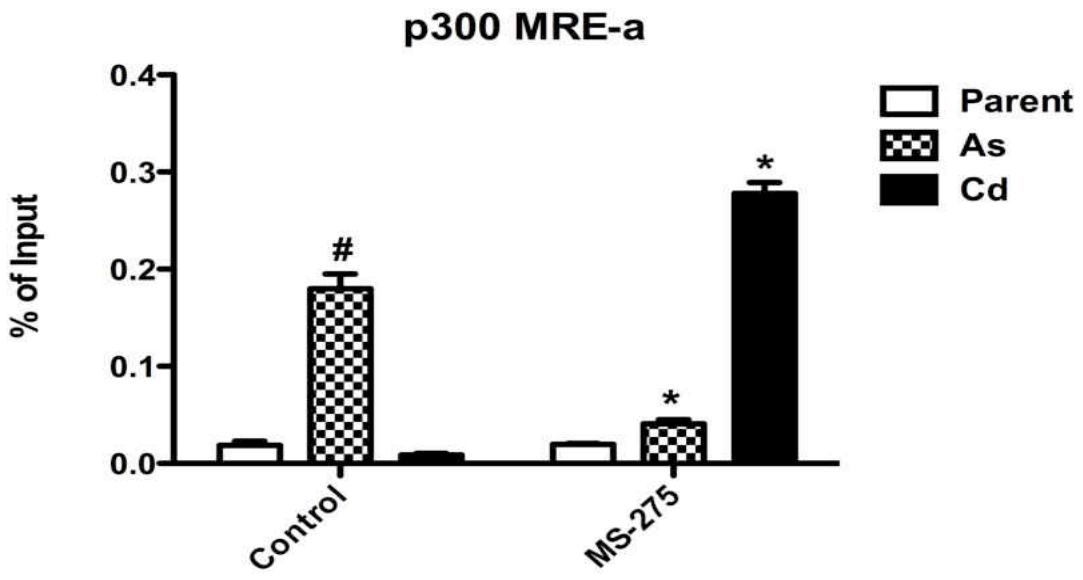

Figure 9. The effect of treatment with MS-275 on p300 binding in the parent, As^{+3} and Cd^{+2} transformed UROtsa cells in the MRE-a region. Statistically significant ($p < 0.05$) when compared to their corresponding cells in the non-treated control group (*), and when compared to the UROtsa parent and Cd^{+2} transformed cells in the non-treated control group (#).

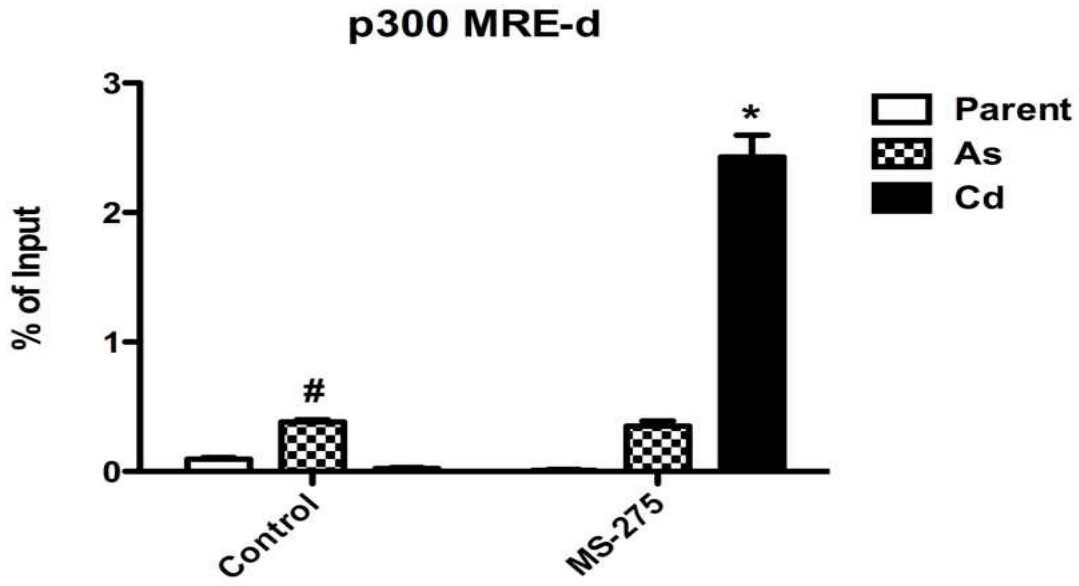

Figure 10. The effect of treatment with MS-275 on p300 binding in the parent, As^{+3} and Cd^{+2} transformed UROtsa cells in the MRE-d region. Statistically significant ($p < 0.05$) when compared to their corresponding cells in the non-treated control group and to all other samples (*), and when compared to the UROtsa parent and Cd^{+2} transformed cells in the non-treated control group (#).

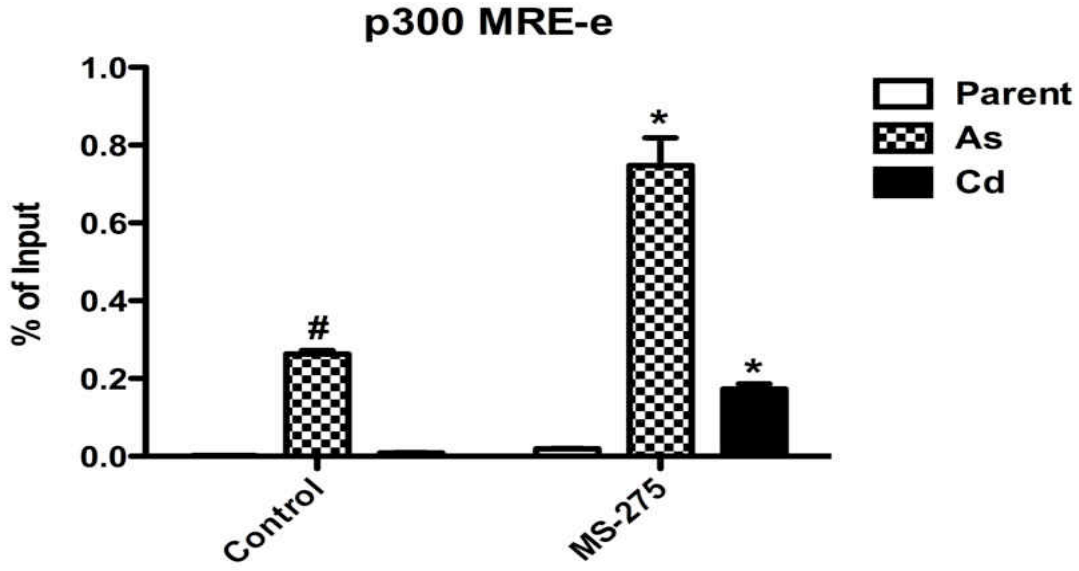

Figure 11. The effect of treatment with MS-275 on p300 binding in the parent, As^{+3} and Cd^{+2} transformed UROtsa cells in the MRE-e region. Statistically significant ($p < 0.05$) when compared to their corresponding cells in the non-treated control group (*), and when compared to the UROtsa parent and Cd^{+2} transformed cells in the non-treated control group (#).

Binding of NF-I to the MT-1X promoter

The NF-I transcription factor is an activator of gene transcription that has been associated with the control of the growth rates of different types of cells and has been associated with a myriad of disease processes (Gronostajski et al., 2000). Results of the ChIP assay for NF-I in the MRE-a region showed that there was a significant amount of binding in the As^{+3} transformed control cells when compared to the parent and the Cd^{+2} transformed cell lines in the same group (Figure 12), and that correlated with the MT-1X mRNA expression in the control group. Treatment with MS-275 resulted in a significant decrease in the NF-I binding in the As^{+3} transformed cells and a non-statistically significant decrease in binding in the parent cells. The Cd^{+2} transformed cells showed a slight increase in binding which was not statistically significant. These results do not correlate with the MT-1X mRNA expression in the MS-275 treatment group (Figure 5).

The binding of NF-I to the MRE-d region was increased significantly in the UROtsa Parent and the As^{+3} transformed cell lines when compared to the Cd^{+2}transformed cells. This correlated to the increased mRNA expression that was seen in the As^{+3} transformed cells (Figure 13). Treatment with MS-275 resulted in a significant increase in NF-I binding in the Cd^{+2} transformed cell lines when compared to the non-treated Cd^{+2} transformed cells. The Parent and the As^{+3} transformed cells in the presence of MS-275 showed a decrease binding which was significant when compared to the non-treated cells. The increase in binding in the Cd^{+2} transformed cells correlated to an increase in MT-1X mRNA. This finding might point to a preferential binding of the transcription factors to different MREs depending on the cells they reside in.

In the MRE-e region, there was a significant amount of NF-I binding in the As^{+3} transformed control cells when compared to the parent and the Cd^{+2} transformed cell lines in the control non-treated cells and that correlated with the MT-1X mRNA expression in the same group (Figure 14). Treatment with MS-275 resulted in a significant increase in NF-I binding in the As^{+3} transformed cell lines, when compared to the non-treated As^{+3} transformed cells, and that correlates with the levels of MT-1X mRNA. Binding of NF-I in the parent and the Cd^{+2} transformed cell lines did not show a significant change after MS-275 treatment when compared to the non-treated control cells.

Based on the data obtained, the As^{+3} transformed cell lines show a more favorable binding in the MRE-e region, while the Cd^{+2} transformed cell lines show a more favorable binding in the MRE-d region.

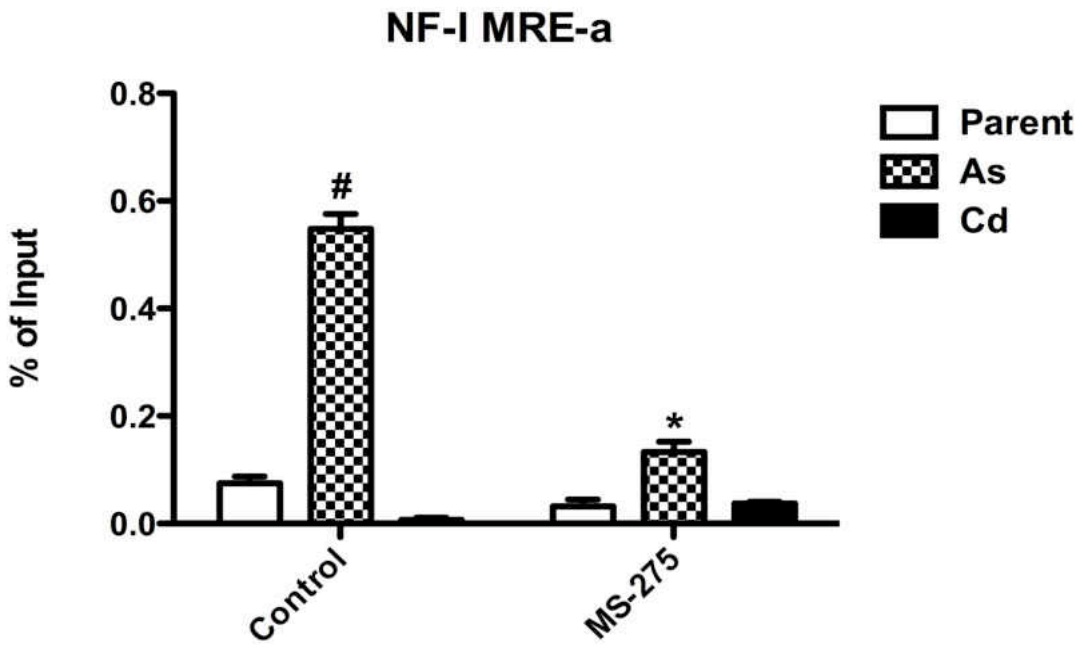

Figure 12. The effect of treatment with MS-275 on NF-I binding in the parent, As^{+3} and Cd^{+2} transformed UROtsa cells in the MRE-a region. Statistically significant ($p < 0.05$) when compared to their corresponding cells in the non-treated control group (*), and when compared to the UROtsa parent and Cd^{+2} transformed cells in the non-treated control group (#).

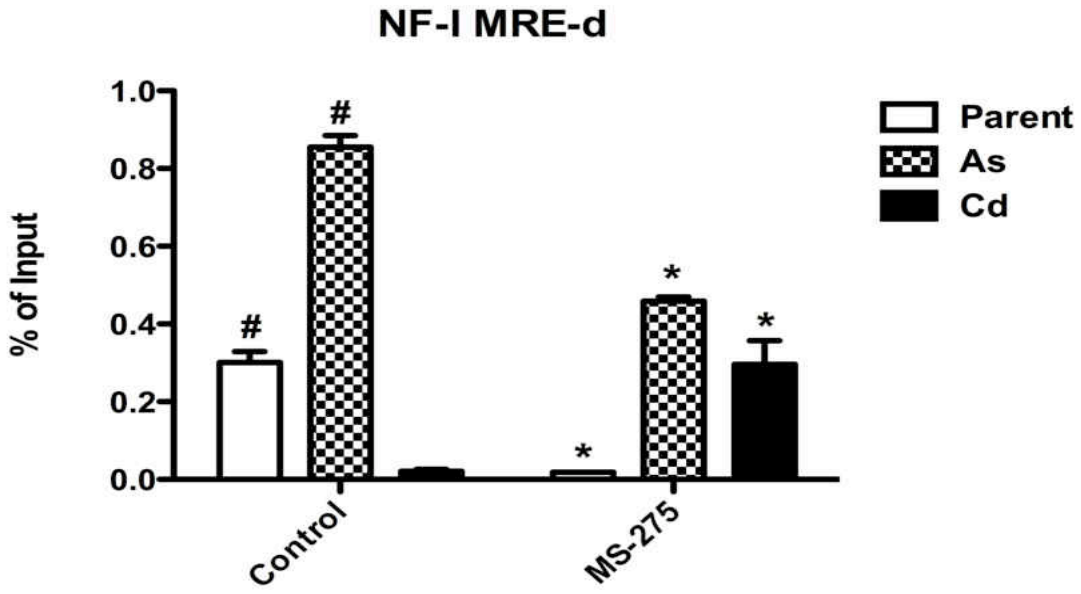

Figure 13. The effect of treatment with MS-275 on NF-I binding in the parent, As^{+3} and Cd^{+2} transformed UROtsa cells in the MRE-d region. Statistically significant ($p < 0.05$) when compared to their corresponding cells in the non-treated control group (*), and when compared to the Cd^{+2} transformed cells in the non-treated control group and to one another (#).

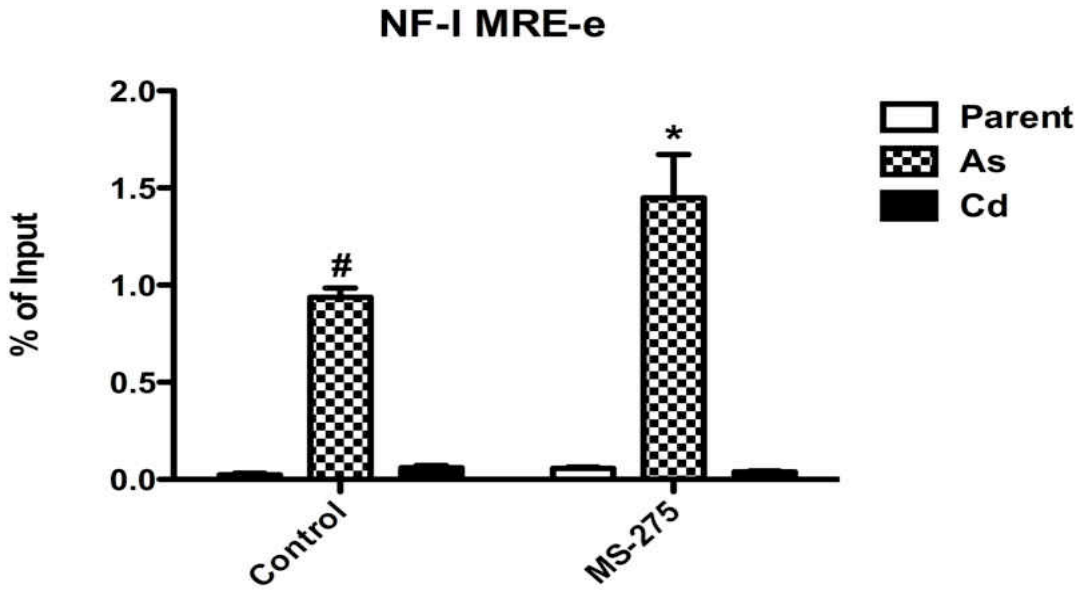

Figure 14. The effect of treatment with MS-275 on NF-I binding in the parent, As^{+3} and Cd^{+2} transformed UROtsa cells in the MRE-e region. Statistically significant ($p < 0.05$) when compared to their corresponding cells in the non-treated control group (*), and when compared to the parent and Cd^{+2} transformed cells in the non-treated control group (#).

Binding of SP1 to the MT-1X promoter

The SP1 transcription factor is a ubiquitously distributed protein that belongs to the Sp1/KLF family of transcriptional activators. Results of the ChIP assay for SP1 in the MRE-a region showed that there was a significant degree of binding in the As^{+3} transformed non-treated control cells when compared to the parent and the Cd^{+2} transformed cell lines in the same group (Figure 15), and that correlated with the MT-1X mRNA expression levels. Treatment with MS-275 resulted in a significant decrease in the amount of SP1 binding in the As^{+3} transformed cell line when compared to its non-treated control. There was no significant change in the amount of SP1 binding in the parent and Cd^{+2} transformed cell lines upon MS-275 treatment. The binding of SP1 to the MRE-a region after MS-275 treatment did not correlate to the levels of MT-1X mRNA in all the three cell lines.

In the MRE-d region, the was a significant amount of SP1 binding in the parent and the As^{+3} transformed control cells when compared to the Cd^{+2} transformed cell lines in the non-treated control group (Figure 16), and this binding correlated with the MT-1X mRNA expression levels in the As^{+3} transformed cell lines. Treatment with MS-275 resulted in a significant decrease in binding of SP1 in the As^{+3} transformed cell lines, when compared to the non-treated controls. There was no change in the amount of SP1 binding in the parent cells after MS-275 treatment, whereas in the Cd^{+2} transformed cell

lines there was no binding of SP1. This data does not correlate to the levels of MT-1X expression that was observed after treatment with MS-275 for all the three cell lines.

In the MRE-e region, there was a significant amount of SP1 binding in the As^{+3} transformed non-treated control cells when compared to the parent and the Cd^{+2} transformed cells (Figure 17). This correlated to the levels of MT-1X expression seen in the non-treated control cells. Treatment with MS-275 resulted in a significant increase in SP1 binding in the Cd^{+2} transformed cell line when compared to the non-treated control. The parent and the As^{+3} transformed cell lines did not show a significant change in SP1 binding when treated with MS-275. The data obtained indicates that treatment with MS-275 resulted in an increase in binding in the Cd^{+2} transformed cell line which correlated to an increase in MT-1X mRNA expression levels. Although treatment with MS-275 did increase the expression of MT-1X in the UROtsa parent cells and in the As^{+3} transformed cell line, this did not result in an increase binding of SP1 to the MRE region. Based on the data obtained, the Cd+2 transformed cells showed enhanced SP1 binding upon in the MRE-e region that was observed following MS-275 treatment.

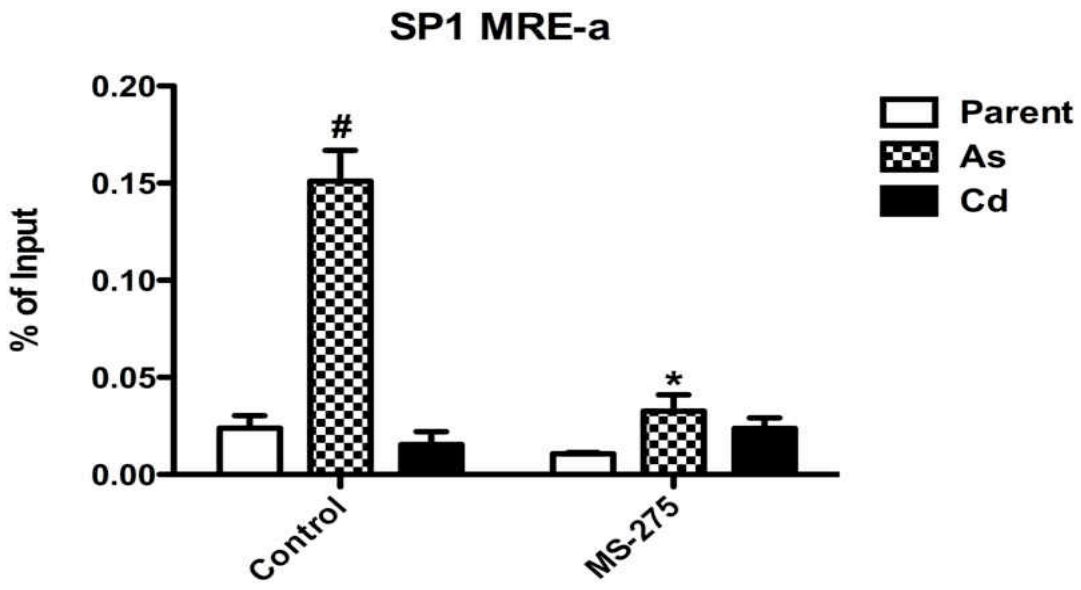

Figure 15. The effect of treatment with MS-275 on SP1 binding in the parent, As^{+3} and Cd^{+2} transformed UROtsa cells in the MRE-a region. Statistically significant ($p < 0.05$) when compared to their corresponding cells in the non-treated control group (*), and when compared to the parent and Cd^{+2} transformed cells in the non-treated control group (#).

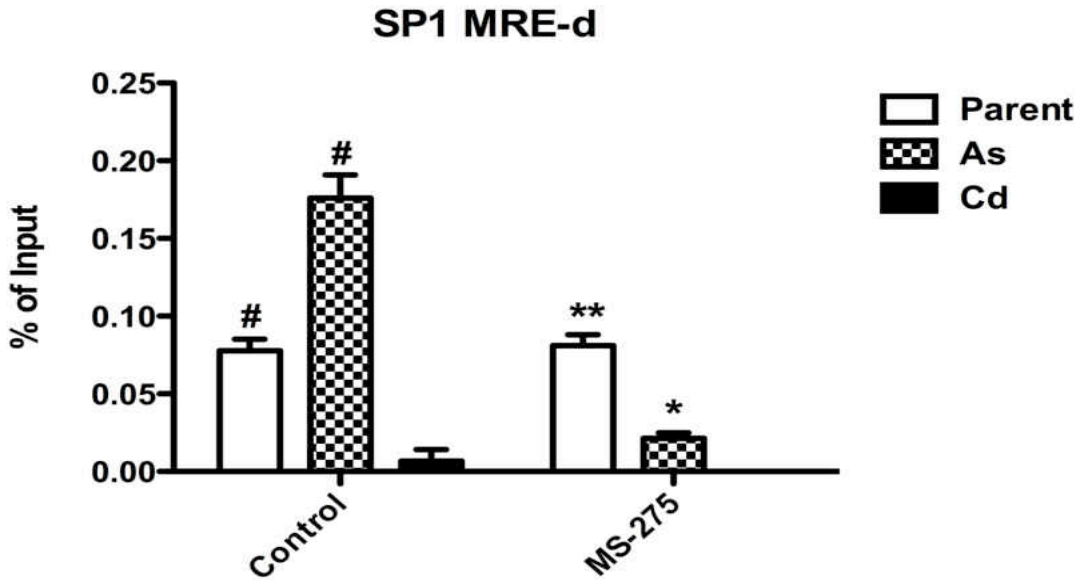

Figure 16. The effect of treatment with MS-275 on SP1 binding in the parent, As^{+3} and Cd^{+2} transformed UROtsa cells in the MRE-d region. Statistically significant ($p < 0.05$) when compared to their corresponding cells in the non-treated control group (*), when compared to the As^{+3} and Cd^{+2} transformed cells treated with MS-275 (**), and when compared to the Cd^{+2} transformed cells in the non-treated control group and to one another (#).

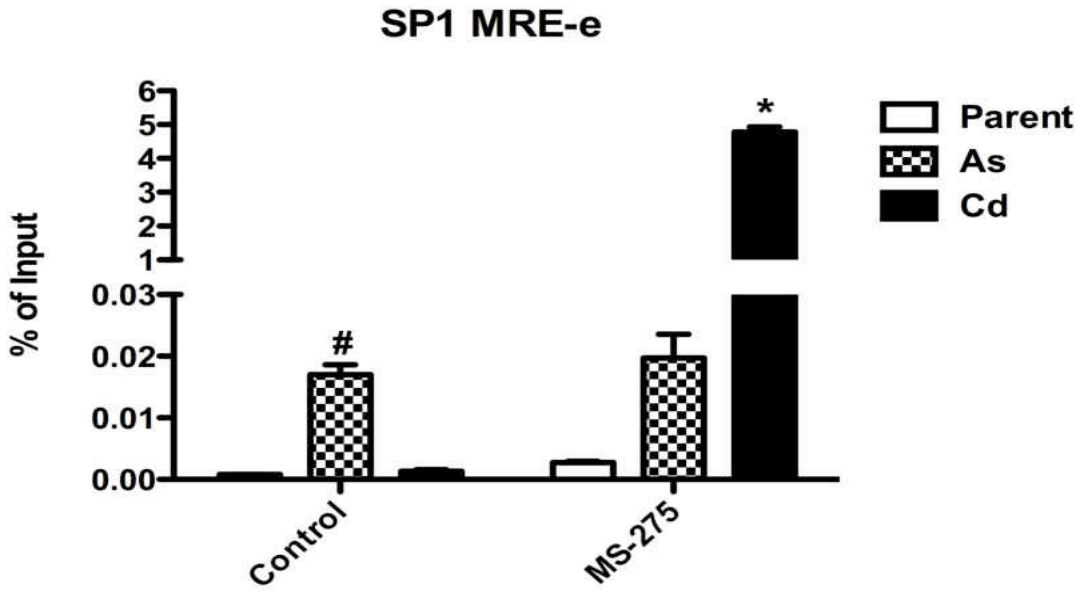

Figure 17. The effect of treatment with MS-275 on SP1 binding in the parent, As^{+3} and Cd^{+2} transformed UROtsa cells in the MRE-e region. Statistically significant ($p < 0.05$) when compared to their corresponding cells in the non-treated control group and to all samples (*), and when compared to the parent and Cd^{+2} transformed cells in the non-treated control group and to one another (#).

Binding of LBP-1 to the MT-1X promoter

The LBP-1 protein is a transcriptional activator that showed potential association with the MT-1X proximal promoter based on the TESS analysis. Results of the ChIP assay for LBP-1 in the MRE-a region showed that there was a significant degree of binding in the parent and the As^{+3} transformed control cells when compared to the Cd^{+2} transformed cell lines in the non-treated control group (Figure 18). Treatment with MS-275 resulted in a significant increase in LBP-1 binding in the As^{+3} and Cd^{+2} transformed cell lines when compared to their non-treated controls, and that increase in binding correlated to the MT-1X mRNA expression. The parent cells showed a decrease in LBP-1 binding that did not correlate to its MT-1X mRNA expression.

ChIP analysis for the detection of LBP-1 binding to the MRE-d region showed that there was no binding in the control non- treated cells. Treatment with MS-275 did not result in an increase the level of binding.

In the MRE-e region, results of the LBP-1 ChIP assay showed that there was a significant degree of binding in the As^{+3} transformed control cell lines when compared to the parent and Cd^{+2} transformed cell lines in the non-treated control group (Figure 19). These results correlated to the MT-1X mRNA expression in the non-treated group. Treatment with MS-275 resulted in a significant increase in the LBP-1 binding in the parent and the As^{+3} transformed cells when compared to their non-treated controls, and this correlated to the increased expression of MT-1X mRNA seen in the MS-275

treated cells. Based on their response to the MS-275 treatment, the UROtsa parent and the Cd+2 transformed cells had increased binding in the MRE-e region, whereas the As^{+3} transformed cells had increased binding in both the MREs a and e regions.

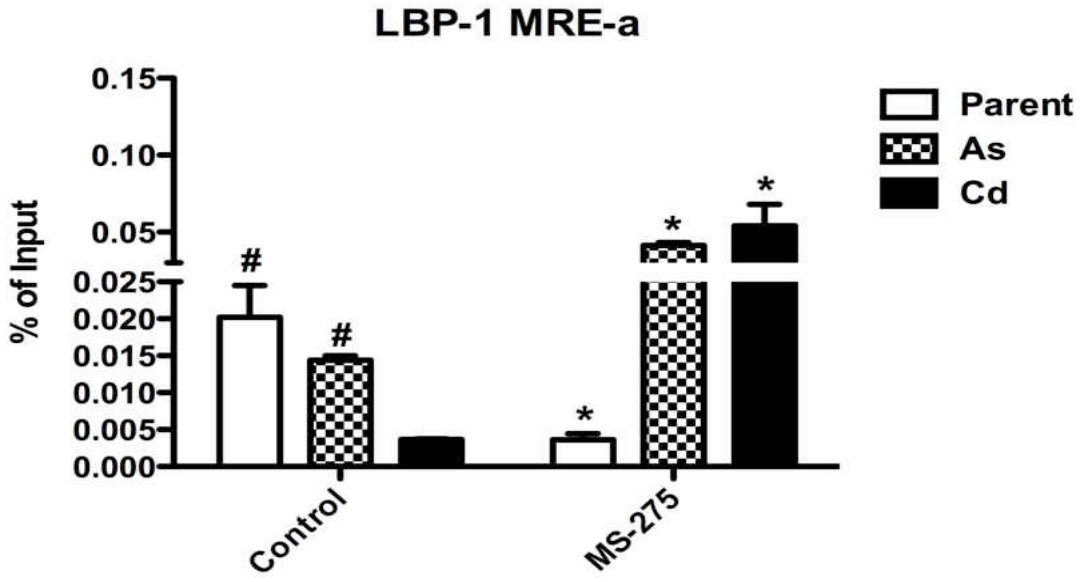

Figure 18. The effect of treatment with MS-275 on LBP-1 binding in the parent, As^{+3} and Cd^{+2} transformed UROtsa cells in the MRE-a region. Statistically significant ($p < 0.05$) when compared to their corresponding cells in the non-treated control group (*), and when compared to the Cd^{+2} transformed cells in the non-treated control group (#).

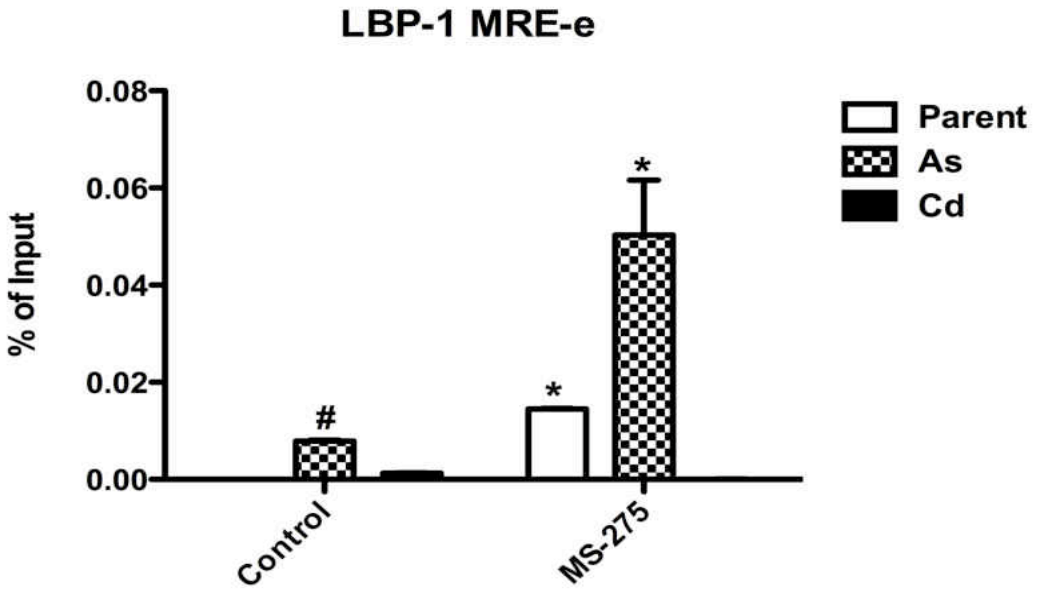

Figure 19. The effect of treatment with MS-275 on LBP-1 binding in the parent, As^{+3} and Cd^{+2} transformed UROtsa cells in the MRE-e region. Statistically significant ($p < 0.05$) when compared to their corresponding cells in the non-treated control group and to one another (*), and when compared to the parent and Cd^{+2} transformed cells in the non-treated control group (#).

Binding of USF1 to the MT-1X promoter

The USF1 is a ubiquitously expressed transcription factor involved in the regulation of different genes and is a crucial member of the transcriptional machinery (Corre *et al*., 2005). Analysis of the USF1 ChIP assay results showed that in the MRE-a region, there was a significant amount of USF1 binding in the UROtsa parent non-treated control control cells when compared to the Cd^{+2} transformed non-treated cells (Figure 20). Treatment with MS-275 resulted in a significant increase in the USF1 binding in the parent and the Cd^{+2} transformed cells, however there was no change in the binding in the As^{+3} transformed cells when compared to the non-treated controls. There was significant increase in binding of USF1 to the MRE-d region of the MT-1X gene in the UROtsa parent cells, when compared to the As^{+3} and Cd^{+2} transformed cells (Figure 21). Treatment of the cells with MS-275 resulted in significant decrease in the amount of USF1 binding in the parent cells when compared to the non-treated cells. In the As^{+3} transformed cell line, treatment with MS-275 did not result in a change in USF1 binding, whereas in the Cd^{+2} transformed cells, there was a decrease in USF1 binding when compared to the non-treated controls. In the MRE-e region, there was significant USF1 binding in the Cd^{+2} transformed cells in the non-treated control group, when compared to the parent and the As^{+3} transformed cell lines (Figure 22). Treatment with

MS-275 resulted in a significant increase in the USF-1 binding in the parent cells when compared to the non-treated parent control. The Cd^{+2} transformed cells showed a decrease in binding of USF1, whereas in the As^{+3} transformed cells there was no change in USF1 binding when compared to the non-treated cells. Based on their response to the MS-275 treatment, the parent cells had increased binding in the MREs a & e regions, the As^{+3} transformed cells had no significant increase in USF1 binding, and the Cd^{+2} transformed cell lines showed enhanced binding in the MRE-a region.

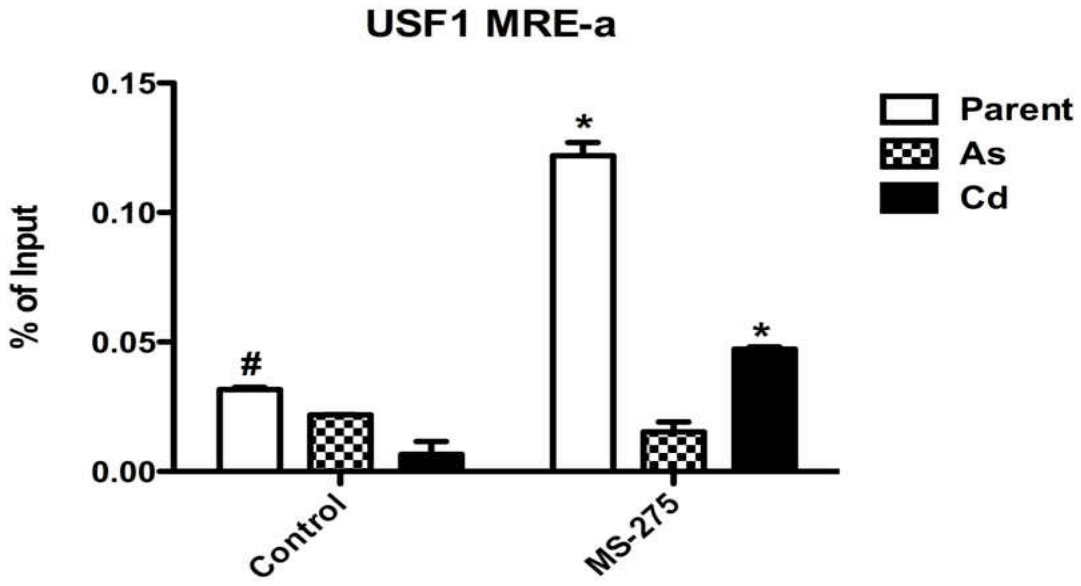

Figure 20. The effect of treatment with MS-275 on USF1 binding in the parent, As^{+3} and Cd^{+2} transformed UROtsa cells in the MRE-a region. Statistically significant ($p < 0.05$) when compared to their corresponding cells in the non-treated control group and to one another (*), and when compared to the Cd^{+2} transformed cells in the non-treated control group (#).

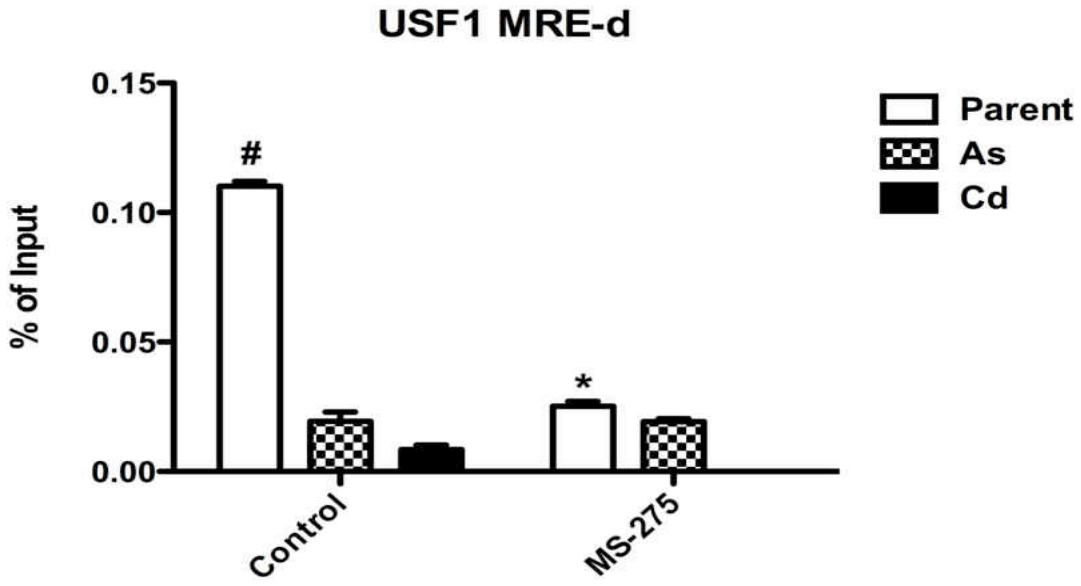

Figure 21. The effect of treatment with MS-275 on USF1 binding in the parent, As^{+3} and Cd^{+2} transformed UROtsa cells in the MRE-d region. Statistically significant ($p < 0.05$) when compared to their corresponding cells in the non-treated control group (*), and when compared to the As^{+3} and Cd^{+2} transformed cells in the non-treated control group (#).

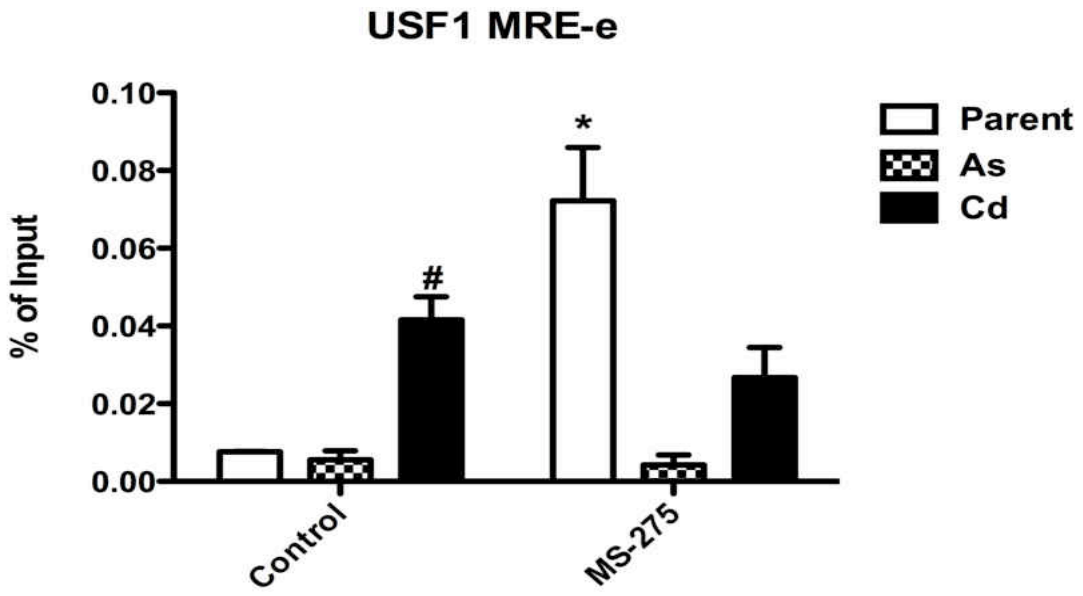

Figure 22. The effect of treatment with MS-275 on USF1 binding in the parent, As^{+3} and Cd^{+2} transformed UROtsa cells in the MRE-e region. Statistically significant ($p < 0.05$) when compared to their corresponding cells in the non-treated control group (*), and when compared to the parent and As^{+3} transformed cells in the non-treated control group (#).

Binding of ELK1 to the MT-1X Promoter

The ELK1 transcription factor is a member of the ETS oncogene family, and has been involved in the activation of various genes. ChIP analysis of binding of ELK1 to the MREs showed that this factor bound only to the MRE-e region of the MT-1X promoter (Figure 23). In the non-treated control group, the As^{+3} transformed cell lines had the most significant binding, when compared to the parent and the Cd^{+2} transformed cell lines. Treatment of the cells with MS-275 resulted in a significant increase in ELK1 binding in the Cd^{+2} transformed cell lines when compared to the non-treated control. In the UROtsa parent and the As^{+3} transformed cells, there was no binding of ELK1 observed when the cells were treated with MS-275.

Binding of TCF-1 to the MT-1X promoter

The TCF-1 is a transcriptional activator that belongs to the high mobility group-box transcription factors, and has been linked to the beta-catenin signaling pathway (Mayer *et al*., 1997). Results of ChIP analysis for TCF-1 showed that there was binding only in the MRE-a region of the MT-1X promoter. In the non-treated control group, only the Cd^{+2} transformed cell line showed any detectable level of binding (Figure 24). Treatment of the cells with MS-275 resulted in a significant increase in the level of TCF-1 binding in all the three cell lines when compared to their non-treated controls. This increase in binding suggests a role for this factor in increasing the transcriptional activation of the MT1X gene in these cell lines.

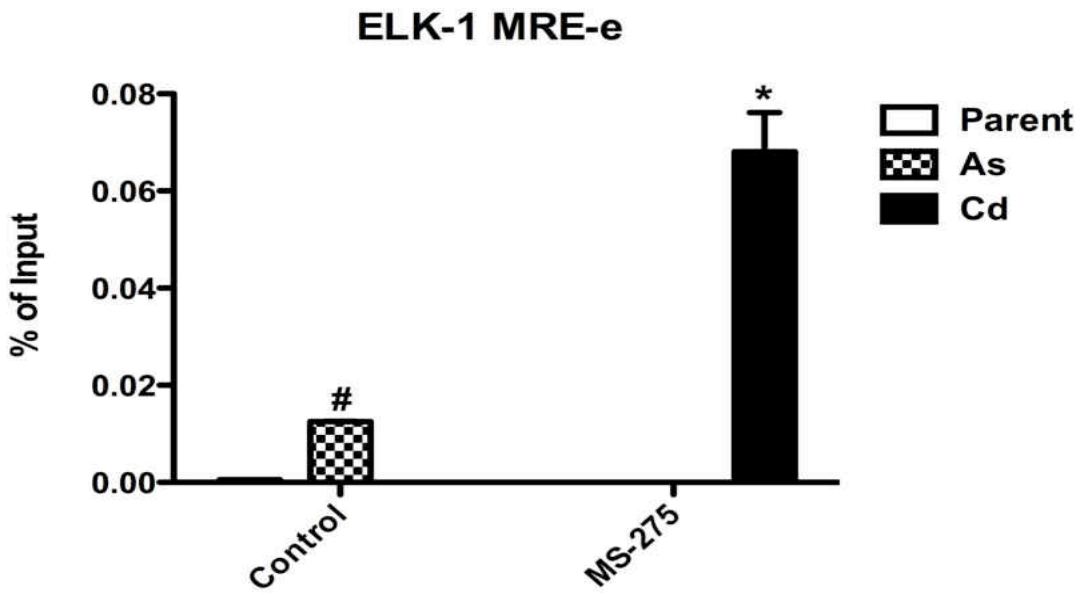

Figure 23. The effect of treatment with MS-275 on ELK-1 binding in the parent, As^{+3} and Cd^{+2} transformed UROtsa cells in the MRE-e region. Statistically significant ($p < 0.05$) when compared to their corresponding cells in the non-treated control group and to all other samples (*), and when compared to the parent and Cd^{+2} transformed cells in the non-treated control group (#).

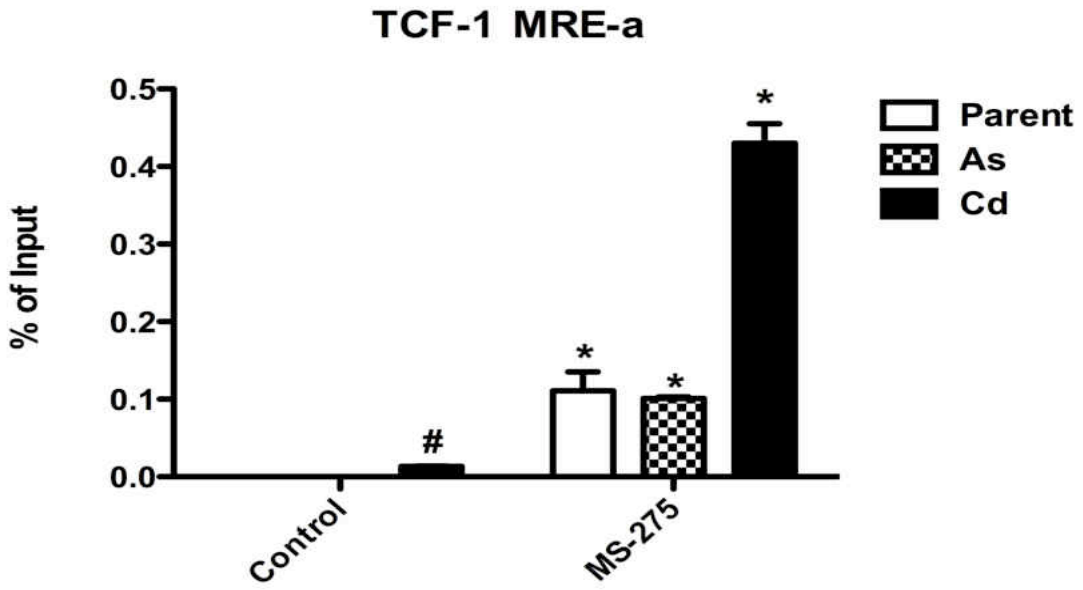

Figure 24. The effect of treatment with MS-275 on TCF-1 binding in the parent, As^{+3} and Cd^{+2} transformed UROtsa cells in the MRE-a region. Statistically significant ($p < 0.05$) when compared to their corresponding cells in the non-treated control group (*), and when compared to the parent and As^{+3} transformed cells in the non-treated control group (#).

Histone Modifications in the MT-1X Proximal Promoter Region

The goal of this set of experiments was to assess the histone modifications in the non-transformed parent cells and to compare them to the As^{+3} and Cd^{+2} transformed cells. In addition, the effect of MS-275 on the histone modifications was also assessed. The end result being to identify histone modifications in the MT-1X promoter which would correlate to expression differences between the normal and metal-transformed cells, thus identifying the mechanism that may be involved in the up-regulation of MT-1X in bladder cancer. The histone modifications analyzed in this study were a combination of modifications that confer activation (trimethyl H3K4, H2A.z, acetyl H4, and H3.3) and others that confer repression (trimethyl H3K9, and trimethyl H3K27). In addition, the levels of the total histone H3 were assessed to compare and correlate to the histone H3 modifications tested. The trimethyl H3K9 modification, which confers a silencing effect on chromatin, was not detected by real time PCR in any of the MREs tested.

Detection of Acetylation on Histone 4 (H4) by ChIP Assay

Histone H4 is one of the core histones, and the addition of an acetyl group to the lysine residues present in histone tails is achieved by the HATs. The addition of the acetyl group neutralizes the positive lysine charges and is thought to lessen the affinity between the histones and DNA permitting the association between the DNA and the transcriptional machinery that results in transcriptional activation.

Analysis of the results of the acetyl H4 ChIP assay in the MRE-a region shows that the non-treated UROtsa parent and the As^{+3} transformed cell lines (controls) showed a significant level of enrichment when compared to the Cd^{+2} transformed cell lines (Figure 25). The level of acetylation of H4 in the As^{+3} transformed cell line correlated to an increased level of expression of MT-1X mRNA in this cell line. Treatment with MS-275 resulted in a significant decrease in the levels of acetyl H4 in the parent and the As^{+3} transformed cell line, while the Cd^{+2} transformed cell lines showed a significant increase in acetylation when compared to the non-treated Cd^{+2} transformed cells. The increase in the mRNA levels of MT-1X in the As^{+3} transformed cells and the UROtsa parent cells treated with MS-275 did not correlate to the levels of acetylation of H4 seen in these cells. However, the increase in H4 acetylation seen in the Cd^{+2} transformed cell line upon MS-275 treatment did correlate to an increase in the mRNA levels of MT-1X. In the MRE-d region, the acetyl H4 expression levels were similar to the findings in the MRE-a region (Figure 26). In the MRE-e region, analysis of the non-treated control group showed that As^{+3} and Cd^{+2} transformed cell lines had significant increased levels of H4 acetylation when compared to the control parent cells (Figure 27), and this increase in acetylation correlated to the increase seen in MT-1X mRNA levels. Treatment with MS-275 resulted in an increase in the acetyl H4 levels in all the three cell lines when compared to their non-treated controls and this increase correlated to the increased mRNA levels of MT-1X.

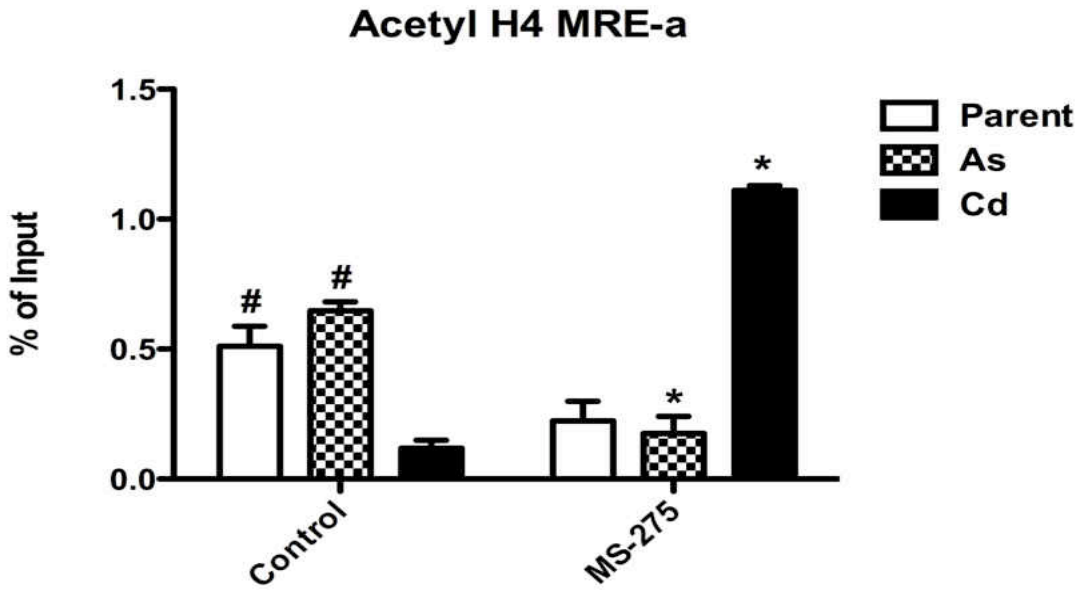

Figure 25. The effect of treatment with MS-275 on acetyl H4 levels in the parent, As^{+3} and Cd^{+2} transformed UROtsa cells in the MRE-a region. Statistically significant ($p < 0.05$) when compared to their corresponding cells in the non-treated control group (*), and when compared to the Cd^{+2} transformed cells in the non-treated control group (#).

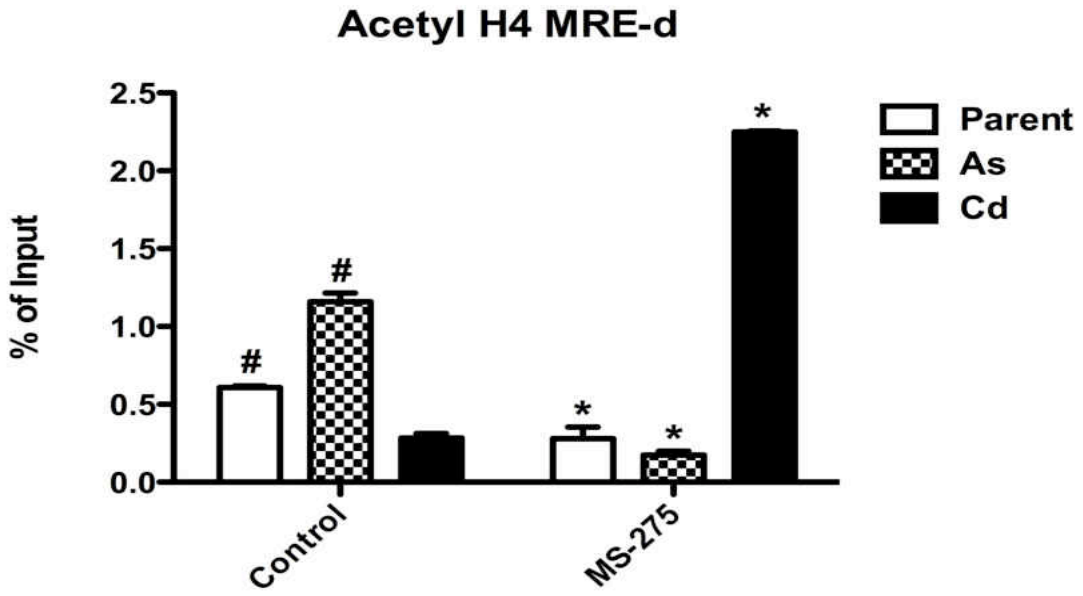

Figure 26. The effect of treatment with MS-275 on acetyl H4 levels in the parent, As^{+3} and Cd^{+2} transformed UROtsa cells in the MRE-d region. Statistically significant ($p < 0.05$) when compared to their corresponding cells in the non-treated control group (*), and when compared to the Cd^{+2} transformed cells in the non-treated control group (#).

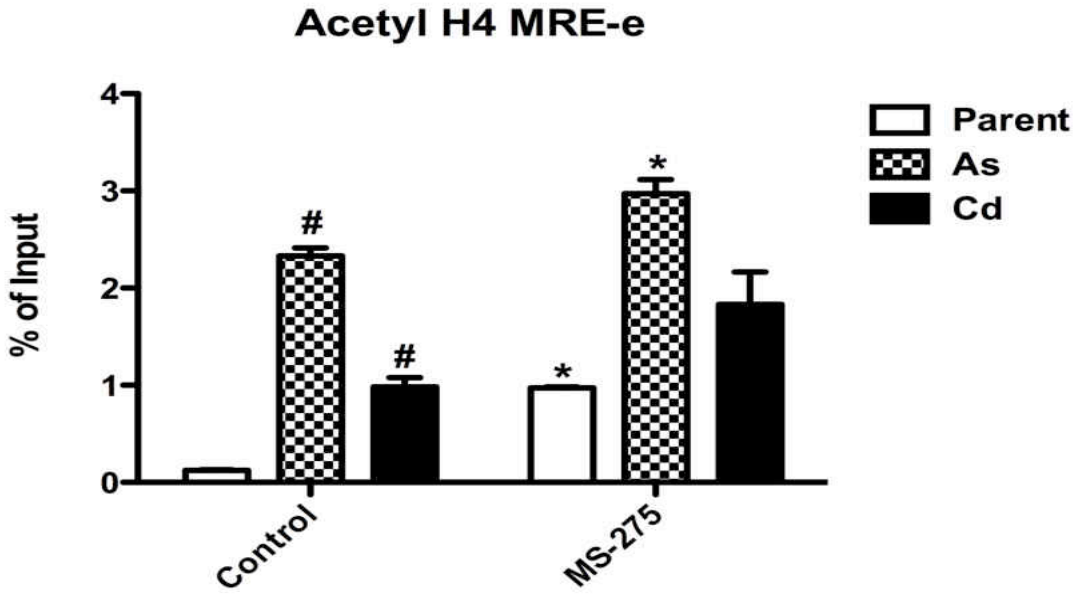

Figure 27. The effect of treatment with MS-275 on acetyl H4 levels in the parent, As^{+3} and Cd^{+2} transformed UROtsa cells in the MRE-e region. Statistically significant ($p < 0.05$) when compared to their corresponding cells in the non-treated control group (*), and when compared to UROtsa parent in the non-treated control group and to one another (#).

The H2A.z ChIP Assay

The Histone variant H2A.z is deposited around the regions of TSS, where its presence denotes an active transcriptional region. Results of the H2A.z ChIP assay showed that, in the MRE-a region there is an increased level of H2A.z in the parent and As^{+3} transformed cell line, when compared to the Cd^{+2} transformed cell line in the non-treated control group (Figure 28). Treatment with MS-275 resulted in a significant decrease in the levels of H2A.z in the parent and As^{+3} transformed cell lines, when compared to their non-treated controls. There was no detectable level of H2A.z in the Cd^{+2} transformed cell line. The decreased level of H2A.z seen after MS-275 treatment did not correlate to an increase the MT-1X mRNA level.

In the MRE-d region, the non-treated As^{+3} transformed cell line showed a significant increase in the levels of H2A.z when compared to the parent and Cd^{+2} transformed cell lines. This increase in H2A.z levels correlated to an increase MT-1X mRNA level that was seen in the As^{+3} transformed cells (Figure 29). Treatment with MS-275 resulted in a significant decrease in the H2A.z levels in the As^{+3} transformed cell lines when compared to its non-treated control, a change that did not correlate with the MT-1X mRNA level. The MS-275 treated parent and Cd^{+2} transformed cell lines did not show a significant change in the H2A.z levels when compared to their non-treated controls.

In the MRE-e region, there were significant levels of H2A.z levels in the non-treated As^{+3} and Cd^{+2} transformed cell lines, when compared to the parent cells (Figure 30). These levels correlated to the increased MT-1X mRNA levels that were seen in the transformed cell lines. Treatment with MS-275 resulted in a decrease in the levels of H2A.z in the As^{+3} and Cd^{+2} transformed cell lines. The parent cells showed an increase in the H2A.z levels when compared to its non-treated control, which correlated to the increase in MT-1X mRNA levels. MS-275 initiates transcriptional activation, and the levels of this histone variant tend to increase in transcriptionally active regions. However, in our experiments the levels of H2A.z decreased upon MS-275 treatment.

Figure 28. The effect of treatment with MS-275 on H2A.z levels in the parent, As^{+3} and Cd^{+2} transformed UROtsa cells in the MRE-a region. Statistically significant ($p < 0.05$) when compared to their corresponding cells in the non-treated control group (*), and when compared to the Cd^{+2} transformed cells in the non-treated control group (#).

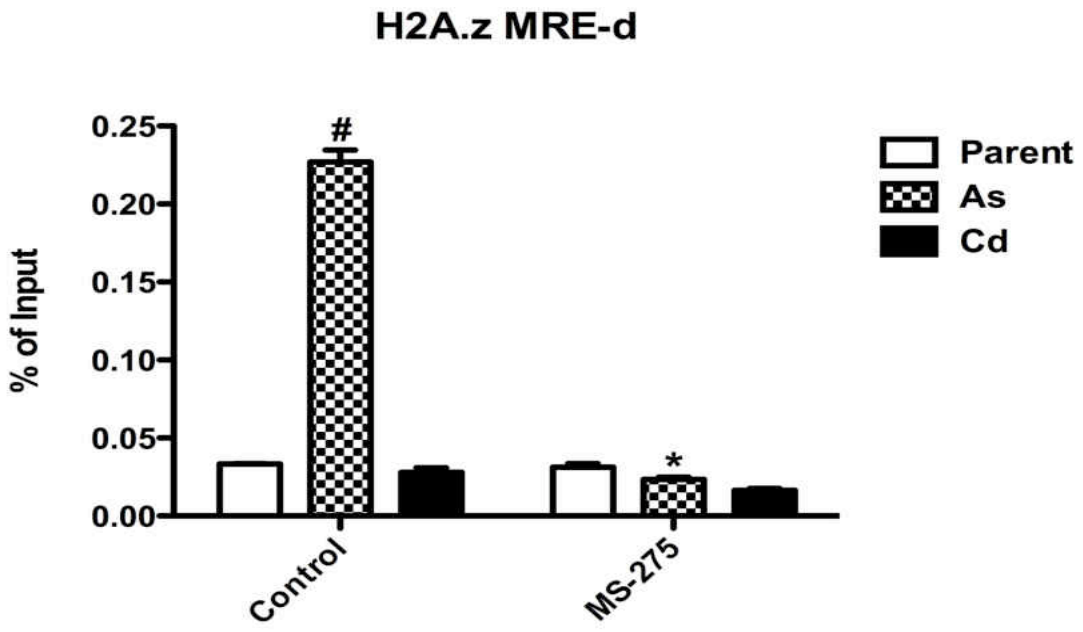

Figure 29. The effect of treatment with MS-275 on H2A.z levels in the parent, As^{+3} and Cd^{+2} transformed UROtsa cells in the MRE-d region. Statistically significant ($p < 0.05$) when compared to their corresponding cells in the non-treated control group (*), and when compared to the parent and Cd^{+2} transformed cells in the non-treated control group and to all other samples (#).

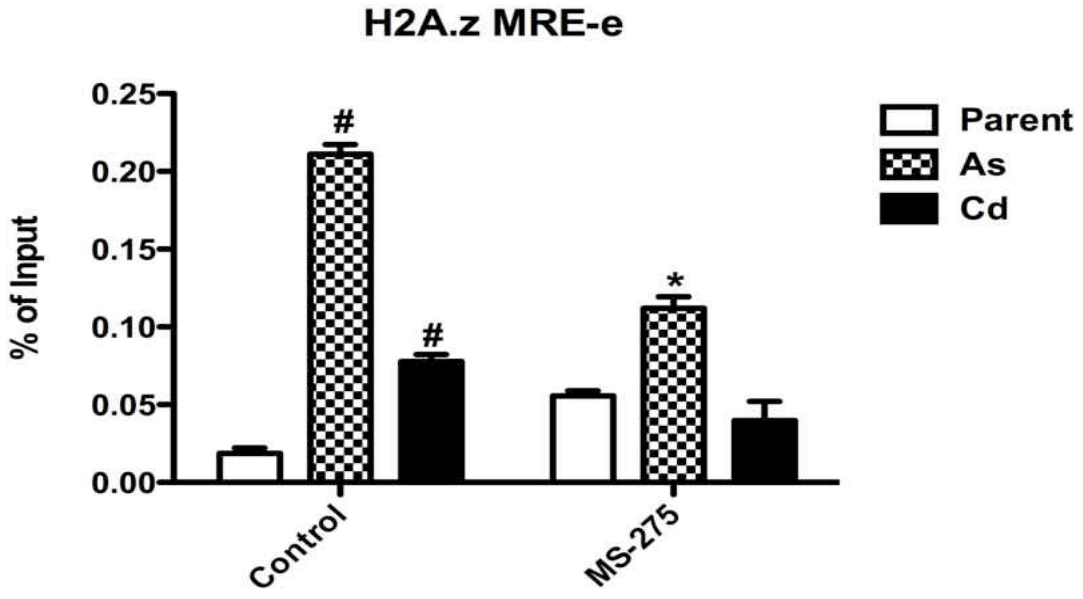

Figure 30. The effect of treatment with MS-275 on H2A.z levels in the parent, As^{+3} and Cd^{+2} transformed UROtsa cells in the MRE-e region. Statistically significant ($p < 0.05$) when compared to their corresponding same cells in the non-treated control group (*), and when compared to the parent cells in the non-treated control group and to one another (#).

The H3.3 ChIP Assay

Histone 3.3 is a variant of the conventional histone H3 that replaces H3 at sites of nucleosomal displacements, marking an actively transcribed gene. Results of the ChIP assay showed that there were detectable levels of H3.3 only in the MRE a & e regions. In the MRE-a region, there were significant levels of H3.3 in the parent and As^{+3} transformed cell line when compared to the Cd^{+2} transformed cell line in the control non-treated group (Figure 31). Treatment with MS-275 resulted in an increase in the level of enrichment in H3.3 in the three cell lines with the highest increase in the Cd^{+2} transformed cell line, which was statistically significant when compared to its non-treated control. This response to treatment with MS-275 correlated with a similar increase in the MT-1X mRNA expression levels.

In the MRE-e region, there was a significant level of H3.3 enrichment in the As^{+3} transformed cell lines when compared to the non-treated parent and Cd^{+2} transformed cell line (Figure 32). This pattern of enrichment correlated with the MT-1X mRNA expression level in the As^{+3} transformed cells. Treatment of the cells with MS-275 resulted in a significant increase in H3.3 levels in the parent and As^{+3} transformed cell lines when compared to their non-treated controls and this pattern of enrichment correlated with the increased MT-1X mRNA level. The Cd^{+2} transformed cell lines had no detectable levels of H3.3.

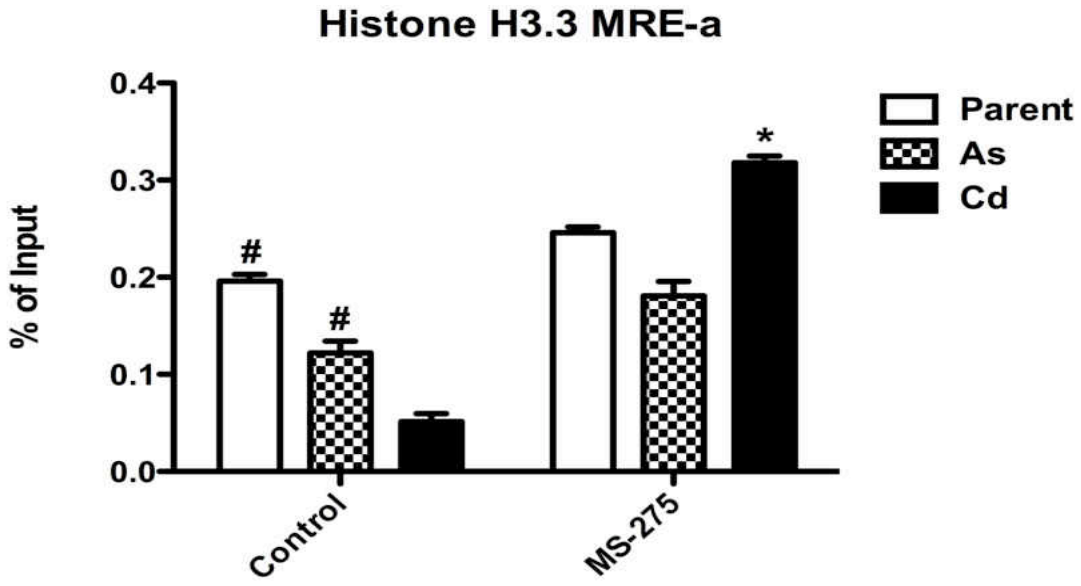

Figure 31. The effect of treatment with MS-275 on histone H3.3 levels in the parent, As^{+3} and Cd^{+2} transformed UROtsa cells in the MRE-a region. Statistically significant ($p < 0.05$) when compared to their corresponding cells in the non-treated control group (*), and when compared to the Cd^{+2} transformed cells in the non-treated control group (#).

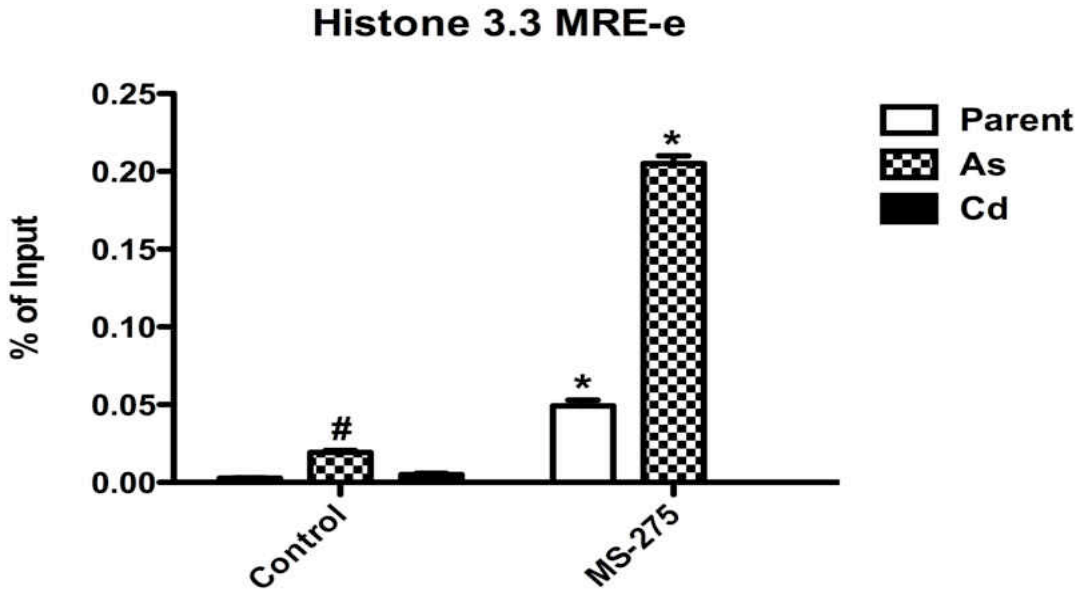

Figure 32. The effect of treatment with MS-275 on histone H3.3 levels in the parent, As^{+3} and Cd^{+2} transformed UROtsa cells in the MRE-e region. Statistically significant ($p < 0.05$) when compared to their corresponding cells in the non-treated control group (*), and when compared to the parent and Cd^{+2} transformed cells in the non-treated control group (#).

The Trimethyl H3K4 ChIP Assay

Trimethylation of the histone H3 tail at the lysine 4 residue, by the lysine methyltransferases (KMTs) confers an active chromatin mark. Results of the trimethyl H3K4 assay in the MRE-a region showed that in this region, there were significant H3K4 levels in the non-treated As^{+3} transformed cell lines, when compared to the parent and Cd^{+2} transformed cell lines of the non-treated control group (Figure 33). The level of methylation at lysine 4 correlated to the MT-1X mRNA expression levels. Treatment with MS-275 resulted in a significant decrease in the levels of H3K4 in the As^{+3} transformed cell lines, while the parent and Cd^{+2} transformed cell lines showed no significant change when compared to their controls. The H3K4 expression levels did not correlate with the MT-1X mRNA expression which increased in all three cell lines after treatment with MS-275.

In the MRE-d region, there were significant H3K4 levels in the parent and As^{+3} transformed cell lines, when compared to the Cd^{+2} transformed cell lines in the non-treated control cells (Figure 34). Treatment with MS-275 resulted in a significant decrease in the levels of H3K4 in the parent and As^{+3} transformed cell lines, while the Cd^{+2} transformed cell line showed no significant change when compared to their non-treated controls. The methylation levels of histone H3 at lysine 4 did not correlate with the MT-1X mRNA levels in the MS-275 treated cells.

In the MRE-e region, there were significant H3K4 levels in the As^{+3} and Cd^{+2} transformed cell lines, when compared to the non-treated parent cell cells (Figure 35). The levels of H3K4 correlated with the MT-1X mRNA expression levels in the control non-treated cells. Treatment with MS-275 resulted in a significant decrease in the levels of H3K4 in the As^{+3} and Cd^{+2} transformed cell lines, while the parent cell lines showed a significant increase when compared to their control. Except for the parent cell lines, the H3K4 levels did not correlate with the MT-1X mRNA expression in the MS-275 treated cells.

The response of the cell lines to the MS-275 treatment by a decrease in their trimethyl H3K4 levels in the three MREs was unexpected. The MS-275 initiates transcriptional activation, and one would have expected that the levels of trimethyl H3K4 would increase since they are enriched in transcriptionally active regions.

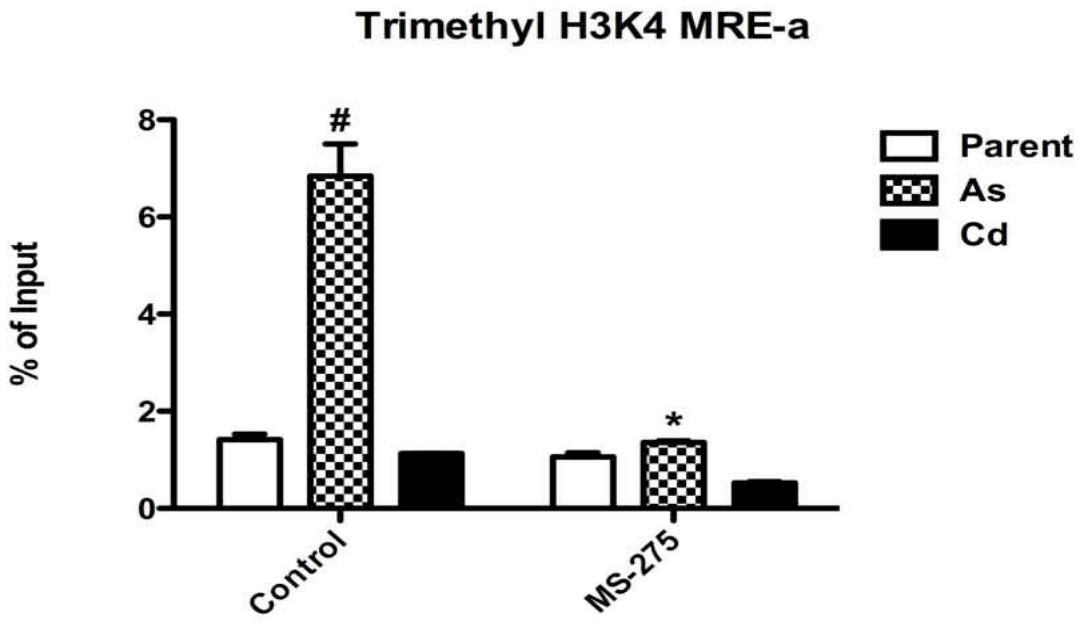

Figure 33. The effect of treatment with MS-275 on H3K4 levels in the parent, As^{+3} and Cd^{+2} transformed UROtsa cells in the MRE-a region. Statistically significant ($p < 0.05$) when compared to their corresponding cells in the non-treated control group (*), and when compared to the parent and Cd^{+2} transformed cells in the non-treated control group and to all other samples (#).

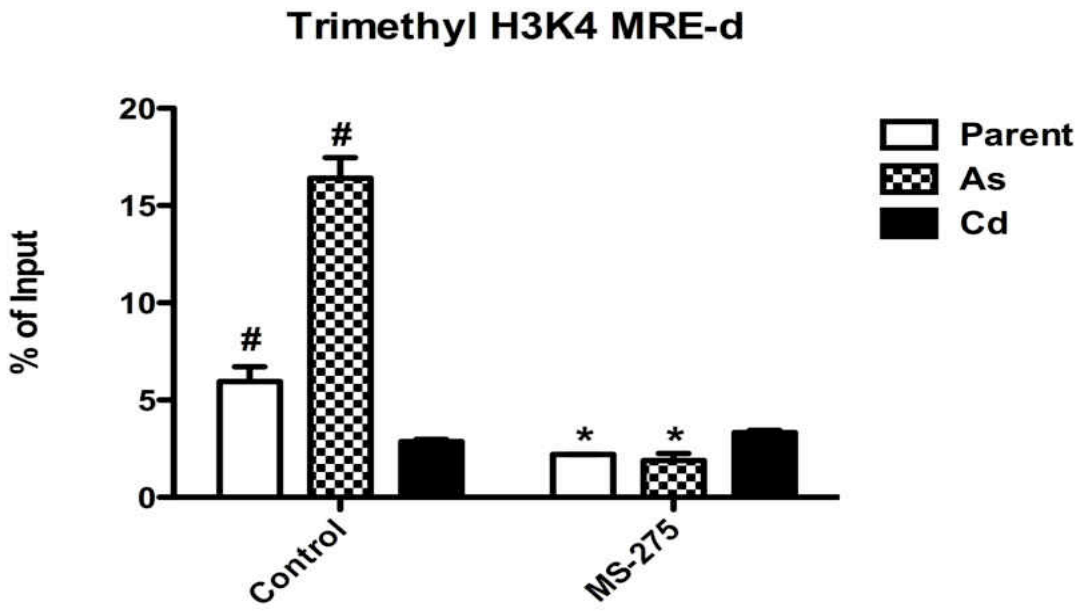

Figure 34. The effect of treatment with MS-275 on H3K4 levels in the parent, As^{+3} and Cd^{+2} transformed UROtsa cells in the MRE-d region. Statistically significant ($p < 0.05$) when compared to their corresponding cells in the non-treated control group (*), and when compared to the Cd^{+2} transformed cells and to one another in the non-treated control group (#).

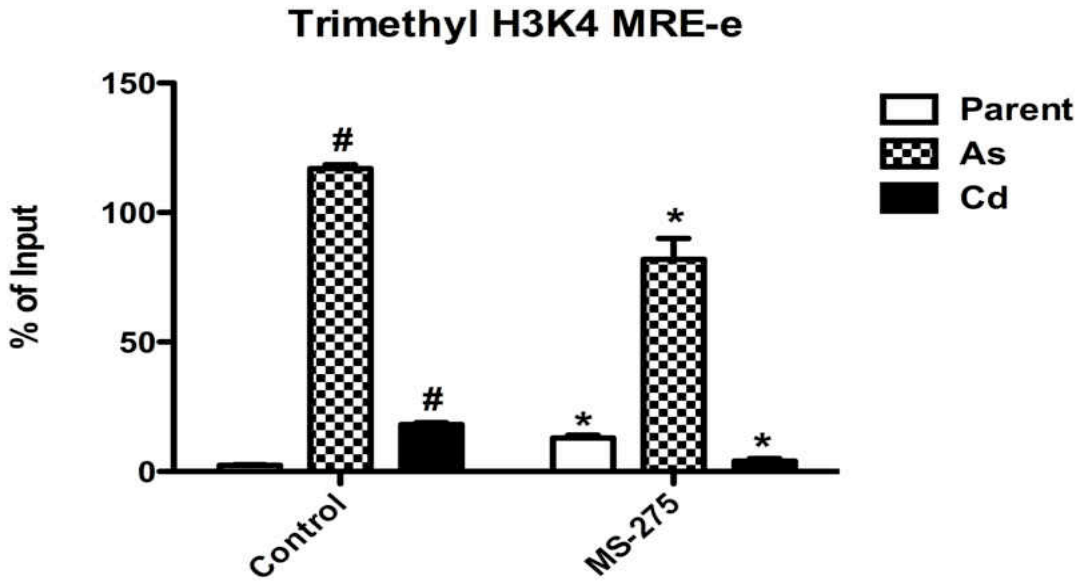

Figure 35. The effect of treatment with MS-275 on H3K4 levels in the parent, As^{+3} and Cd^{+2} transformed UROtsa cells in the MRE-e region. Statistically significant ($p < 0.05$) when compared to their corresponding cells in the non-treated control group (*), and when compared to the parent cells and to one another in the non-treated control group (#).

The Trimethyl H3K27 ChIP Assay

Trimethylation of the lysine 27 of the histone H3 tail results in the propagation of heterochromatin and gene silencing. Analysis of the ChIP assay results show that in the MRE-a region, the parent cell lines had the highest levels of H3K27 levels, when compared to the As^{+3} and Cd^{+2} transformed cell lines of the non-treated control cells (Figure 36). Treatment with MS-275 resulted in a significant increase in the levels of H3K27 in the Cd^{+2} transformed cell line, while the parent and As^{+3} transformed cell lines did not show a significant change in the H3K27 levels when compared to their controls.

In the MRE-d region, there was a significant level of H3K27 in the Cd^{+2} transformed cell line, when compared to the parent and As^{+3} transformed cell lines in the control non-treated cells (Figure 37). Treatment with MS-275 resulted in a significant increase in the levels of H3K27 in the Cd^{+2} transformed cell line, while the parent and As^{+3} transformed cell lines did not show detectable levels of H3K27.

In the MRE-e region, there was a significant level of H3K27 in the As^{+3} transformed cell line, when compared to the parent and Cd^{+2} transformed cell lines in the non-treated control group (Figure 38). Treatment with MS-275 resulted in a significant increase in the levels of H3K27 in the As^{+3} and Cd^{+2} transformed cell lines when compared to the control non-treated cells, while the parent cell line showed a slight increase in H3K27 levels when compared to its control. The increased level of trimethyl H3K27 seen in the MREs of the cell lines after treatment with MS-275 was unexpected, as the transcriptional activation by MS-275 should have resulted in a decrease in the repressive trimethyl H3K27 chromatin marks.

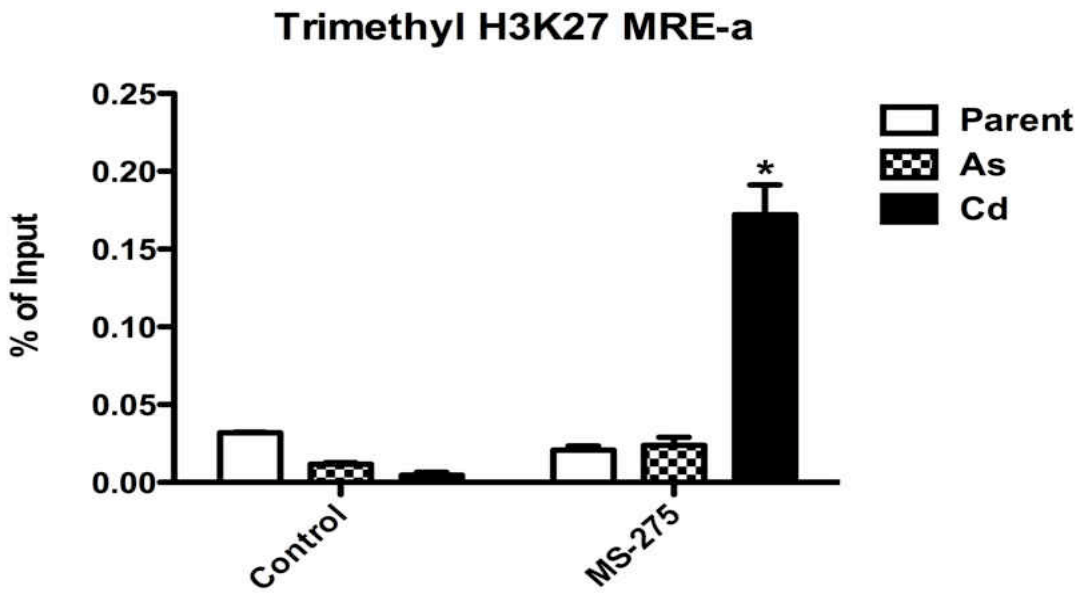

Figure 36. The effect of treatment with MS-275 on H3K27 levels in the parent, As^{+3} and Cd^{+2} transformed UROtsa cells in the MRE-a region. Statistically significant ($p < 0.05$) when compared to their corresponding cells in the non-treated control group, and to all samples (*).

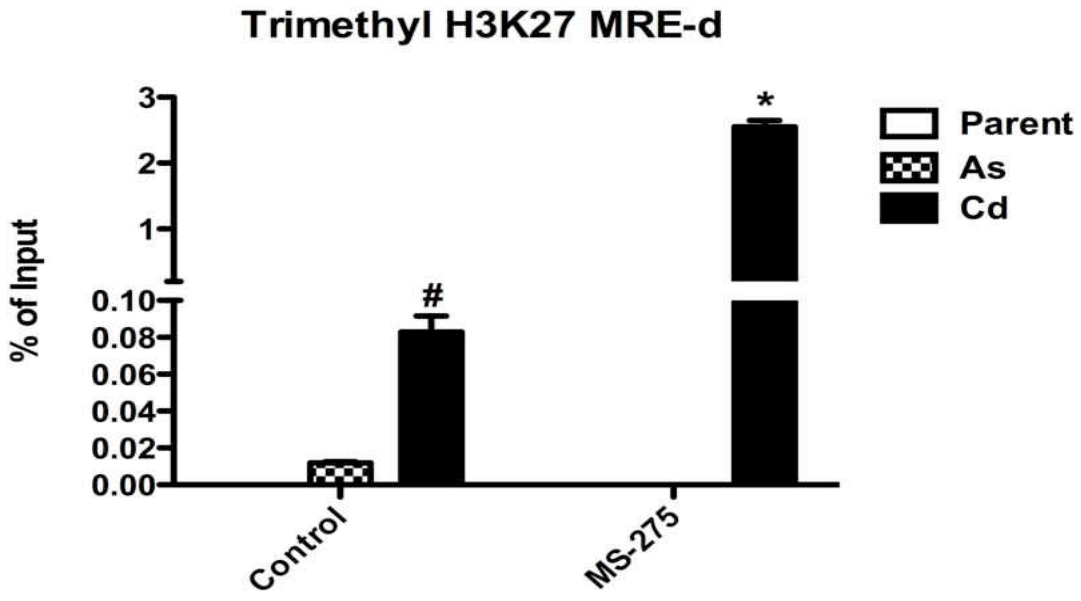

Figure 37. The effect of treatment with MS-275 on H3K27 levels in the parent, As^{+3} and Cd^{+2} transformed UROtsa cells in the MRE-d region. Statistically significant ($p < 0.05$) when compared to their corresponding cells in the non-treated control group (*), and when compared to the parent and As^{+3} transformed cells in the non-treated control group (#).

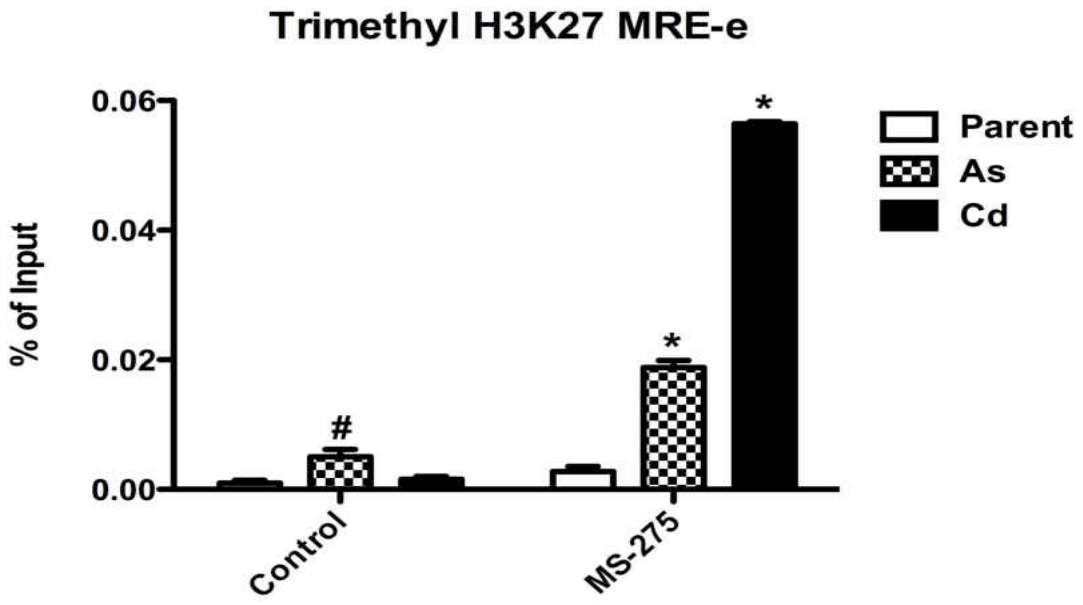

Figure 38. The effect of treatment with MS-275 on H3K27 levels in the parent, As^{+3} and Cd^{+2} transformed UROtsa cells in the MRE-e region. Statistically significant ($p < 0.05$) when compared to their corresponding cells in the non-treated control group and to each other (*), and when compared to the parent and Cd^{+2} transformed cells in the non-treated control group (#).

The Histone H3 ChIP Assay

ChIP assay on total histone H3 was performed to compare and correlate its levels to the histone H3 modifications tested. In the MRE-a region, there were significant levels of H3 in the parent and As^{+3} transformed cell lines when compared to the Cd^{+2} transformed cell lines in the non-treated control group (Figure 39). Treatment with MS-275 resulted in a significant decrease in the level of H3 in the parent and As^{+3} transformed cell lines, when compared to their controls. There was a significant increase in the levels of H3 in the Cd^{+2} transformed cell lines, when compared to its control.

In the MRE-d region, there were significantly increased levels of H3 in the As^{+3} transformed cell line when compared to the parent and Cd^{+2} transformed cell lines in the non-treated control group (Figure 40). Treatment with MS-275 resulted in a significant decrease in the level of H3 in the As^{+3} transformed cell line, and a significant increase in its levels in the Cd^{+2} transformed cell line, when compared to their non-treated control. The parent cell line showed no change in the H3 levels.

In the MRE-e region, there were significant levels of H3 in the As^{+3} transformed cell line when compared to the parent and Cd^{+2} transformed cell lines in the non-treated control cells (Figure 41). Treatment with MS-275 did not result in any significant change in the three cell lines, when compared to their non-treated controls.

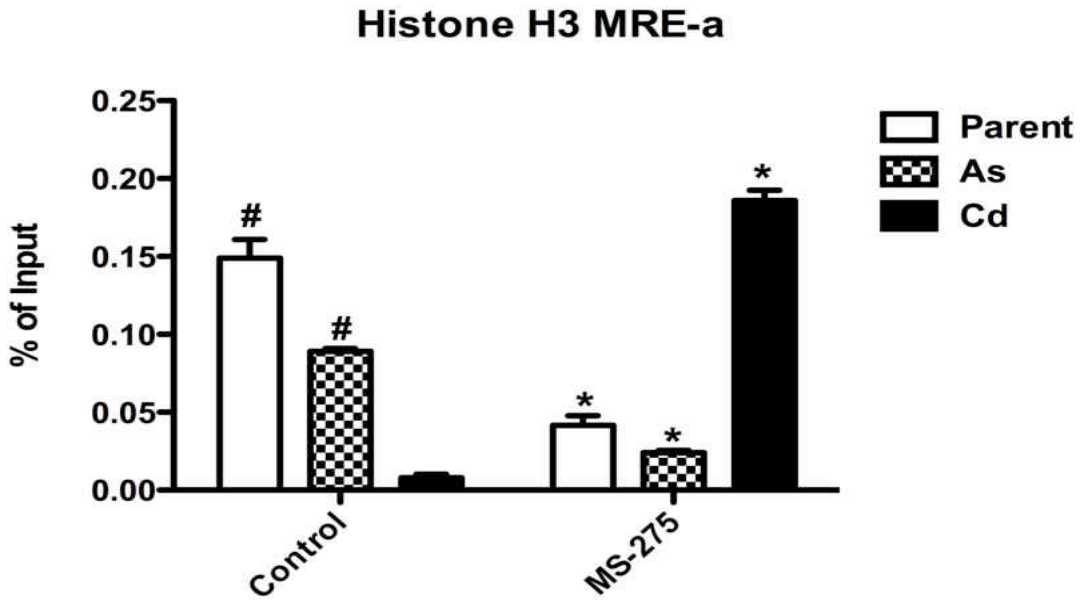

Figure 39. The effect of treatment with MS-275 on histone H3 levels in the parent, As^{+3} and Cd^{+2} transformed UROtsa cells in the MRE-a region. Statistically significant ($p < 0.05$) when compared to their corresponding cells in the non-treated control group (*), and when compared to the Cd^{+2} transformed cells in the non-treated control group (#).

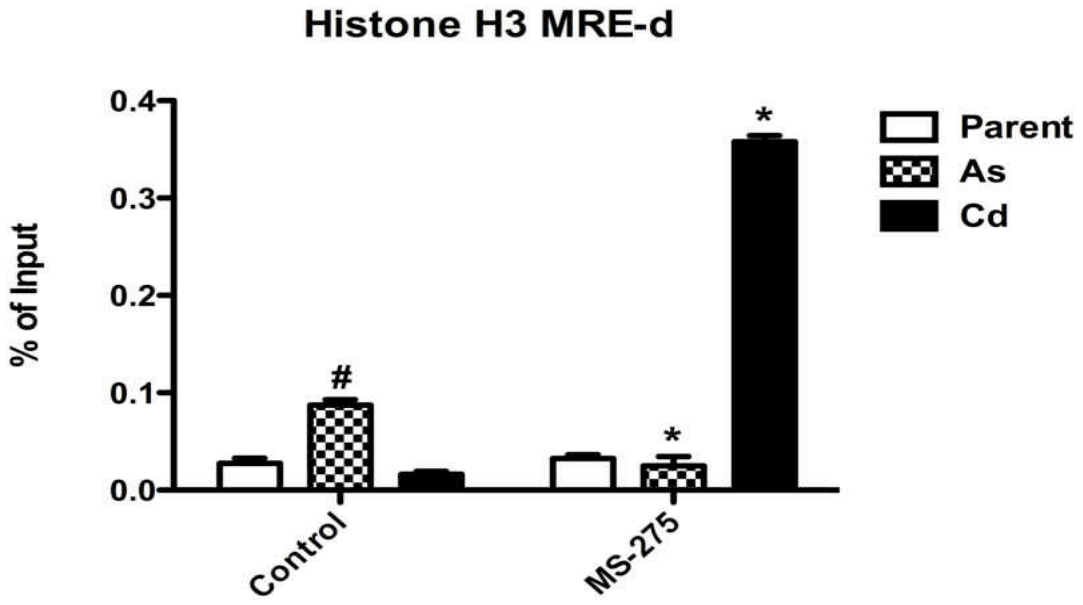

Figure 40. The effect of treatment with MS-275 on histone H3 levels in the parent, As^{+3} and Cd^{+2} transformed UROtsa cells in the MRE-d region. Statistically significant ($p < 0.05$) when compared to their corresponding cells in the non-treated control group and to one another (*), and when compared to the parent and Cd^{+2} transformed cells in the non-treated control group (#).

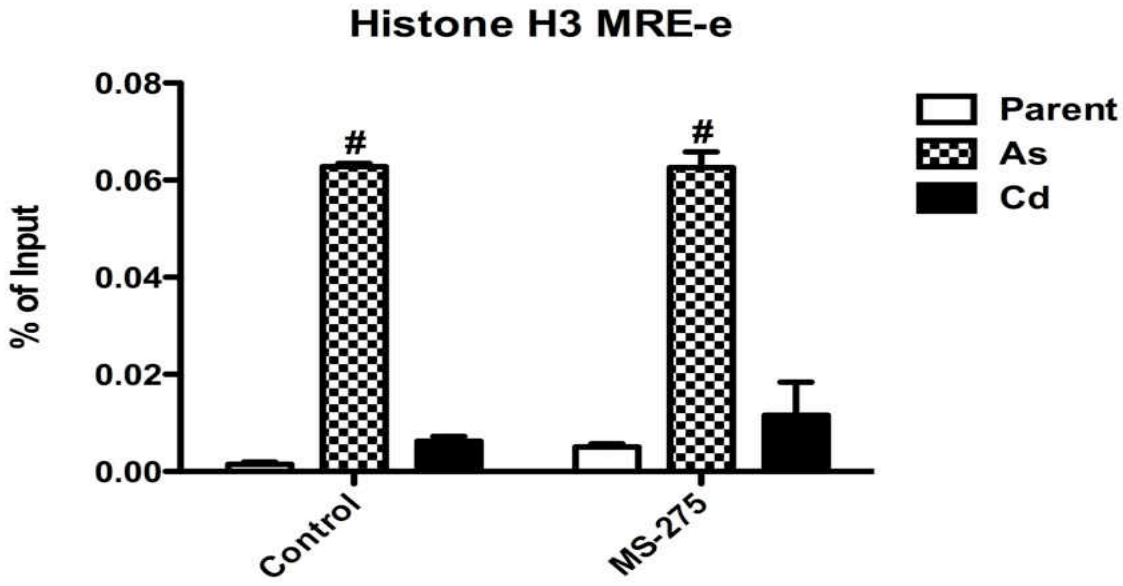

Figure 41. The effect of treatment with MS-275 on histone H3 levels in the parent, As^{+3} and Cd^{+2} transformed UROtsa cells in the MRE-e region. Statistically significant ($p < 0.05$) when compared to other cells in the same treatment group (#).

Part II: Kindlin-2

Selection of Kindlin-2 for Analysis of Gene Expression in Urothelial Cancer

Each of the 13 independent isolates of As^{+3} and Cd^{+2} transformed UROtsa cell lines were characterized for their pattern of gene expression against the UROtsa parental cell line using the Affymetrix human Genome U133 plus 2.0 array chip. The data were then analyzed for differences between the 3 transformed cell lines able to effectively generate peritoneal tumors (As# 1, As# 3, and Cd# 1) and those that formed no peritoneal tumors (As# 2, As# 5, and As# 6; Cd# 2 to Cd# 7). Those cell lines designated as effective for generating peritoneal tumors produced >100 separate tumor nodules per mouse. One cell line (As# 4) generated a low number of peritoneal tumors, between 3 and 20 among the 6 mice tested, and was not used in the analysis. A set of 5 genes were identified that were the most consistently repressed in the cell lines able to form peritoneal tumors when compared with those unable to form peritoneal tumors. Similarly, a set of 5 genes were identified that were the most induced in the cell lines able to form peritoneal tumors when compared with those unable to form peritoneal tumors. These 10 genes are identified in (Table 2). The *PLEKHC1* gene, also known as Kindlin-2, was chosen for further characterization based on the fact that it was the gene most consistently differentially repressed between the 2 sets of cell lines.

Table 2: Differentially expressed genes in peritoneal tumor forming, metal-transformed UROtsa cells. The fold change and the Log 2-fold change represent the average fold change in the cell lines able to form peritoneal tumors compared with the non-tumor forming ones.

Gene Symbol	Gene	Log 2-fold Change	Fold Change
CALB1	Calbindin 1, 28 kDa	4.80	27.87
SPRR3	Small proline-rich protein 3	3.32	10.05
ADH7	Alcohol dehydrogenase 7	3.14	8.83
ODZ2	Odz, odd Oz/ten-m homologue 2	2.98	7.94
ZNF703	Zinc finger protein 703	2.65	6.32
KRT7	Keratin 7	−3.36	0.10
PTN	Pleiotrophin	−3.17	0.11
CTHRC1	Collagen triple helix repeat containing 1	−3.07	0.12
LRRN1	Leucine rich repeat neuronal 1	−2.84	0.14
PLEKHC1	Pleckstrin homology domain containing, family C member 1	−2.60	0.16

Kindlin-2 mRNA and Protein Expression in Parental UROtsa, As^{+3} and Cd^{+2} Transformed Cell Lines, and their Sc Tumors

The expression of Kindlin-2 mRNA was determined on the parental UROtsa cells and the As^{+3} and Cd^{+2} transformed cell lines (Figure 42 A). The results of this analysis demonstrated that Kindlin-2 mRNA was expressed in the parental UROtsa cell line. The 2 A^{+3} transformed cell lines (As# 1, As# 3) and the 1 Cd^{+2} transformed cell line (Cd# 1), which were able to effectively form peritoneal tumors, had reduced expression of Kindlin-2 mRNA when compared with the parental cell line and all other As^{+3} and Cd^{+2} transformed cell lines (Figure 42 A). The 3 As^{+3} transformed and the 6 Cd^{+2} transformed cell lines unable to form peritoneal tumors displayed Kindlin-2 mRNA levels similar to, or elevated above, those of the parental cell line. A corresponding analysis of Kindlin-2 protein expression by Western blotting generally followed the above pattern of Kindlin-2 mRNA expression (Figure 42 B). Western blotting showed that the parental cell line expressed Kindlin-2 protein. The relative amount of Kindlin-2 protein expression in the parental cells was below that of the 9 As^{+3} and Cd^{+2} transformed cell lines unable to form peritoneal tumors. In contrast, the relative amount of Kindlin-2 protein expression in the parental cells was above that of the 2 As^{+3} transformed cell lines (As# 1, As# 3) and the 1 Cd^{+2} transformed cell line (Cd# 1) that were able to effectively form peritoneal tumors. Overall, the determination of Kindlin-2 mRNA and protein in each cell line confirmed the observation regarding Kindlin-2 expression in the initial microarray-based analysis. The expression of Kindlin-2 mRNA and protein was also determined for the SC tumors generated from the 6 As^{+3} and 7 Cd^{+2} transformed cell lines (Figure 43 A & B).

Kindlin-2 mRNA was expressed in all the Cd^{+2} transformed cell lines (Figure 43 A). The expression of Kindlin-2 mRNA was similar in tumors generated from the Cd# 1, Cd# 4, Cd# 5, and Cd# 7 cell lines and, in comparison with these tumors, elevated in the tumors derived from the Cd# 2, Cd# 3, and Cd# 6 cell lines. The corresponding analysis of Kindlin-2 protein in the Cd^{+2} transformed cell lines by Western blotting demonstrated that all the cell lines expressed Kindlin-2 protein, but that there was no correlation between the levels of Kindlin-2 mRNA expression and that of the corresponding protein (Figure 43 B). Acute studies of Kindlin-2 expression were not performed on the parental UROtsa cell line.

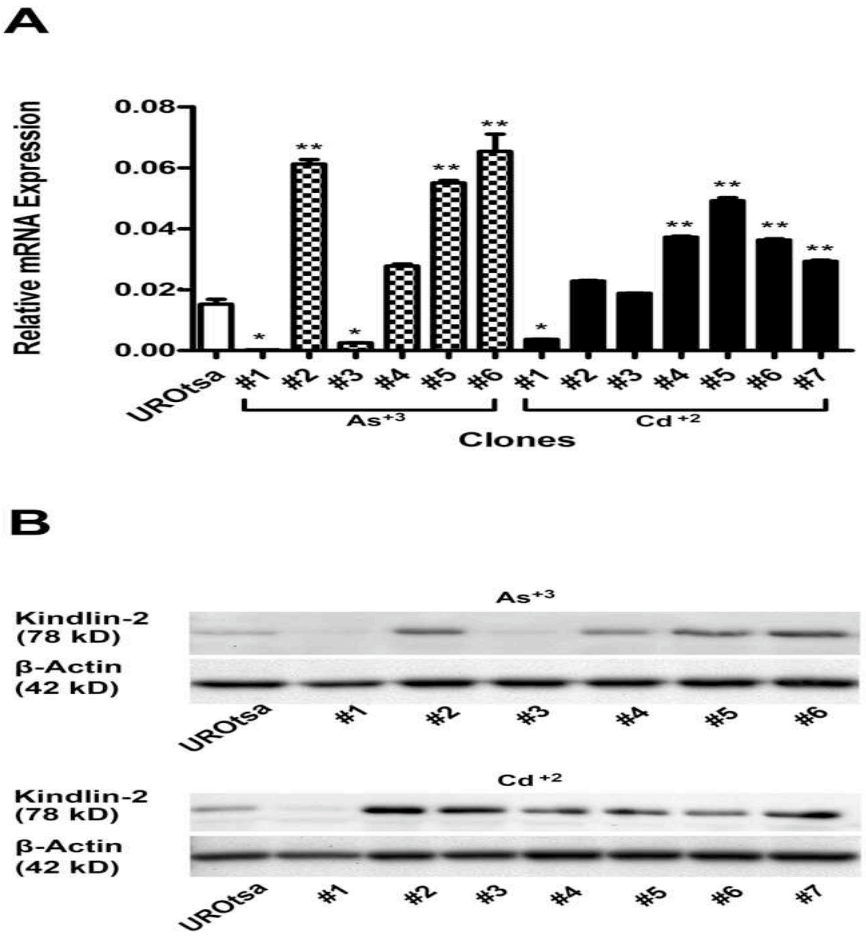

Figure 42. Expression of Kindlin-2 mRNA and protein in UROtsa parent, As^{+3} and Cd^{+2} transformed isolates and SC tumor heterotransplants. RT-PCR analysis of Kindlin-2 in UROtsa parent and transformed isolates (A). Western analysis of Kindlin-2 in UROtsa and transformed isolates (B). All statistical significance is denoted at *P* <.05. Reduced compared with parental cells and other cell lines (*), and elevated compared with parental cells (**) (Talaat *et al.,* 2011).

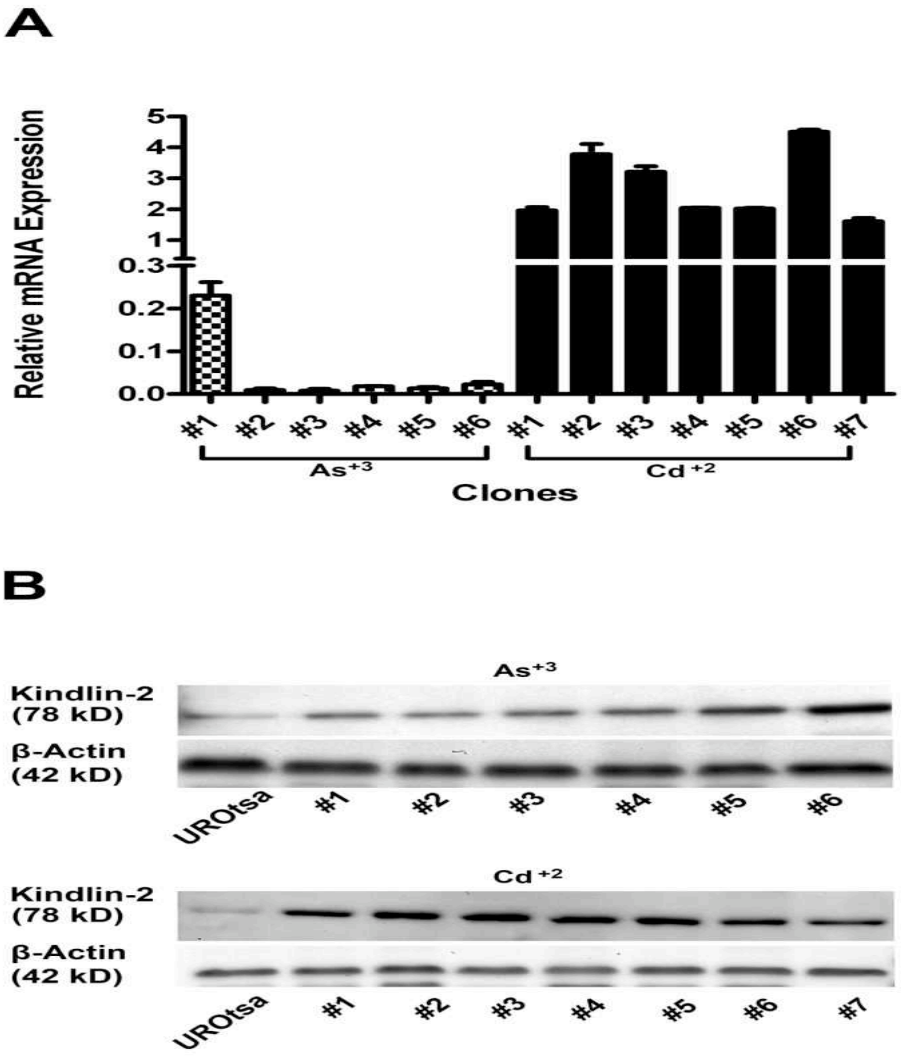

Figure 43. Expression of Kindlin-2 mRNA and protein in UROtsa parent, As^{+3} and Cd^{+2} transformed isolates and sc tumor heterotransplants. RT-PCR analysis of Kindlin-2 in the SC tumor heterotransplants (A). Western analysis of Kindlin-2 in the SC tumor heterotransplants (B). All statistical significance is denoted at *P* <.05. Reduced compared with parental cells and other cell lines (*), and elevated compared with parental cells (**) (Talaat *et al.,* 2011).

Immunohistochemical Staining of Kindlin-2 in Tumor Heterotransplants

The immunohistochemical analysis of Kindlin-2 expression in the SC tumors showed no staining of Kindlin-2 in the urothelial tumor cells produced by any of the As^{+3} or Cd^{+2} transformed cell lines. In contrast, the stromal components of all the urothelial tumors were moderately to strongly positive for the expression of Kindlin-2 protein. The stromal components of the tumors are presumably of murine origin and recruited to the tumor site. There were also occasional blood vessels within the tumors that were weakly to moderately immunoreactive for Kindlin-2. An example of this immunostaining pattern of Kindlin-2 is illustrated for SC tumors generated from 2 As^{+3} and 2 Cd^{+2} transformed cell lines (Figure 44 A-D). An identical result for Kindlin-2 staining was obtained for the IP tumors produced from the Cd# 1 and As# 1 and As# 3 cell lines, with the urothelial cancer cells negative and the stromal cells positive for Kindlin-2 expression. An example is shown for the As# 1 and Cd# 1 cell lines (Figure 44 E &F).

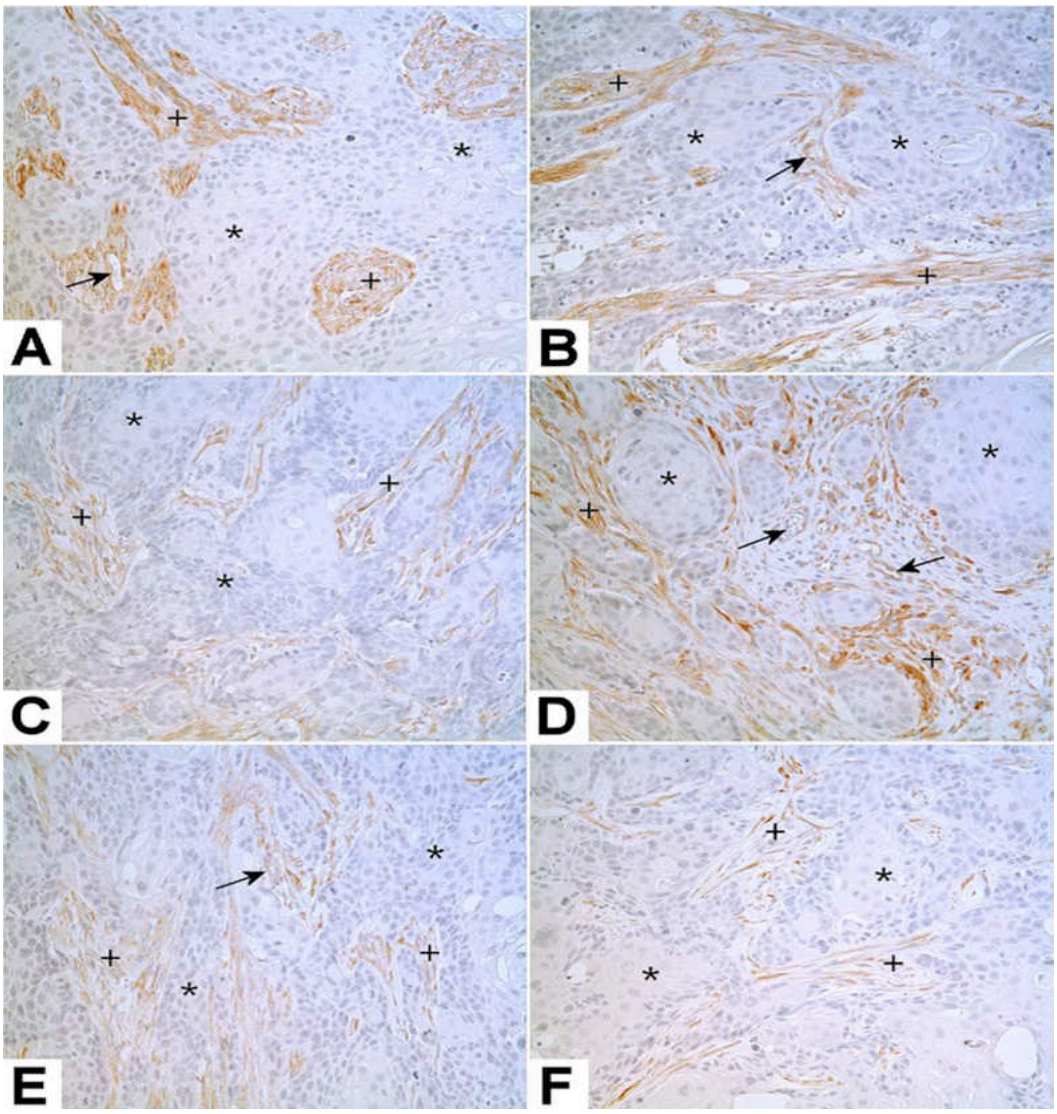

Figure 44. Immunostaining of Kindlin-2 in tumor heterotransplants. Kindlin-2 is shown in representative mouse subcutaneous heterotranplants from As#2 (A), As#4 (B), Cd#2 (C), Cd#3 (D) cell lines, and intraperitoneal heterotransplants from As#1 (E), Cd#1 (F) cell lines. The tumorous epithelium is negative for Kindlin-2 (*), but the stroma is moderately to strongly positive for Kindlin-2 (+), Some small blood vessels in the tumor shown weak to moderate staining of Kindlin-2 (arrows) (Talaat *et al.,* 2011). Original magnification:200X.

Immunohistochemical Staining of Kindlin-2 in Benign Human Bladder and Urothelial Cancer

The immunohistochemical staining of Kindlin-2 was determined on 6 archival specimens of benign human bladder, 5 cases of low-grade carcinoma, 6 cases of noninvasive high-grade carcinoma, and 16 cases of invasive high-grade carcinoma. There was no staining of Kindlin-2 in the normal urothelial cells present in all 6 cases of benign human bladder (Figure 45 A). In all 6 cases of benign human bladder, there was Kindlin-2 staining of the stromal, endothelial, and smooth muscle cells (Figure 45 A). There was no staining of Kindlin-2 in the tumorous epithelium in all 5 cases of low-grade carcinoma (Figure 45 B). In all 5 cases, there were some stromal cells and small blood vessels in the papillary core that were moderately positive for Kindlin-2. The 6 cases of noninvasive high-grade urothelial cancer showed no staining of Kindlin-2 in the tumorous epithelium, but did show moderate to strong staining for Kindlin-2 in the stroma and small blood vessels in the papillary core (Figure 45 C & D). In contrast to the noninvasive low- and high-grade cancers, 2 of the 16 cases of invasive, high-grade urothelial cancer were found to have areas of Kindlin-2 expression in the tumorous epithelium. Kindlin-2 expression in the malignant cells was focal in expression and comprised approximately 30% of the tumor cells (Figure 45 E & F). In all the cases of high-grade invasive urothelial cancer, the stromal cells and small blood vessels were stained for Kindlin-2.

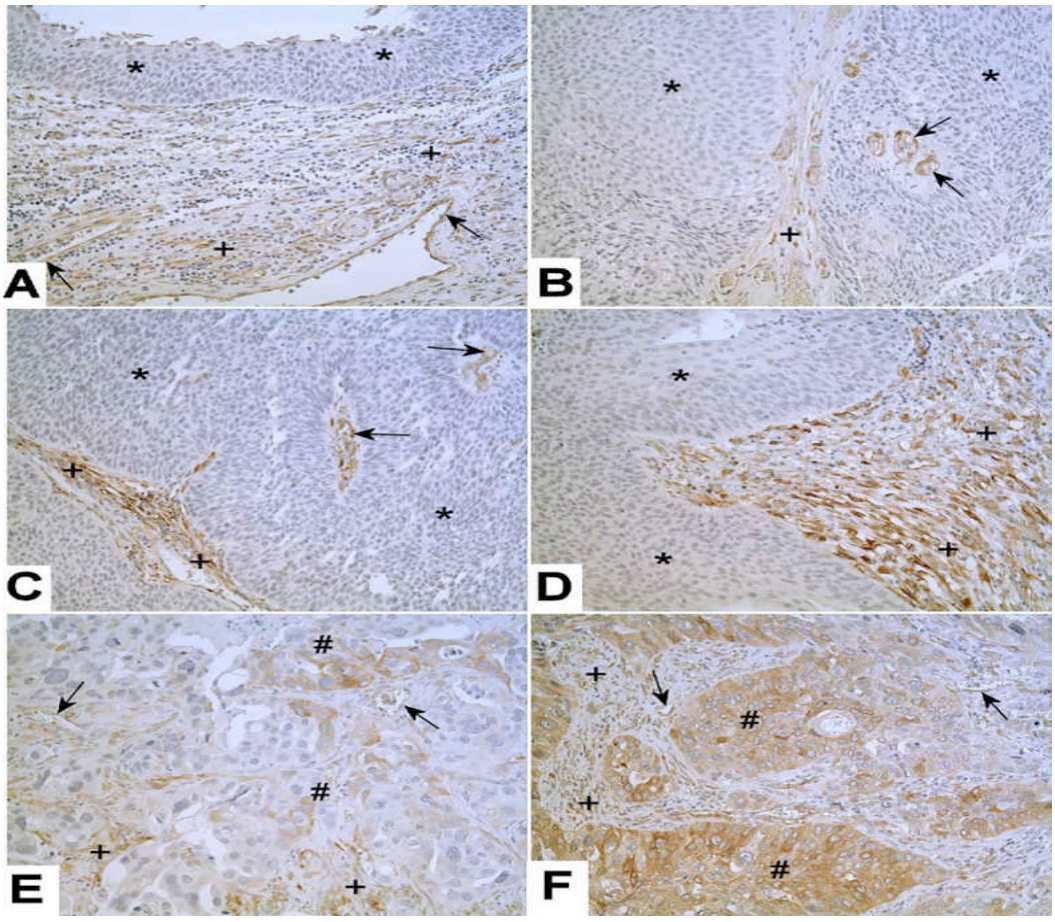

Figure 45. Immunostaining of Kindlin-2 in Benign Human Bladder and Urothelial Carcinoma. Kindlin-2 is shown in representative benign human bladder (A), low-grade urotheliel carcinoma (B), high-grade noninvasive carcinoma (C, D), and high-grade invasive carcinoma (E, F). There is no staining of Kindlin-2 in benign urothelium, and the tumorous epithelium from low grade carcinoma and high grade noninvasive carcinoma (*, A-D), but in 2 cases of high grade invasive carcinoma, the tumorous epithelium shows focal positivity of Kindlin-2 (#, E and F). The stromal cells from benign bladder and urothelial carcinoma are positive for Kindlin-2 (+); some small blood vessels from both benign bladder and urothelial carcinoma are also positive for Kindlin-2 (arrows) (Talaat *et al.,* 2011).

Chapter V

Discussion

Part I: MT-1X

The mRNA Changes in the UROtsa Cells as They Undergo the Process of Malignant Transformation

The UROtsa cell culture system was derived from the normal urothelial lining of the ureter of a 12-year-old female. Although these cells were immortalized through the use of a simian virus 40 (SV40) large T-antigen, they have been proven to be non-tumorogenic through their inability to form colonies when grown on soft agar, and when injected in nude mice (Petzoldt *et al*., 1995). The UROtsa cells were suggested for use as a cell culture model system to study the effects of environmental insults and cell stressors on the urothelium (Rossi *et al.*, 2001). Cadmium and As^{+3} are environmental toxicants that are associated with many types of cancer, but there has been no direct evidence, other than numerous epidemiological studies, that linked As^{+3} and Cd^{+2} to the development of bladder cancer. In an effort to develop an *in vitro* model system of agent-induced bladder cancer, Sens & colleagues were the first to report the successful malignant transformation of UROtsa cells after long-term exposure to As^{+3} and Cd^{+2} (Sens *et al*., 2004). In addition to their expression in response to different oxidative and cell stress conditions, the expression of MTs in different types of cancers has long been under investigation, and among these is bladder cancer.

A previous study by members of this laboratory has shown the absence of MT I/II expression in normal bladder tissues and a correlation between the intensity of MT I/II staining and bladder cancer tumor grade (Somji *et al*., 2001). This study has also shown that there was positive staining for MT I/II in all high-grade tumor samples. Due to the fact that the antibody used in immunohistochemical staining cannot distinguish between the MT-I & MT-II isoforms, mRNA analysis was done to discern the different MT I/II isoforms expressed. Findings determined that there was a significant increase in the MT-1X mRNA expression in all three grades of bladder cancer examined: carcinoma in situ and low and high-grade transitional cell carcinomas. Another study reported the absence of MT I/II immunohistochemical staining in benign lesions and in low-grade bladder cancer, and a high degree of expression in high-grade muscle-invasive bladder cancer. This study also reported positive stromal staining for MT I/II in heterotransplant tumors formed following the SC injection of As^{+3} and Cd^{+2} transformed tumor cells in athymic nude mice. One of the conclusions of that study was that MT I/II might be developed as a prognostic biomarker in the progression of advanced bladder cancer (Zhou *et al*., 2006). The overall conclusions from the two previous studies discussed were that MT I/II isoforms showed strong expression in high-grade muscle-invasive bladder cancers, and that MT-1X might be the predominant isoform responsible for these elevated levels.

Based on the previous studies, there was an interest to further investigate the role of MT-1X in bladder cancer. The murine MT-1, as well as the human MT2-A promoters have been extensively studied, but there are very few studies examining the MT-1X

promoter. This lack of data led us to further characterize the MT-1X promoter in an effort to determine the mechanism involved in the increased expression of MT-1X in bladder cancer.

The first goal of this study was to identify, through an *in silico* analysis, the potential transcription factor binding sites especially the MREs, and to design specific primers that would span the MREs to which MTF-1 binds and subsequently stimulates the transcription of MTs. Results of this analysis showed that there were five MREs in the promoter of MT-1X, and five primer sets to amplify these MREs were designed and tested for specificity and efficiency. Of these five primer sets, only the primers covering MREs a, d, & e were specific for MT-1X and attained a favorable PCR efficiency that was close to 100%. The difficulty in designing primers that are specific for each paralog can be largely attributed to the fact that these paralogs arose as a result of MT-1 gene duplication events during the process of primate evolution to the modern human (Moleirinho *et al*., 2011). Consequently, the significant degree of gene promoter sequence homology that these paralogs share presents a technical challenge in designing isoform-specific primers in either the coding region or the immediate upstream region of each MT gene.

Previous studies from this laboratory have shown that the MT-1X mRNA was up-regulated in bladder cancer (Somji *et al*., 2001). In order to determine the mechanism that regulates the expression of MT-1X during cellular transformation, UROtsa cells were exposed to 1 µM of As^{+3} or Cd^{+2} for either 48 h (short term) or were sub-cultured in the presence of these metals for 5 passages (long term, P5). Total RNA was extracted

from the harvested cells, and used to examine the MT-1X mRNA expression in the short- and long-term exposure to metals, and to compare its expression pattern in these experiments to that of the UROtsa cells transformed by As^{+3} and Cd^{+2}. The goal being to look at changes in MT-X mRNA levels that may occur during the process of malignant transformation (Appendix A). Results of these experiments determined that MT-1X was induced nearly 10 fold by exposure to 1 µM Cd^{+2}, whereas exposure to 1 µM As^{+3} exhibited only a modest increase in expression, similar to what was observed in a previous study (Sens *et al*., 2003). Cadmium is well known for its potent MT-inducing properties (Klaassen *et al*., 1999), thus during the pre-transformation phase, MT-1X was induced and to the greatest extent with Cd^{+2}. Analysis of MT-1X expression in the metal transformed cells, analyzed under no current metal exposure, showed that the MT-1X levels remained elevated in the As^{+3} transformed cells, but were back to near basal levels in the Cd^{+2} transformed cells. In addition, exposure to MS-275, Zn^{+2}, or MS-275+Zn^{+2} treatments resulted in an increase in MT-1X expression in the three experiments (48h, P5, and metal-transformed) in the three cell lines to varying degrees (Appendix A) when compared to their non-treated controls. Therefore, based on the previous studies that documented the elevated levels of MT I/II protein and increased expression of MT-1X mRNA in bladder cancer, and our studies that show increased levels of MT-1X mRNA in As^{+3} transformed cells, it is possible to speculate that exposure to As^{+3} may increase MT-1X in malignant tumors of the urinary bladder, and that this increase correlates with poor prognosis.

The Binding of MTF-1 to the MREs: MTF-1 protein domains and preferential binding to MREs

Transcriptional activation of MTs is dependent on the binding of MTF-1 to the MT promoter. MTF-1 regulates the transcription of many genes including MTs, which in turn, regulate Zn^{+2} homeostasis within the cell. Zinc is an element that is essential for the cell's homeostasis but is toxic to the cell if present in excessive amounts; therefore its levels have to be highly regulated. MTF-1 is a Zn^{+2} sensor, and upon sensing an excessive amount of Zn^{+2}, it translocates from the cytoplasm to the nucleus where it recognizes, and binds to several non-identical MREs in the MT promoter. The binding of MTF-1 to specific MREs stimulates MT transcription through the recruitment of, and interactions with elements of the RNA polymerase II transcriptional machinery, the p300 HAT, and several transcription factors. MTF-1 is essential for both the basal and heavy metal-induction of MTs (Haq *et al.* 2003, Smirnova *et al*. 2000, Westin *et al*. 1988, and Heuchel *et al*. 1994).

MTF-1 has several domains, the most conserved of which is the DNA-binding domain, containing six zinc fingers near its N-terminal end, and is involved in the Zn^{+2} sensing function of MTF-1 and in the metal-dependent transcriptional activation of MTs. There are three other domains in the MTF-1 protein namely: the acidic domain, the proline-rich domain, and the serine/threonine rich domain. These domains are less conserved than the DNA-binding domain, and vary between different species (Laity *et al.*, 2007). Although the DNA binding domain is the one involved in the metal-dependent transcriptional activation of MTs, this does not exclude the possibility of one of the other less conserved domains, or other factors, being responsible for the metal-

dependent transcriptional activation of MTs. Deletion mutants of the human MTF-1 provided evidence about the importance of the acidic and the proline-rich domains in the metal induction of MT (Radtke *et al.*, 1995). Another study characterized the presence of a cysteine-rich cluster in the human MTF-1 that is located C-terminal to the serine/threonine rich domain, and can directly bind Zn^{+2} to activate MT transcription independent of the zinc-finger domain. It was concluded that this complex alters the interaction of MTF-1 with the chromatin and with the other proteins and cofactors that are involved in the transcriptional activation of MTs (Chen *et al*., 2003).

The third goal of this study was to assess the difference in the accessibility of MTF-1 to the MT-1X MREs between the parental and As^{+3} and Cd^{+2} transformed UROtsa cells. The effect of treatment of the cells with MS-275, Zn^{+2}, or the combined exposure to both agents on the binding of MTF-1 to the MREs was also investigated. The results of these experiments showed that while there were various degrees of MTF-1 binding in the MREs in the no treatment and in the MS-275 treated groups, there was no detectable binding in any of the Zn^{+2} treated cell lines in any of the MREs tested (Appendix B). As discussed in the preceding section, MTF-1 is a Zn^{+2} sensor, and upon sensing an excessive amount of Zn^{+2} it binds to the MREs in the MT promoter to initiate MT transcription. Thus, the lack of detectable binding upon Zn^{+2} treatment came rather as a surprise. More perplexing was the fact that the MS-275 followed by the Zn^{+2} treatment resulted in a significant increase in binding in the parental, and As^{+3} and Cd^{+2} transformed UROtsa cells. The author currently has one hypothesis that might explain these findings and it involves the inability to generate MT-1X specific primers for MREs b

& c. This can be largely attributed to the high degree of homology between the different MT-1 paralogs, as discussed earlier, and can point to an important function for MREs b & c (Haq *et al*., 2003) that can involve the initiation of transcription in the MT-1X promoter. It is also noteworthy that the MREs differ between one another in their binding of MTF-1 and their response to heavy metals (Stuart *et al*., 1984). Therefore, this hypothesis assumes that the initiation of transcription of MT-1X involves the association of MTF-1 with MREs a, d, & e under Zn^{+2} deficient conditions and that under Zn^{+2} treatment conditions, MTF-1 preferentially binds either or both of MREs b & c (Appendix B). This hypothesis might explain the absence of detectable binding in MREs a, d, & e upon Zn^{+2} treatment but does not account for the marked increase in MT-1X mRNA expression observed under the combined MS-275 and Zn^{+2} treatment conditions, when compared to the MS-275-only treatment group, and might point to the possible involvement of additional factors.

Transcription Factor Binding and Histone Modifications in the MT-1X Promoter are Under the Effects of Epigenetic Regulation

Inside the cell, approximately, every 147 base pairs of DNA are wound around an octamer histone core and this ever-changing state of DNA packaging is named "chromatin". The octamer histone core consists of four histones: H2A, H2B, H3 and H4. Histones are generally globular in nature, with unstructured N-terminal tails, and a distinguishing feature of these histones is the presence of a large number of modified residues, particularly on their N-terminal tails. At least eight types of post-translational modifications have been identified, and these include: acetylation, methylation, phosphorylation, ubiquitylaion, sumoylation, and ADP-ribosylation (Kouzarides *et al.*,

2007). These post-translational modifications, along with DNA methylation are epigenetic marks that are essential in the regulation and propagation of heritable gene expression (Martinez-Zamudio *et al*., 2011).

A study by Somji & colleagues revealed that the MT-3 promoter was under epigenetic control, and that it was in a "poised state" carrying both marks of activation and repression in a "transcription-ready" state (Somji *et al*., 2011). This finding raised the possibility that the MT-1X promoter could also be under epigenetic control, and that this type of regulation contributes to its long-term up-regulation in human bladder cancers. Thus the fourth goal of this study was to utilize the ChIP technique to assess transcription factor binding and histone modifications across the non-transformed parent, compared to the Cd^{+2} and As^{+3} transformed cells in the MT-1X proximal promoter. Superimposed on these experiments was the treatment of cells with MS-275, and determining the effect of this exposure on factor binding and histone modifications. ChIP assays that were conducted in this study have provided evidence that all of the transcription factors tested showed a pattern of binding to the MT-1X promoter that correlated to MT-1X mRNA expression differences between the normal and the metal-transformed cells. The binding of these factors was augmented following treatment with MS-275, and what was worth noting is that the parental and As^{+3} or Cd^{+2} transformed cells each had their own "signature" of being more enhanced in certain MREs over that of the other ones (Appendices C & D).

The NF-I is a Coordinator of Transcriptional Activation

The NF-I transcription factor is an activator of gene transcription that has been associated with the control of the growth rates of different types of cells and has been associated with a myriad of disease processes (Gronostajski *et al.*, 2000). A study of the *c-fos* promoter revealed that the mitogen-activated protein kinase signaling and its associated transcription factor ELK1 resulted in the recruitment of p300, and this, in turn, increased the acetylation status of the *c-fos* promoter. One study has observed that NF-I cannot bind chromatin unless it is in a loose conformation status, which can be achieved through histone acetylation. Following this acetylation, NF-I can bind the chromatin and allow a more permissive state for the binding of the transcriptional machinery and other transcription factors (O'Donnell *et a*l., 2008). One study examining MT transcriptional activation determined that upon Zn^{+2} induction, a multiprotein complex forms consisting of MTF-1, p300 and SP1 and results in the activation of MT transcription (Li *et al*, 2008). Another study, underscored the role of NF-I as a synergistic coactivator with MTF-1 in the induction of MT transcription (LaRochelle *et al*., 2008). Therefore, in a way similar to the *c-fos* promoter induction, a model for MT-1X transcriptional activation could be the following: upon Zn^{+2} stimulation, MTF-1 translocates to the nucleus and binds the MREs b & c, and this is followed by the recruitment of p300 and the subsequent histone acetylation that results in a change in the chromatin structure to a less compacted state that favors the binding of NF-I**.** Comparative analysis between the binding of p300 and NF-I and the correlation to the acetyl H4 levels in each of the MRE regions (Appendix C) shows that there is a definite

correlation between the levels of the two transcription factors' binding and the Acetyl H4 modification. Examination of the MRE-a ChIP results, as an example, shows that there is a significant correlation between the binding levels of NF-I and p300 in the control non-treated group, and that this binding correlates to the levels of acetylated H4 lysines in the same treatment group. Similarly, changes in the level of this binding in reponse to treatment with MS-275 shows a similar correlation. The same correlation holds true for the results of these ChIP assays in MREs d & e (Appendix C).

This correlation between the transcriptional activation of NF-I, p300, and acetyl H4 that was observed in this study triggered a more in-depth literature search regarding the role of NF-I in transcriptional activation. The results of this search revealed some roles for NF-I in transcriptional activation that have not been extensively studied. The first of these roles involves the direct recruitment of p300 by NF-I. Although many studies have cited NF-I as a transcriptional activator of many genes, its role has been mostly supplementary to other transcriptional initiators (Belikov *et al*., 2004, and LaRochelle *et al*., 2008). One study confirmed the direct interaction between NF-I and CBP using a mammalian two-hybrid assay (Leahy *et al.*, 1999) where the CBP/p300 co-activator complex is responsible for the acetylation and thus the activation of numerous genes (Chen *et al*., 2011). Another study determined that NF-I binding of DNA is affected by Zn^{+2} concentration and that NF-I can affect the transcription of murine MT-1 through its translocation to the nucleus in response to changes in Zn^{+2} concentration. This study also highlighted the fact that the different NF-I isoforms (A, B, C, and X) can have different effects on transcription based on the type of tissues and promoters

involved (Oh *et al*., 2012). Another interesting aspect is the discovery that NF-I acts as a chromatin remodeler that directly interacts with histone H3 (Muller *et al*., 2000). All of these observations point to the possibility of NF-I initiating MT-1X transcription in response to Zn^{+2} treatment and then acting in concert with MTF-1 to potentiate its response to MS-275 treatment when the cells are treated with Zn^{+2} and MS-275 together.

There are several other aspects about the role of NF-I in the transcriptional regulation of MT-1X that require further exploration. One of these aspects is investigating the effect of Zn^{+2} and the combined MS-275 + Zn^{+2} treatments on NF-I binding. Another aspect involves identifying the specific isosforms that are involved in the transcriptional regulation of MT-1X, given the fact that the antibody used for the detection of NF-I binding in this study detected all of the NF-I isoforms.

Transcriptional Activation of MT-1X Results in Nucleosomal Rearrangement Events

The nucleosome consists of an octamer of histone proteins consisting of two molecules of each of the canonical highly conserved histones: H2A, H2B, H3, and H4 histones (Luger *et al*., 1997). Each of these histones has a globular body that partners with the other histone (H2A with H2B and H3 with H4), and a tail protruding from the nucleosomal unit. Post-translational modifications of histones occur in the amino acids residues present in the tails and these modifications can confer active or repressive marks by altering the association between the histones and the DNA double helix wrapped around them (Kouzarides *et al.*, 2007).

Upon transcriptional activation, especially in active promoter sites, changes in the nucleosomal structure frequently occur. One model for this chromatin remodeling involves the binding of a transcription factor following transcriptional activation, and this factor then recruits chromatin-remodeling complexes. The nucleosomal changes might involve total nucleosomal removal from its current site, rearrangement of the nucleosomal structure through exchange of canonical histones with histone variants, or displacement of the nucleosomal structure through a process of 'sliding' to make the chromatin more accessible to the transcriptional machinery and the different transcription factors (Aalfs *et al*., 2000). Although the action of the chromatin remodeling complexes is crucial in altering the nucleosomal structure, the inherent ability of the nucleosomal unit to be disrupted or displaced in position plays an important role in transcriptional activation. Histone-histone and histone-DNA interactions play an important role in preparing the nucleosomal for such displacement. The presence of either, or both of the histone variants H2A.z and H3.3 (double-histone variant) in the promoter region makes the nucleosomes harboring them particularly sensitive to the disruption of its structure (Jin *et al*., 2007). Noteworthy is the fact that double-variant nucleosomes have been mapped around nucleosome deficient regions (NDRs) and represent nucleosomes that are in the process of disruption (Jin *et al*., 2009).

Histone H3.3 is a histone variant that replaces the canonical H3 histone. Contrary to that observed with the canonical H3, the deposition of histone H3.3 is not limited to the S phase of the cell cycle; therefore it is capable of replacing the histones that are

being displaced during the course of transcriptional activation. Some studies have suggested that the presence of histone H3.3 in transcriptionally active genes casts a "mark" on this region to keep it in an open conformation state, and that its levels increase upon transcriptional activation (Heinkoff *et al*., 2004). The histone H2A.z variant replaces canonical H2A histone, and its presence in a promoter site denotes RNA polymerase II occupancy (Hardy *et al*., 2009). It has been noted that upon transcriptional activation, the H2A.z variant is evicted from the nucleosome to be replaced by the canonical histone H2A and this pattern is repeated again as the transcriptional needs of the cell dictates (Talbert *et al*., 2010). This fact might explain the decreasing H2A.z levels that were observed in this study upon the transcriptional activation of MT-1X following the MS-275 treatment.

ChIP results of the H2A.z histone modifications (Appendix E) showed that there was decreased enrichment in the parental, and As^{+3} and Cd^{+2} transformed cell lines upon transcriptional activation by MS-275 in MREs a, d, and e. Similarly, a comparison between the ChIP results of histones H3 and H3.3 in the MRE-a region (Appendix E), showed that upon transcriptional activation by MS-275, the levels of H3 decreased in the parent and As^{+3} transformed cell lines and this decrease correlated to an increase in the level of H3.3 in the same cell lines and indicates that H3.3 is replacing the canonical histone H3 in these lines. This comparison did not show the same correlation for the Cd^{+2} transformed cell line. For the MRE-e region, comparison of the ChIP results of histones H3 and H3.3 shows that although there was minimal change in histone H3 levels between the control and the MS-275 treated As^{+3} transformed cell lines, there

was a significant increase in the H3.3 enrichment upon MS-275 treatment in the same cell line. These results point to a high likelihood that there is nucleosomal disruption in MREs a & e in the As^{+3} transformed cell lines. There were no detectable levels for the H3.3 modification in the MRE-d region for all of the three cell lines.

A recent study by Okumura and colleagues (Okumura *et al.*, 2011) on the promoter of the murine MT-1 concluded that upon Zn^{+2} stimulation, MTF-1 and its associated HAT p300 are recruited to the promoter region. This recruitment results in nucleosomal disruption that is characterized by the decreased levels of total histone H3, trimethyl H3K4, and acetylated H3K9 that was accompanied by an increase in the level of H3.3. Comparison of the levels of histone H3, trimethyl H3K4, and trimethyl H3K27 observed in this study (Appendix F) showed that: the decrease in the level of histone H3 in the As^{+3} transformed cell lines in MREs a, d, & e observed earlier upon the transcriptional activation with MS-275, correlated to a decrease in the level of trimethyl H3K4 in the same cell lines in the three MREs. This denotes that removal of the histone H3 from the nucleosomal unit is taking place and that, in turn, is translated to a decrease in H3K4 levels since H3 is being replaced by H3.3. The trimethyl H3K27 levels did not generally correlate with those of H3 in the three MREs. Trimethyl H3K27 invokes a repressive mark on the chromatin and would be expected to have a decrease in its level of enrichment upon transcriptional activation, but instead showed mostly an increase in the parental, As^{+3} and Cd^{+2} transformed cell lines. The author currently has no valid explanation for this phenomenon, except that it is possible that the significant increase

in the trimethyl H3K27 following treatment with MS-275 correlates with the decrease in the MT-1X mRNA expression observed in the Cd^{+2} transformed cell lines.

The general conclusion is that there are two potential models for the transcriptional activation of MT-1X based on the results of the experiments conducted in this study on MRES a, d, & e. The first model involves the activation of MT-1X transcription under basal conditions (no Zn^{+2} treatment): where MTF-1 binds the chromatin and recruits the HAT p300, which causes a hyperacetylation state. This hyperacetylation state loosens the chromatin structure and facilitates the binding of NF-I, which in turn, recruits the chromatin remodeling complexes. The chromatin remodelers cause the removal of H3 histones from the nucleosomal units and its replacement with the variant histone H3.3, and this makes the nucleosomal unit ready for disruption or displacement. The second model involves the transcriptional activation under Zn^{+2} treatment conditions: this involves the binding of NF-I to the chromatin that is followed by its interaction with p300 causing the hyperacetylation state. Chromatin remodelers are either recruited by p300, or NF-I acts as a chromatin remodeler through its interactions with the histone H3 discussed earlier. This is followed by the nucleosomal rearrangement events that facilitate the association of the RNA polymerase II with the MT-1X promoter and the initiation of transcription.

Another conclusion is that there is positive response to the epigenetic remodeler MS-275, which is manifested by an increase in the binding of transcription factors and in the histone modifications tested. The most significant changes occurred in the MRE-e

region of the As^{+3} transformed cells, and points to a significant role that this region might play in the process of malignant transformation.

Future Directions

UROtsa cells were previously transformed by the continual passaging of the cells in the presence of 1.0 μM Cd^{+2} or As^{+3}. It required passages between 30 and 40 to attain the ability to form colonies in soft agar and tumors in nude mice. Since studies in this dissertation showed that these metals induced MT-1X during exposure for 48 hr and five passages, it appears that at the point of transformation, the MT-1X gene attains metal-independent increases in gene expression. The question that remains is whether transformation is required for metal-independent increase in MT-1X expression. In previous studies, cells were frozen down in intermediate passages, and these cells can be returned to culture to assess whether metal-independent increases in MT-1X expression had occurred and whether the passage at which this does occur, corresponds to cellular transformation. Once this has been established, the findings of this dissertation can be applied, specifically to determine whether NF-I and p300 binding with its associated H4 acetylation also increases at this point. It will also be interesting to note the specific isoforms of NF-I that would be responsible for this altered state of the MT-1X promoter as well as the combination of active versus repressive histone modifications within the various regions of the promoter. Other factors may come into play, and it will be especially interesting to assess whether MTF-1 will have a role in this transition point. The current data concerning this major MT-transcriptional regulator, suggests a minor role in the transformation process.

As a prelude to these studies, ChIP assays for p300 binding were done for the 48 h and P5 experimental cells. A comparison between the results of these assays was done to compare the p300 binding levels in these experiments to those of the transformed cells (Appendix G). Results of this comparison showed a correlation between the p300 binding and the MT-1X mRNA expression (Appendix A) in these three experiments (48 h, P5, and metal-transformation).

Part II: Kindlin-2

Kindlin-2 is one of three family members belonging to the Kindlin family of focal adhesion proteins that have been proven to play a significant role in integrin activation. The Kindlins (1-3) share significant structural homology and are evolutionarily conserved, and they have the function of an "adaptor protein" that is recruited to intracellular integrin-containing adhesion sites that are termed focal adhesions. The Kindlins possess what is known as the FERM (four point one protein, ezrin, radixin, and moesin) domain that has been deemed essential in integrin activation. The FERM domain is bipartite and is interrupted by a pleckstrin homology (PH) domain. The Kindlins can bind directly to different classes of integrin receptors and can participate in the bi-directional integrin signaling (Lai-Cheong et al., 2010). Kindlin-2 localizes to the sites of cell-ECM adhesions through the direct binding of its C-terminal end to the beta integrin receptor. Through its N-terminal end, Kindlin-2 interacts with the protein migfilin that associates with other proteins including filamin, which acts as a "cross-linking" protein through its ability to connect together two actin filaments, and to promote the formation of loose gel-like actin "sheets". These "sheets" of actin can

form projections from the cell surface that are termed “lamellipodia” that help the cell move on solid surfaces (Alberts *et al*., 2008).

Study of Kindlin-2 knockout mice showed that Kindlin-2 deficiency resulted in death of the animals around the embryonic age of 7.5 days due to detachment of the epiblast and endoderm. Through the use of Northern analysis, Kindlin-2 mRNA has been detected in the heart, lung, skeletal muscle, kidney, bladder, and stomach. Kindlin-2 protein has been shown to be present in fibroblasts, muscle, and epithelial and endothelial cells (Ussar *et al.*, 2006). At present, there are no published studies examining the localization of Kindlin-2 protein in the normal human bladder and human urothelial carcinomas, and this study appears to be the first to characterize its expression in the normal human bladder and bladder carcinomas.

Results of the present study showed that there was no expression of Kindlin-2 in the urothelium of normal human bladder but that there was a modest degree of expression in the non-epithelial stromal elements including: fibroblasts, smooth muscle cells and in some blood vessels. In the present study, the microarray screen showed that the 3 cell lines repressed in the expression of Kindlin-2 mRNA were those that were able to establish peritoneal tumors when injected into the peritoneal cavity. The results of this analysis were confirmed in extracts of these cell lines, showing that Kindlin-2 protein expression correlated with the ability of these cell lines to form peritoneal tumors. Examination of extracts from SC and peritoneal heterotransplants showed that there was no expression of Kindlin-2 protein in the urothelial cells of any of the SC or peritoneal tumors. Examination of archival human specimens from low and high-grade

urothelial carcinomas detected the presence of Kindlin-2 protein in all the stromal components, and this expression was more pronounced in the high-grade lesions. Blood vessels within the papillary core were also positive for Kindlin-2 expression. Of special significance was the presence of areas of Kindlin-2 focal expression within the tumor tissues of high-grade invasive urothelial carcinomas. Although this finding did not correlate with the results of the microarray study, never-the-less it was significant since it pointed to a potential role for Kindlin-2 as a prognostic biomarker in a subset of high-grade invasive urothelial cancers that are destined to progression and metastasis. It is predicted that the role that Kindlin-2 plays in the control of cell motility might be a factor in the finding observed in this study about its role in tumor progression.

APPENDICES

APPENDIX A

A comparisonbetween MT-1X mRNA expression differences between UROtsa cells subjected to the short (48 h) and long term (P5) exposures to As^{+3} and Cd^{+2} and UROtsa cells transformed by the same metals.

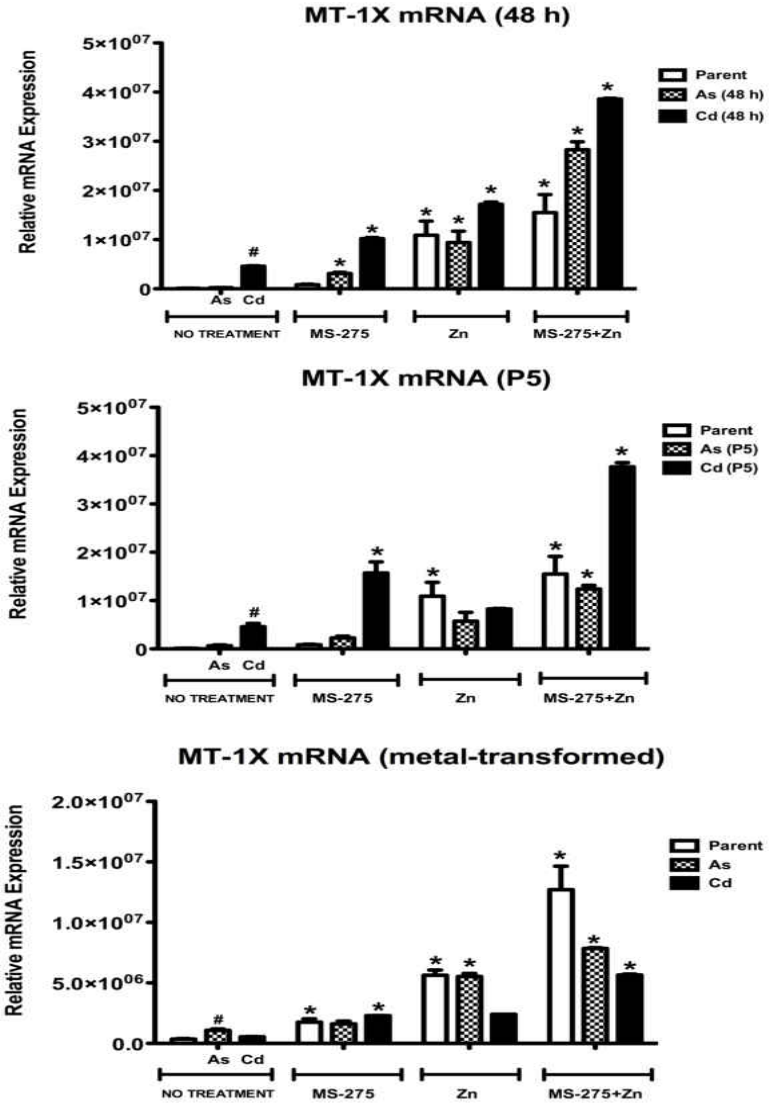

APPENDIX B

A comparison between MT-1X mRNA expression, and the MTF-1 binding, and the effect of Zn^{+2}, MS-275, or the combined treatment with both agents on the expression and binding levels when compared to the As^{+3} and Cd^{+2} transformed cell lines cell lines receiving no treatment.

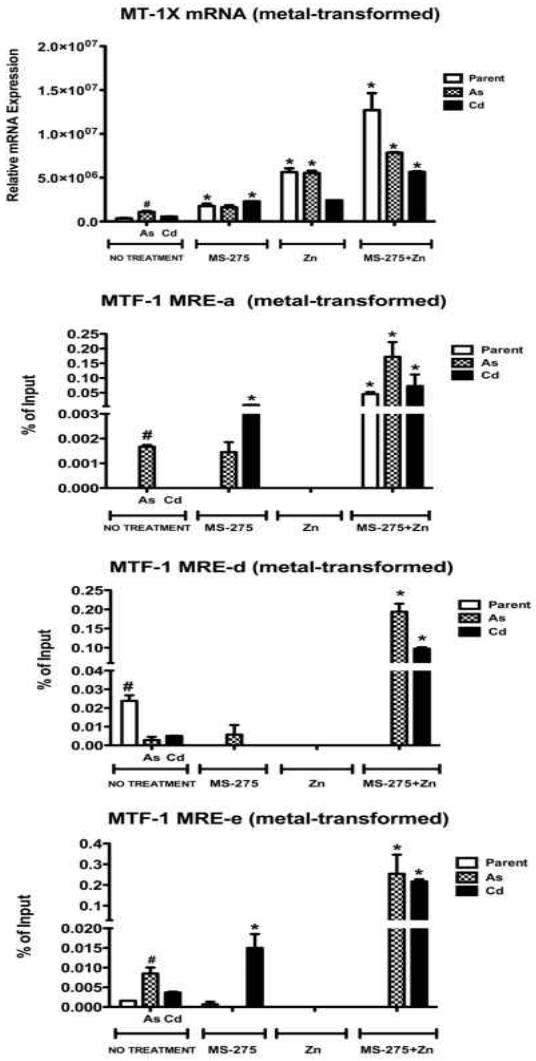

APPENDIX C

A comparison between the binding of NF-I and p300 transcription factors, and their correlation to the level of acetyl H4 enrichments in MREs a, d, & e in the MT-1X promoter of As^{+3} and Cd^{+2} transformed UROtsa cells.

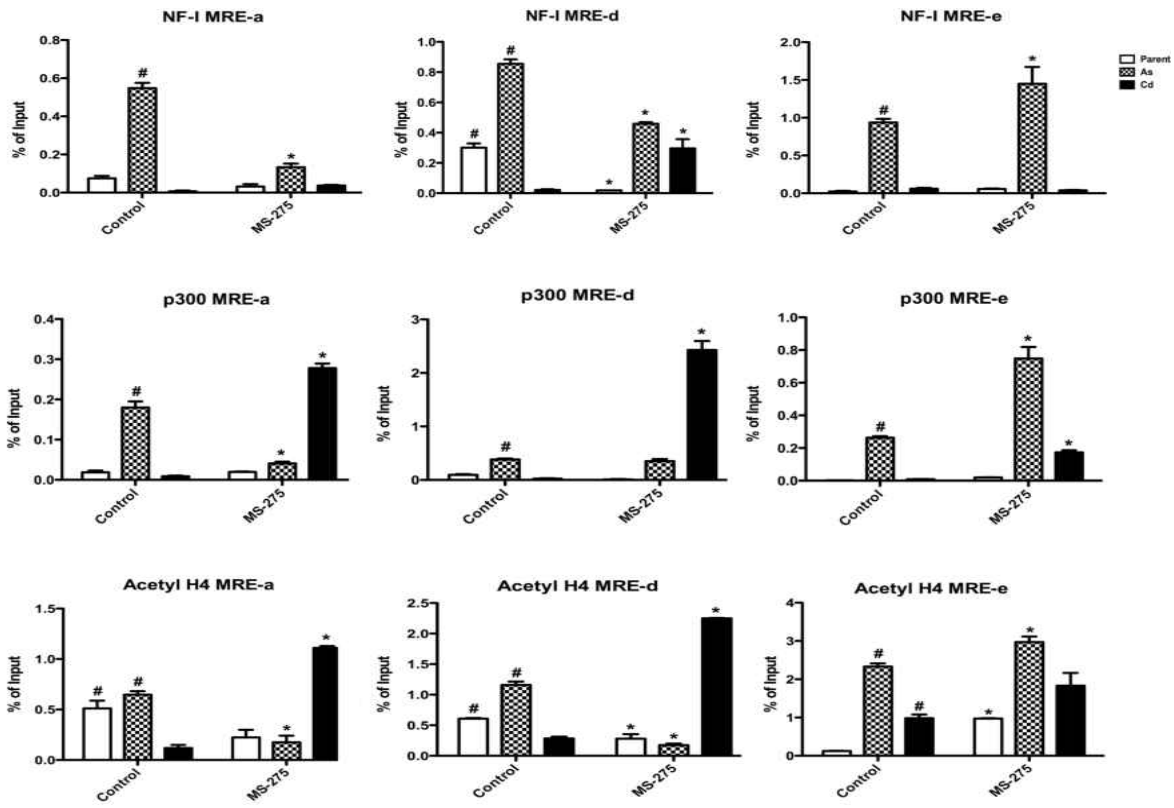

APPENDIX D

A comparison between the binding of USF1, LBP-1, and SP1 transcription factors in MREs a, d, & e in the MT-1X promoter of As^{+3} and Cd^{+2} transformed UROtsa cells.

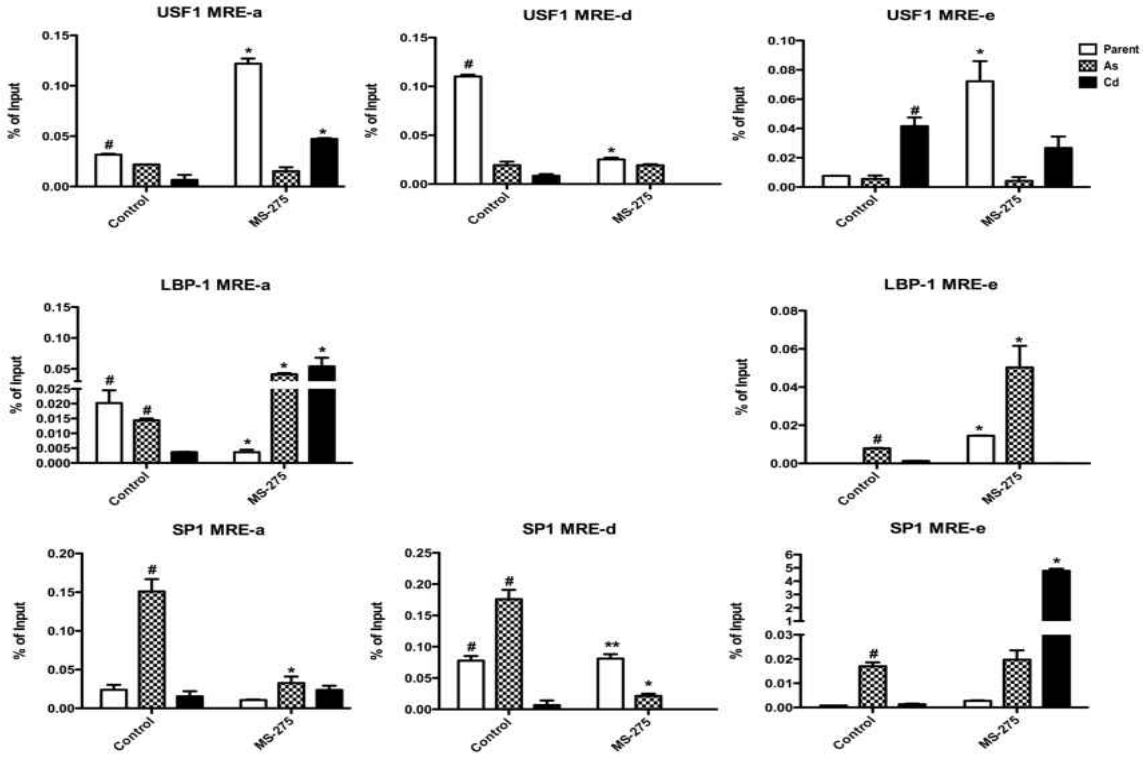

APPENDIX E

A comparison between the levels of histones H2A.z, H3.3, and histone H3 histone modifications in MREs a, d, & e in the MT-1X promoter of As^{+3} and Cd^{+2} transformed UROtsa cells.

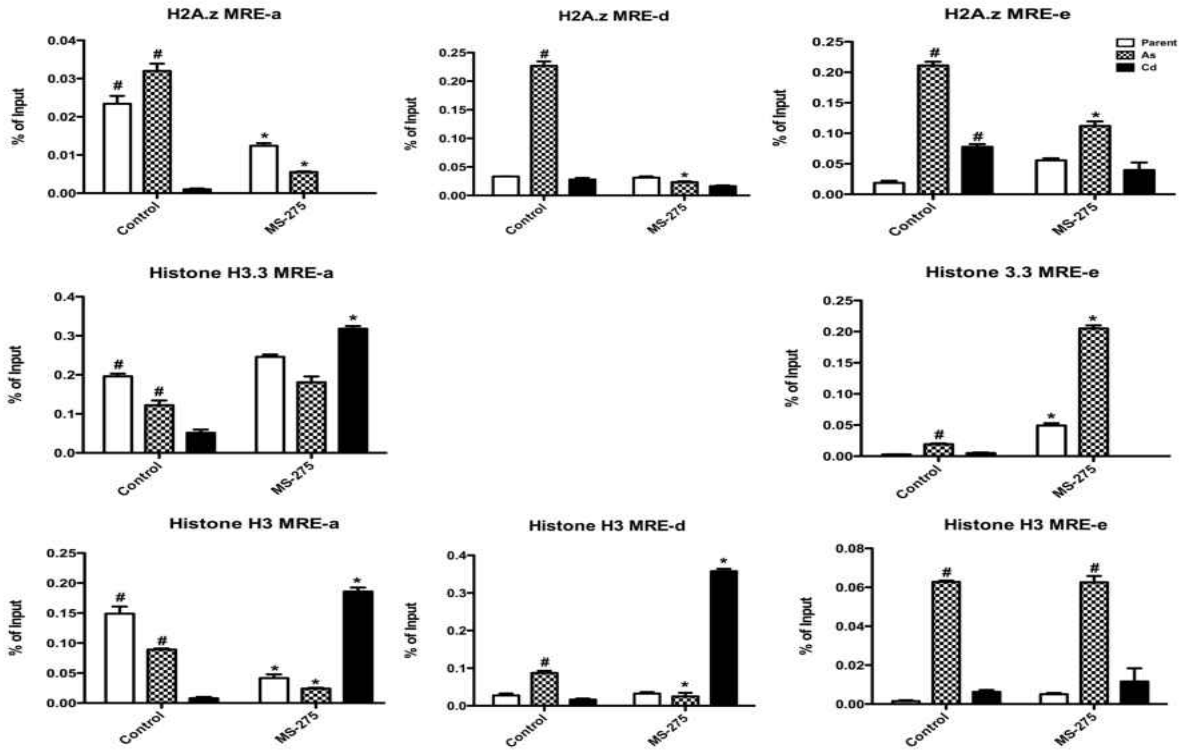

APPENDIX F

A comparison between the levels of histone H3, trimethyl H3K4, and trimethyl H3K27 histone modifications in MREs a, d, & e in the MT-1X promoter of As^{+3} and Cd^{+2} transformed UROtsa cells.

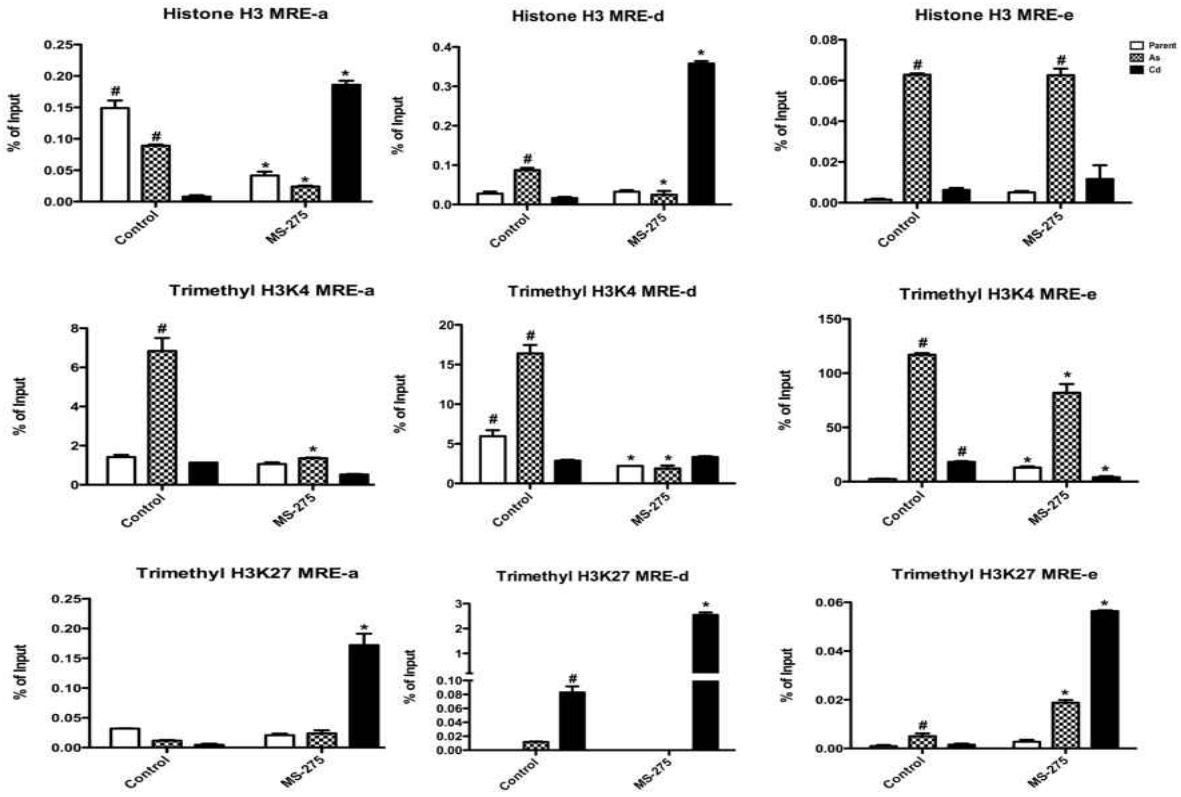

APPENDIX G

A comparison between MREs a, d, & e to examine the differences in p300 binding between UROtsa cells subjected to the short (48 h) and long term (P5) exposures to As^{+3} and Cd^{+2} and UROtsa cells transformed by the same metals.

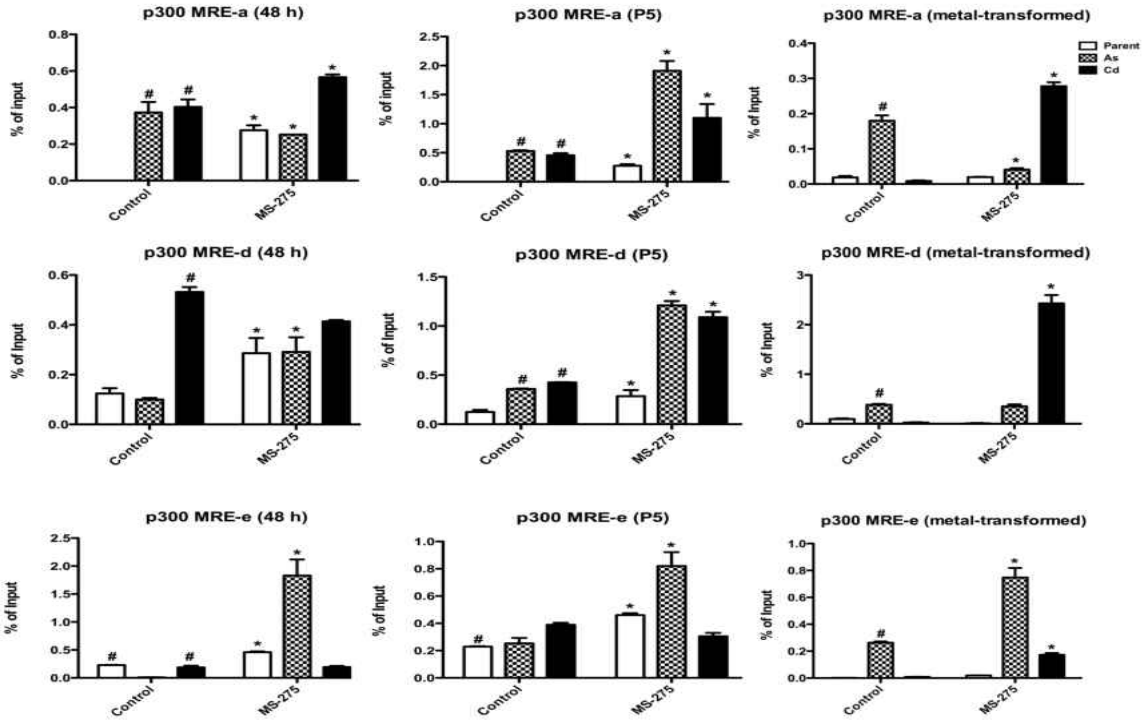

REFERENCES

1. Alberts B, Johnson A, Lewis J, Raff M, Roberts K, Walter P. Molecular Biology of The Cell. Fifth ed. New York: Garland Science; 2008. Chapter 16, The Cytoskeleton; p.1008-1009.

2. Aalfs JD, Kingston RE. What does 'chromatin remodeling' mean?. Trends Biochem Sci. 2000 Nov; 25 (11) :548-55. PubMed PMID:11084367.

3. Ahlborn GJ, Nelson GM, Ward WO, Knapp G, Allen JW, Ouyang M, Roop BC, Chen Y, O'Brien T, Kitchin KT, Delker DA. Dose response evaluation of gene expression profiles in the skin of K6/ODC mice exposed to sodium arsenite. Toxicol Appl Pharmacol. 2008 Mar 15; 227 (3) :400-16. PubMed PMID:18191166.

4. Ali AH, Kondo K, Namura T, Senba Y, Takizawa H, Nakagawa Y, Toba H, Kenzaki K, Sakiyama S, Tangoku A. Aberrant DNA methylation of some tumor suppressor genes in lung cancers from workers with chromate exposure. Mol Carcinog. 2011 Feb; 50 (2) :89-99. PubMed PMID:21229606.

5. Bahnson RR, Banner BF, Ernstoff MS, Lazo JS, Cherian MG, Banerjee D, Chin JL. Immunohistochemical localization of metallothionein in transitional cell carcinoma of the bladder. J Urol. 1991 Dec; 146 (6) :1518-20. PubMed PMID:1942331.

6. Bahnson RR, Becich M, Ernstoff MS, Sandlow J, Cohen MB, Williams RD. Absence of immunohistochemical metallothionein staining in bladder tumor specimens predicts response to neoadjuvant cisplatin, methotrexate and vinblastine chemotherapy. J Urol. 1994 Dec; 152 (6 Pt 2) :2272-5. PubMed PMID:7966723.

7. Bednar J, Dimitrov S. Chromatin under mechanical stress: from single 30 nm fibers to single nucleosomes. FEBS J. 2011 Jul; 278 (13) :2231-43. PubMed PMID:21535477.

8. Belikov S, Holmqvist PH, Astrand C, Wrange O. Nuclear factor 1 and octamer transcription factor 1 binding preset the chromatin structure of the mouse mammary tumor virus promoter for hormone induction. J Biol Chem. 2004 Nov 26; 279 (48) :49857-67. PubMed PMID:15381691.

9. Benbrahim-Tallaa L, Waterland RA, Dill AL, Webber MM, Waalkes MP. Tumor suppressor gene inactivation during cadmium-induced malignant transformation of human prostate cells correlates with overexpression of de novo DNA methyltransferase. Environ Health Perspect. 2007 Oct; 115 (10) :1454-9. PubMed PMID:17938735; PubMed Central PMCID: PMC2022656.

10. Bertolero F, Pozzi G, Sabbioni E, Saffiotti U. Cellular uptake and metabolic reduction of pentavalent to trivalent arsenic as determinants of cytotoxicity and morphological transformation. Carcinogenesis. 1987 Jun; 8 (6) :803-8. PubMed PMID:3608077.

11. Bonasio R, Tu S, Reinberg D. Molecular signals of epigenetic states. Science. 2010 Oct 29; 330 (6004) :612-6. PubMed PMID:21030644.

12. Cao L, Zhou XD, Sens MA, Garrett SH, Zheng Y, Dunlevy JR, Sens DA, Somji S. Keratin 6 expression correlates to areas of squamous differentiation in multiple independent isolates of As(+3)-induced bladder cancer. J Appl Toxicol. 2010 Jul; 30 (5) :416-30. PubMed PMID:20186695; PubMed Central PMCID: PMC3100548.

13. Carter DE, Aposhian HV, Gandolfi AJ. The metabolism of inorganic arsenic oxides, gallium arsenide, and arsine: a toxicochemical review. Toxicol Appl Pharmacol. 2003 Dec 15; 193 (3) :309-34. PubMed PMID:14678742.

14. Chen CJ, Chuang YC, Lin TM, Wu HY. Malignant neoplasms among residents of a blackfoot disease-endemic area in Taiwan: high-arsenic artesian well water and cancers. Cancer Res. 1985 Nov; 45 (11 Pt 2) :5895-9. PubMed PMID:4053060.

15. Chen H, Li S, Liu J, Diwan BA, Barrett JC, Waalkes MP. Chronic inorganic arsenic exposure induces hepatic global and individual gene hypomethylation: implications for arsenic hepatocarcinogenesis. Carcinogenesis. 2004 Sep; 25 (9) :1779-86. PubMed PMID:15073043.

16. Chen J, Li Q. Life and death of transcriptional co-activator p300. Epigenetics. 2011 Aug; 6 (8) :957-61. PubMed PMID:21730760.

17. Chen X, Zhang B, Harmon PM, Schaffner W, Peterson DO, Giedroc DP. A novel cysteine cluster in human metal-responsive transcription factor 1 is required for heavy metal-induced transcriptional activation in vivo. J Biol Chem. 2004 Feb 6; 279 (6) :4515-22. PubMed PMID:14610091.

18. Cheng L, Zhang S, MacLennan GT, Williamson SR, Lopez-Beltran A, Montironi R. Bladder cancer: translating molecular genetic insights into clinical practice. Hum Pathol. 2011 Apr; 42 (4) :455-81. PubMed PMID:21106220.

19. Corre S, Galibert MD. Upstream stimulating factors: highly versatile stress-responsive transcription factors. Pigment Cell Res. 2005 Oct; 18 (5) :337-48. PubMed PMID:16162174.

20. Ebadi M, Iversen PL, Hao R, Cerutis DR, Rojas P, Happe HK, Murrin LC, Pfeiffer RF. Expression and regulation of brain metallothionein. Neurochem Int. 1995 Jul; 27 (1) :1-22. PubMed PMID:7655341.

21. Eneman JD, Potts RJ, Osier M, Shukla GS, Lee CH, Chiu JF, Hart BA. Suppressed oxidant-induced apoptosis in cadmium adapted alveolar epithelial cells and its potential involvement in cadmium carcinogenesis. Toxicology. 2000 Jul 5; 147 (3) :215-28. PubMed PMID:10924803.

22. Gibb HJ, Lees PS, Pinsky PF, Rooney BC. Lung cancer among workers in chromium chemical production. Am J Ind Med. 2000 Aug; 38 (2) :115-26. PubMed PMID:10893504.

23. Gius D, Cui H, Bradbury CM, Cook J, Smart DK, Zhao S, Young L, Brandenburg SA, Hu Y, Bisht KS, Ho AS, Mattson D, Sun L, Munson PJ, Chuang EY, Mitchell JB, Feinberg AP. Distinct effects on gene expression of chemical and genetic manipulation of the cancer epigenome revealed by a multimodality approach. Cancer Cell. 2004 Oct; 6 (4) :361-71. PubMed PMID:15488759.

24. Glatt S, Alfieri C, Müller CW. Recognizing and remodeling the nucleosome. Curr Opin Struct Biol. 2011 Jun; 21 (3) :335-41. PubMed PMID:21377352.

25. Goering PL, Waalkes MP, Klaassen CD, Toxicology of Cadmium, in: R.A. Goyer, M.G. Cherian (Eds.), Handbook of Experimental Pharmacology: Toxicology of Metals, Biochemical Effects, vol. 115, Springer-Verlag, New York, 1994, pp. 189–214.

26. Gozgit JM, Pentecost BT, Marconi SA, Otis CN, Wu C, Arcaro KF. Use of an aggressive MCF-7 cell line variant, TMX2-28, to study cell invasion in breast cancer. Mol Cancer Res. 2006 Dec; 4 (12) :905-13. PubMed PMID:17189381.

27. Gregoretti IV, Lee YM, Goodson HV. Molecular evolution of the histone deacetylase family: functional implications of phylogenetic analysis. J Mol Biol. 2004 Apr 16; 338 (1) :17-31. PubMed PMID:15050820.

28. Gronostajski RM. Roles of the NFI/CTF gene family in transcription and development. Gene. 2000 May 16; 249 (1-2) :31-45. PubMed PMID:10831836.

29. Günther V, Lindert U, Schaffner W. The taste of heavy metals: Gene regulation by MTF-1. Biochim Biophys Acta. 2012 Jan 20; PubMed PMID:22289350.

30. Haq F, Mahoney M, Koropatnick J. Signaling events for metallothionein induction. Mutat Res. 2003 Dec 10; 533 (1-2) :211-26. PubMed PMID:14643422.

31. Hardy S, Jacques PE, Gévry N, Forest A, Fortin ME, Laflamme L, Gaudreau L, Robert F. The euchromatic and heterochromatic landscapes are shaped by antagonizing effects of transcription on H2AZ deposition. PLoS Genet. 2009 Oct; 5 (10) :e1000687. PubMed PMID:19834540; PubMed Central PMCID: PMC2754525.

32. Hartwig A. Mechanisms in cadmium-induced carcinogenicity: recent insights. Biometals. 2010 Oct; 23 (5) :951-60. PubMed PMID:20390439.

33. He Z, Ma WY, Liu G, Zhang Y, Bode AM, Dong Z. Arsenite-induced phosphorylation of histone H3 at serine 10 is mediated by Akt1, extracellular signal-regulated kinase 2, and p90 ribosomal S6 kinase 2 but not mitogen- and stress-activated protein kinase 1. J Biol Chem. 2003 Mar 21; 278 (12) :10588-93. PubMed PMID:12529330.

34. Henikoff S, Furuyama T, Ahmad K. Histone variants, nucleosome assembly and epigenetic inheritance. Trends Genet. 2004 Jul; 20 (7) :320-6. PubMed PMID:15219397.

35. Heuchel R, Radtke F, Georgiev O, Stark G, Aguet M, Schaffner W. The transcription factor MTF-1 is essential for basal and heavy metal-induced metallothionein gene expression. EMBO J. 1994 Jun 15; 13 (12) :2870-5. PubMed PMID:8026472; PubMed Central PMCID: PMC395168.

36. Himeno S, Yanagiya T, Fujishiro H. The role of zinc transporters in cadmium and manganese transport in mammalian cells. Biochimie. 2009 Oct; 91 (10) :1218-22. PubMed PMID:19375483.

37. Hu E, Dul E, Sung CM, Chen Z, Kirkpatrick R, Zhang GF, Johanson K, Liu R, Lago A, Hofmann G, Macarron R, de los Frailes M, Perez P, Krawiec J, Winkler J, Jaye M. Identification of novel isoform-selective inhibitors within class I histone deacetylases. J Pharmacol Exp Ther. 2003 Nov; 307 (2) :720-8. PubMed PMID:12975486.

38. Huang C, Li J, Ding M, Wang L, Shi X, Castranova V, Vallyathan V, Ju G, Costa M. Arsenic-induced NFkappaB transactivation through Erks- and JNKs-dependent pathways in mouse epidermal JB6 cells. Mol Cell Biochem. 2001 Jun; 222 (1-2) :29-34. PubMed PMID:11678607.

39. Hynes RO. Integrins: bidirectional, allosteric signaling machines. Cell. 2002 Sep 20; 110 (6) :673-87. PubMed PMID:12297042.

40. International Agency for Research on Cancer (1987*)*. Overall Evaluations of Carcinogenicity: An Updating of IARC Monographs Volumes 1 to 42. IARC Monographs on the Evaluation of Carcinogenic Risks to Humans. Supplement 7. IARC, Lyon, France.

41. International Agency for Research on Cancer (2012*)*. A Review of Human Carcinogens: Arsenic, Metals, Fibres, and Dusts. IARC Monographs on the Evaluation of Carcinogenic Risks to Humans. Vol. 100C. IARC, Lyon, France.

42. Jacobson-Kram D, Montalbano D. The reproductive effects assessment group's report on the mutagenicity of inorganic arsenic. Environ Mutagen. 1985; 7 (5) :787-804. PubMed PMID:3899634.

43. Jin C, Zang C, Wei G, Cui K, Peng W, Zhao K, Felsenfeld G. H33/H2AZ double variant-containing nucleosomes mark 'nucleosome-free regions' of active promoters and other regulatory regions. Nat Genet. 2009 Aug; 41 (8) :941-5. PubMed PMID:19633671; PubMed Central PMCID: PMC3125718.

44. Jin C, Felsenfeld G. Nucleosome stability mediated by histone variants H33 and H2AZ. Genes Dev. 2007 Jun 15; 21 (12) :1519-29. PubMed PMID:17575053; PubMed Central PMCID: PMC1891429.

45. KAGI JH, VALLEE BL. Metallothionein: a cadmium and zinc-containign protein from equine renal cortex II Physico-chemical properties. J Biol Chem. 1961 Sep; 236:2435-42. PubMed PMID:13750714.

46. Kato K, Shiozawa T, Mitsushita J, Toda A, Horiuchi A, Nikaido T, Fujii S, Konishi I. Expression of the mitogen-inducible gene-2 (mig-2) is elevated in human uterine leiomyomas but not in leiomyosarcomas. Hum Pathol. 2004 Jan; 35 (1) :55-60. PubMed PMID:14745725.

47. Kaufman DS, Shipley WU, Feldman AS. Bladder cancer. Lancet. 2009 Jul 18; 374 (9685) :239-49. PubMed PMID:19520422.

48. Kellen E, Zeegers MP, Hond ED, Buntinx F. Blood cadmium may be associated with bladder carcinogenesis: the Belgian case-control study on bladder cancer. Cancer Detect Prev. 2007; 31 (1) :77-82. PubMed PMID:17296271.

49. Kerckaert GA, LeBoeuf RA, Isfort RJ. Use of the Syrian hamster embryo cell transformation assay for determining the carcinogenic potential of heavy metal compounds. Fundam Appl Toxicol. 1996 Nov; 34 (1) :67-72. PubMed PMID:8937893.

50. Kitchin KT. Recent advances in arsenic carcinogenesis: modes of action, animal model systems, and methylated arsenic metabolites. Toxicol Appl Pharmacol. 2001 May 1; 172 (3) :249-61. PubMed PMID:11312654.

51. Klaassen CD, Liu J, Choudhuri S. Metallothionein: an intracellular protein to protect against cadmium toxicity. Annu Rev Pharmacol Toxicol. 1999; 39:267-94. PubMed PMID:10331085.

52. Kondo K, Takahashi Y, Hirose Y, Nagao T, Tsuyuguchi M, Hashimoto M, Ochiai A, Monden Y, Tangoku A. The reduced expression and aberrant methylation of p16(INK4a) in chromate workers with lung cancer. Lung Cancer. 2006 Sep; 53 (3) :295-302. PubMed PMID:16828922.

53. Kotoh S, Naito S, Sakamoto N, Goto K, Kumazawa J. Metallothionein expression is correlated with cisplatin resistance in transitional cell carcinoma of the urinary tract. J Urol. 1994 Oct; 152 (4) :1267-70. PubMed PMID:8072117.

54. Kouzarides T. Chromatin modifications and their function. Cell. 2007 Feb 23; 128 (4) :693-705. PubMed PMID:17320507.

55. Lai-Cheong JE, Parsons M, McGrath JA. The role of kindlins in cell biology and relevance to human disease. Int J Biochem Cell Biol. 2010 May; 42 (5) :595-603. PubMed PMID:19854292.

56. Laity JH, Andrews GK. Understanding the mechanisms of zinc-sensing by metal-response element binding transcription factor-1 (MTF-1). Arch Biochem Biophys. 2007 Jul 15; 463 (2) :201-10. PubMed PMID:17462582.

57. Larjava H, Plow EF, Wu C. Kindlins: essential regulators of integrin signalling and cell-matrix adhesion. EMBO Rep. 2008 Dec; 9 (12) :1203-8. PubMed PMID:18997731; PubMed Central PMCID: PMC2603460.

58. LaRochelle O, Labbé S, Harrisson JF, Simard C, Tremblay V, St-Gelais G, Govindan MV, Séguin C. Nuclear factor-1 and metal transcription factor-1 synergistically activate the mouse metallothionein-1 gene in response to metal ions. J Biol Chem. 2008 Mar 28; 283 (13) :8190-201. PubMed PMID:18230604.

59. Laukens D, Waeytens A, De Bleser P, Cuvelier C, De Vos M. Human metallothionein expression under normal and pathological conditions: mechanisms of gene regulation based on in silico promoter analysis. Crit Rev Eukaryot Gene Expr. 2009; 19 (4) :301-17. PubMed PMID:19817707.

60. Leahy P, Crawford DR, Grossman G, Gronostajski RM, Hanson RW. CREB binding protein coordinates the function of multiple transcription factors including nuclear factor I to regulate phosphoenolpyruvate carboxykinase (GTP) gene transcription. J Biol Chem. 1999 Mar 26; 274 (13) :8813-22. PubMed PMID:10085123.

61. Li J, Gorospe M, Barnes J, Liu Y. Tumor promoter arsenite stimulates histone H3 phosphoacetylation of proto-oncogenes c-fos and c-jun chromatin in human diploid fibroblasts. J Biol Chem. 2003 Apr 11; 278 (15) :13183-91. PubMed PMID:12547826.

62. Li Y, Kimura T, Huyck RW, Laity JH, Andrews GK. Zinc-induced formation of a coactivator complex containing the zinc-sensing transcription factor MTF-1, p300/CBP, and Sp1. Mol Cell Biol. 2008 Jul; 28 (13) :4275-84. PubMed PMID:18458062; PubMed Central PMCID: PMC2447150.

63. Lombardi PM, Cole KE, Dowling DP, Christianson DW. Structure, mechanism, and inhibition of histone deacetylases and related metalloenzymes. Curr Opin Struct Biol. 2011 Dec; 21 (6) :735-43. PubMed PMID:21872466; PubMed Central PMCID: PMC3232309.

64. Ludwig S, Hoffmeyer A, Goebeler M, Kilian K, Häfner H, Neufeld B, Han J, Rapp UR. The stress inducer arsenite activates mitogen-activated protein kinases extracellular signal-regulated kinases 1 and 2 via a MAPK kinase 6/p38-dependent pathway. J Biol Chem. 1998 Jan 23; 273 (4) :1917-22. PubMed PMID:9442025.

65. Luger K, Mäder AW, Richmond RK, Sargent DF, Richmond TJ. Crystal structure of the nucleosome core particle at 28 A resolution. Nature. 1997 Sep 18; 389 (6648) :251-60. PubMed PMID:9305837.

66. Marsit CJ, Karagas MR, Danaee H, Liu M, Andrew A, Schned A, Nelson HH, Kelsey KT. Carcinogen exposure and gene promoter hypermethylation in bladder cancer. Carcinogenesis. 2006 Jan; 27 (1) :112-6. PubMed PMID:15987713.

67. Martinez-Zamudio R, Ha HC. Environmental epigenetics in metal exposure. Epigenetics. 2011 Jul; 6 (7) :820-7. PubMed PMID:21610324; PubMed Central PMCID: PMC3230540.

68. Mayer K, Hieronymus T, Castrop J, Clevers H, Ballhausen WG. Ectopic activation of lymphoid high mobility group-box transcription factor TCF-1 and overexpression in colorectal cancer cells. Int J Cancer. 1997 Aug 7; 72 (4) :625-30. PubMed PMID:9259402.

69. Moleirinho A, Carneiro J, Matthiesen R, Silva RM, Amorim A, Azevedo L. Gains, losses and changes of function after gene duplication: study of the metallothionein family. PLoS One. 2011 Apr 25; 6 (4) :e18487. PubMed PMID:21541013; PubMed Central PMCID: PMC3081807.

70. Müller K, Mermod N. The histone-interacting domain of nuclear factor I activates simian virus 40 DNA replication in vivo. J Biol Chem. 2000 Jan 21; 275 (3) :1645-50. PubMed PMID:10636857.

71. Namdarghanbari M, Wobig W, Krezoski S, Tabatabai NM, Petering DH. Mammalian metallothionein in toxicology, cancer, and cancer chemotherapy. J Biol Inorg Chem. 2011 Oct; 16 (7) :1087-101. PubMed PMID:21822976.

72. O'Donnell A, Yang SH, Sharrocks AD. MAP kinase-mediated c-fos regulation relies on a histone acetylation relay switch. Mol Cell. 2008 Mar 28; 29 (6) :780-5. PubMed PMID:18374651.

73. Ogryzko VV, Schiltz RL, Russanova V, Howard BH, Nakatani Y. The transcriptional coactivators p300 and CBP are histone acetyltransferases. Cell. 1996 Nov 29; 87 (5) :953-9. PubMed PMID:8945521.

74. Oh HJ, Lee HK, Park SJ, Cho YS, Bae HS, Cho MI, Park JC. Zinc balance is critical for NFI-C mediated regulation of odontoblast differentiation. J Cell Biochem. 2012 Mar; 113 (3) :877-87. PubMed PMID:22228435.

75. Okumura F, Li Y, Itoh N, Nakanishi T, Isobe M, Andrews GK, Kimura T. The zinc-sensing transcription factor MTF-1 mediates zinc-induced epigenetic changes in chromatin of the mouse metallothionein-I promoter. Biochim Biophys Acta. 2011 Jan; 1809 (1) :56-62. PubMed PMID:21035574.

76. Peng D, Hu TL, Jiang A, Washington MK, Moskaluk CA, Schneider-Stock R, El-Rifai W. Location-specific epigenetic regulation of the metallothionein 3 gene in esophageal adenocarcinomas. PLoS One. 2011; 6 (7) :e22009. PubMed PMID:21818286; PubMed Central PMCID: PMC3139601.

77. Petzoldt JL, Leigh IM, Duffy PG, Sexton C, Masters JR. Immortalisation of human urothelial cells. Urol Res. 1995; 23 (6) :377-80. PubMed PMID:8788275.

78. Peyre M, Commo F, Dantas-Barbosa C, Andreiuolo F, Puget S, Lacroix L, Drusch F, Scott V, Varlet P, Mauguen A, Dessen P, Lazar V, Vassal G, Grill J. Portrait of ependymoma recurrence in children: biomarkers of tumor progression identified by dual-color microarray-based gene expression analysis. PLoS One. 2010 Sep 24; 5 (9) :e12932. PubMed PMID:20885975; PubMed Central PMCID: PMC2945762.

79. Quaife CJ, Findley SD, Erickson JC, Froelick GJ, Kelly EJ, Zambrowicz BP, Palmiter RD. Induction of a new metallothionein isoform (MT-IV) occurs during differentiation of stratified squamous epithelia. Biochemistry. 1994 Jun 14; 33 (23) :7250-9. PubMed PMID:8003488.

80. Radtke F, Georgiev O, Müller HP, Brugnera E, Schaffner W. Functional domains of the heavy metal-responsive transcription regulator MTF-1. Nucleic Acids Res. 1995 Jun 25; 23 (12) :2277-86. PubMed PMID:7610056; PubMed Central PMCID: PMC307018.

81. Rehn L (1895). Blasengeschwulte bei fuchsin-arbeitern. Arch. Klin. Chir. 50**,** 588.

82. Reichard JF, Schnekenburger M, Puga A. Long term low-dose arsenic exposure induces loss of DNA methylation. Biochem Biophys Res Commun. 2007 Jan 5; 352 (1) :188-92. PubMed PMID:17107663; PubMed Central PMCID: PMC1866367.

83. Rojas E, Herrera LA, Poirier LA, Ostrosky-Wegman P. Are metals dietary carcinogens?. Mutat Res. 1999 Jul 15; 443 (1-2) :157-81. PubMed PMID:10415439.

84. Rossi MR, Masters JR, Park S, Todd JH, Garrett SH, Sens MA, Somji S, Nath J, Sens DA. The immortalized UROtsa cell line as a potential cell culture model of human urothelium. Environ Health Perspect. 2001 Aug; 109 (8) :801-8. PubMed PMID:11564615; PubMed Central PMCID: PMC1240407.

85. Schwamborn K, Gaisa NT, Henkel C. Tissue and serum proteomic profiling for diagnostic and prognostic bladder cancer biomarkers. Expert Rev Proteomics. 2010 Dec; 7 (6) :897-906. PubMed PMID:21142890.

86. Schwerdtle T, Walter I, Mackiw I, Hartwig A. Induction of oxidative DNA damage by arsenite and its trivalent and pentavalent methylated metabolites in cultured human cells and isolated DNA. Carcinogenesis. 2003 May; 24 (5) :967-74. PubMed PMID:12771042.

87. Sens D, Rossi M, Park S, Gurel V, Nath J, Garrett S, Sens MA, Somji S. Metallothionein isoform 1 and 2 gene expression in a human urothelial cell line (UROtsa) exposed to CdCl2 and NaAsO2. J Toxicol Environ Health A. 2003 Nov 14; 66 (21) :2031-46. PubMed PMID:14555400.

88. Sens DA, Park S, Gurel V, Sens MA, Garrett SH, Somji S. Inorganic cadmium- and arsenite-induced malignant transformation of human bladder urothelial cells. Toxicol Sci. 2004 May; 79 (1) :56-63. PubMed PMID:14976345.

89. Sens MA, Somji S, Lamm DL, Garrett SH, Slovinsky F, Todd JH, Sens DA. Metallothionein isoform 3 as a potential biomarker for human bladder cancer. Environ Health Perspect. 2000 May; 108 (5) :413-8. PubMed PMID:10811567; PubMed Central PMCID: PMC1638035.

90. Sens MA, Somji S, Garrett SH, Beall CL, Sens DA. Metallothionein isoform 3 overexpression is associated with breast cancers having a poor prognosis. Am J Pathol. 2001 Jul; 159 (1) :21-6. PubMed PMID:11438449; PubMed Central PMCID: PMC1850423.

91. Shi X, Wu C. A suppressive role of mitogen inducible gene-2 in mesenchymal cancer cell invasion. Mol Cancer Res. 2008 May; 6 (5) :715-24. PubMed PMID:18505917.

92. Siemiatycki J, Dewar R, Nadon L, Gérin M. Occupational risk factors for bladder cancer: results from a case-control study in Montreal, Quebec, Canada. Am J Epidemiol. 1994 Dec 15; 140 (12) :1061-80. PubMed PMID:7998589.

93. Siu LL, Banerjee D, Khurana RJ, Pan X, Pflueger R, Tannock IF, Moore MJ. The prognostic role of p53, metallothionein, P-glycoprotein, and MIB-1 in muscle-invasive urothelial transitional cell carcinoma. Clin Cancer Res. 1998 Mar; 4 (3) :559-65. PubMed PMID:9533522.

94. Smirnova IV, Bittel DC, Ravindra R, Jiang H, Andrews GK. Zinc and cadmium can promote rapid nuclear translocation of metal response element-binding transcription factor-1. J Biol Chem. 2000 Mar 31; 275 (13) :9377-84. PubMed PMID:10734081.

95. Smith AH, Hopenhayn-Rich C, Bates MN, Goeden HM, Hertz-Picciotto I, Duggan HM, Wood R, Kosnett MJ, Smith MT. Cancer risks from arsenic in drinking water. Environ Health Perspect. 1992 Jul; 97:259-67. PubMed PMID:1396465; PubMed Central PMCID: PMC1519547.

96. Smith CJ, Livingston SD, Doolittle DJ. An international literature survey of "IARC Group I carcinogens" reported in mainstream cigarette smoke. Food Chem Toxicol. 1997 Oct-Nov; 35 (10-11) :1107-30. PubMed PMID:9463546.

97. Somji S, Sens MA, Lamm DL, Garrett SH, Sens DA. Metallothionein isoform 1 and 2 gene expression in the human bladder: evidence for upregulation of MT-1X mRNA in bladder cancer. Cancer Detect Prev. 2001; 25 (1) :62-75. PubMed PMID:11270423.

98. Somji S, Garrett SH, Zhou XD, Zheng Y, Sens DA, Sens MA. Absence of Metallothionein 3 Expression in Breast Cancer is a Rare, But Favorable Marker of Outcome that is Under Epigenetic Control. Toxicol Environ Chem. 2010 Oct; 92 (9) :1673-1695. PubMed PMID:21170156; PubMed Central PMCID: PMC3002175.

99. Somji S, Garrett SH, Toni C, Zhou XD, Zheng Y, Ajjimaporn A, Sens MA, Sens DA. Differences in the epigenetic regulation of MT-3 gene expression between parental and Cd+2 or As+3 transformed human urothelial cells. Cancer Cell Int. 2011 Feb 8; 11 (1) :2. PubMed PMID:21303554; PubMed Central PMCID: PMC3041731.

100. Stuart GW, Searle PF, Chen HY, Brinster RL, Palmiter RD. A 12-base-pair DNA motif that is repeated several times in metallothionein gene promoters confers metal regulation to a heterologous gene. Proc Natl Acad Sci U S A. 1984 Dec; 81 (23) :7318-22. PubMed PMID:6095286; PubMed Central PMCID: PMC392137.

101. Takiguchi M, Achanzar WE, Qu W, Li G, Waalkes MP. Effects of cadmium on DNA-(Cytosine-5) methyltransferase activity and DNA methylation status during cadmium-induced cellular transformation. Exp Cell Res. 2003 Jun 10; 286 (2) :355-65. PubMed PMID:12749863.

102. Talaat S, Somji S, Toni C, Garrett SH, Zhou XD, Sens MA, Sens DA. Kindlin-2 expression in arsenite- and cadmium-transformed bladder cancer cell lines and in archival specimens of human bladder cancer. Urology. 2011 Jun; 77 (6) :1507.e1-7. PubMed PMID:21624607; PubMed Central PMCID: PMC3105253.

103. Talbert PB, Henikoff S. Histone variants--ancient wrap artists of the epigenome. Nat Rev Mol Cell Biol. 2010 Apr; 11 (4) :264-75. PubMed PMID:20197778.

104. Thirumoorthy N, Manisenthil Kumar KT, Shyam Sundar A, Panayappan L, Chatterjee M. Metallothionein: an overview. World J Gastroenterol. 2007 Feb 21; 13 (7) :993-6. PubMed PMID:17373731.

105. Tsai SM, Wang TN, Ko YC. Mortality for certain diseases in areas with high levels of arsenic in drinking water. Arch Environ Health. 1999 May-Jun; 54 (3) :186-93. PubMed PMID:10444040.

106. Tseng CH. Arsenic methylation, urinary arsenic metabolites and human diseases: current perspective. J Environ Sci Health C Environ Carcinog Ecotoxicol Rev. 2007 Jan-Mar; 25 (1) :1-22. PubMed PMID:17365340.

107. Tu Y, Wu S, Shi X, Chen K, Wu C. Migfilin and Mig-2 link focal adhesions to filamin and the actin cytoskeleton and function in cell shape modulation. Cell. 2003 Apr 4; 113 (1) :37-47. PubMed PMID:12679033.

108. Ussar S, Wang HV, Linder S, Fässler R, Moser M. The Kindlins: subcellular localization and expression during murine development. Exp Cell Res. 2006 Oct 1; 312 (16) :3142-51. PubMed PMID:16876785.

109. Vahter M. Mechanisms of arsenic biotransformation. Toxicology. 2002 Dec 27; 181-182:211-7. PubMed PMID:12505313.

110. Vahter M. Methylation of inorganic arsenic in different mammalian species and population groups. Sci Prog. 1999; 82 (Pt 1):69-88. PubMed PMID:10445007.

111. Waddington CH The epigenotype. Endeavour 1, 18–20 (1942)

112. Waalkes MP. Cadmium carcinogenesis. Mutat Res. 2003 Dec 10; 533 (1-2) :107-20. PubMed PMID:14643415.

113. Westin G, Schaffner W. A zinc-responsive factor interacts with a metal-regulated enhancer element (MRE) of the mouse metallothionein-I gene. EMBO J. 1988 Dec 1; 7 (12) :3763-70. PubMed PMID:3208749; PubMed Central PMCID: PMC454951.

114. Wu C. Migfilin and its binding partners: from cell biology to human diseases. J Cell Sci. 2005 Feb 15; 118 (Pt 4) :659-64. PubMed PMID:15701922.

115. Wu MM, Kuo TL, Hwang YH, Chen CJ. Dose-response relation between arsenic concentration in well water and mortality from cancers and vascular diseases. Am J Epidemiol. 1989 Dec; 130 (6) :1123-32. PubMed PMID:2589305.

116. Wülfing C, van Ahlen H, Eltze E, Piechota H, Hertle L, Schmid KW. Metallothionein in bladder cancer: correlation of overexpression with poor outcome after chemotherapy. World J Urol. 2007 Apr; 25 (2) :199-205. PubMed PMID:17253087.

117. Zhao CQ, Young MR, Diwan BA, Coogan TP, Waalkes MP. Association of arsenic-induced malignant transformation with DNA hypomethylation and aberrant gene expression. Proc Natl Acad Sci U S A. 1997 Sep 30; 94 (20) :10907-12. PubMed PMID:9380733; PubMed Central PMCID: PMC23527.

118. Zhong CX, Mass MJ. Both hypomethylation and hypermethylation of DNA associated with arsenite exposure in cultures of human cells identified by methylation-sensitive arbitrarily-primed PCR. Toxicol Lett. 2001 Jul 6; 122 (3) :223-34. PubMed PMID:11489357.

119. Zhong S, Fields CR, Su N, Pan YX, Robertson KD. Pharmacologic inhibition of epigenetic modifications, coupled with gene expression profiling, reveals novel targets of aberrant DNA methylation and histone deacetylation in lung cancer. Oncogene. 2007 Apr 19; 26 (18) :2621-34. PubMed PMID:17043644.

120. Zhou X, Li Q, Arita A, Sun H, Costa M. Effects of nickel, chromate, and arsenite on histone 3 lysine methylation. Toxicol Appl Pharmacol. 2009 Apr 1; 236 (1) :78-84. PubMed PMID:19371620; PubMed Central PMCID: PMC2684878.

121. Zhou XD, Sens DA, Sens MA, Namburi VB, Singh RK, Garrett SH, Somji S. Metallothionein-1 and -2 expression in cadmium- or arsenic-derived human malignant urothelial cells and tumor heterotransplants and as a prognostic indicator in human bladder cancer. Toxicol Sci. 2006 Jun; 91 (2) :467-75. PubMed PMID:16565513.

122. Zlotta AR, Cohen SM, Dinney C, Droller M, van der Kwast TH, van Rhijn BW, Bochner B, Ameil G, Jewett MA. BCAN Think Tank session 1: Overview of risks for and causes of bladder cancer. Urol Oncol. 2010 May-Jun; 28 (3) :329-33. PubMed PMID:20439032.